UNIVERSITY
OF TRENTO - Italy
DEPARTMENT OF INDUSTRIAL ENGINEERING

XXVII cycle

Doctoral School in Materials Science and Engineering

Bottom-up Tissue Engineering: The Effect of 3D Tissue Fabrication Strategies on Cellular Behavior.

Volha Liaudanskaya

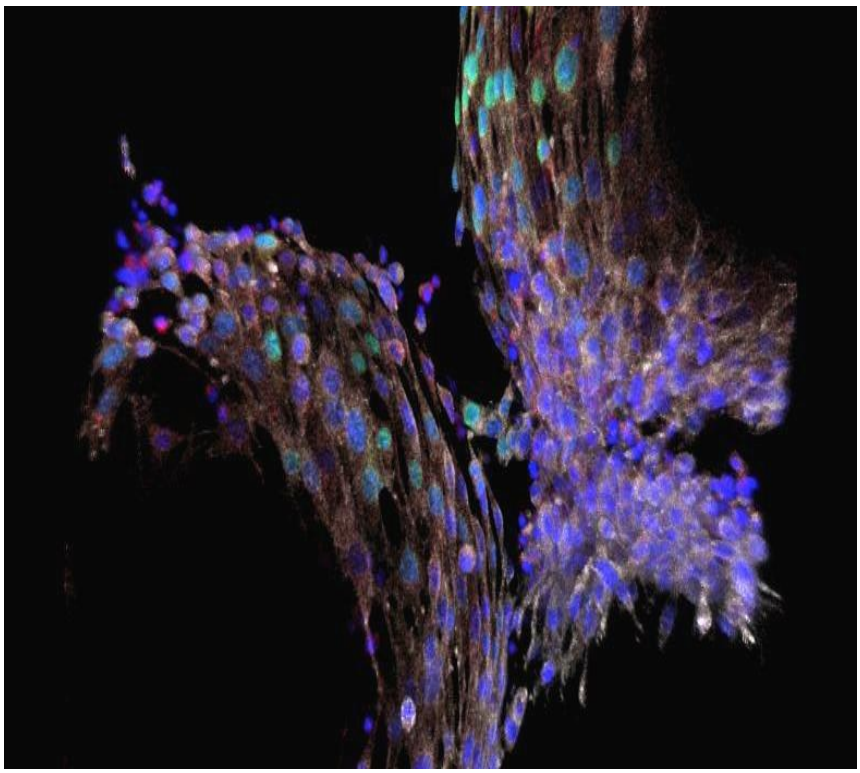

April 2015

Bottom-up Tissue Engineering: the effect of 3D tissue fabrication strategies on cellular behavior.

Volha Liaudanskaya
E-mail: volha.liaudanskaya@gmail.com

Advisors

Prof. Claudio Migliaresi,
Department of Industrial Engineering,
Universita degli Studi di Trento, Italy.

Doctoral Committee

Prof. Gian Domenico Soraru,
Department of Industrial Engineering,
Universita degli Studi di Trento, Italy.

Prof. Antonella Motta,
Department of Industrial Engineering,
Universita degli Studi di Trento, Italy.

Prof. Ralf Riedel,
Institut für Materialwissenschaft,
Technische Universität Darmstadt,
Germany.

PhD internsip advisor:
Prof. Utkan Demirci,
Stanford University School of Medicine,
Canary Center
Department of Radiology, USA.

Prof. Sabine Fuchs,
Department of Traumatology,
Experimental Trauma Surgery,
University Hospital Schleswig-Holstein,
Germany.

University of Trento,
Department of Industrial Engineering
April 2015

... To those who have dreams, but have doubts how to reach them…. Never give up, never get discouraged, just keep work hard and be dedicated to your dreams and life will reward you in the moment when you least expect this.

Table of contents

List of Tables

List of Figures

List of abbreviations and acronyms

TE	Tissue Engineering
PGA	Poly (glycolic acid)
UV	Ultraviolet light
3D bioprinting	Three-dimensional bioprinting
ECM	Extracellular matrix
TCP	Tissue culture plate
Gd	Gadolinium salt
EHDJ	Electro-hydro dynamic jetting
PI	Photoinitiator
hESCs	Human embryonic stem cells
PHEMA	Poly (hydroxyethyl metacrylate)
PVA	Poly (vinyl alcohol)
HA	Hyaluronic acid
GelMA	Gelatin metacrylate

Abstract

Organ failure is one the biggest problems, doctors face every day. Many patients are not able to get a transplant, but even those who recieved it, may undergo painful process of organ rejection and be on the transplant waiting list again. Organ transplants shortage is severe problem in current medicine that has many ethical and medical issues. To solve this problem, the new direction in regenerative medicine was formed, organ prinitng. The main goal of organ printing is fabrication of organ replacements that would mimic the original ones in terms of complexity and functionality. By direct fabrication and maturation of organs in vitro, the problem of organ shortage can be solved, moreover, based on the advances in cell therapy, these organs can be printed with patients own cells, which will eliminte the problem of transplant rejection.

Organ printing is multistep and complex process, composed of three main steps: tissue design, or theoretical modelling of replacement composition; tissue fabrication, or direct cell encapsulation and controlled assembly of building units; at last, tissue maturation to reach desirable functionality of the replacement. In the past decade, there was developed a variety of methods for the second step of organ printing, cell encapsulation, which is practicaly the main procedure for tissue fabrication. However, all these methods of cell encapsulation are complex and they might affect cells viability and functionality, which will result in changed tissue function.

Thus, starting from the detailed analysis of the tissue fabrication process (encapsulation and assembly methods) the list of possible cell behavior affectors was composed. Based on this list, we designed a multistep protocol for coherent evaluation of cells behavior parameters, in terms of viability, functionality and activity during the tissue fabrication and its maturation steps. Three main materials were used for this study, two naturally (alginate and modified gelatin) and one synthetically (polyethilene glycol) derived polymers.

The encapsulation step was performed with two different methods based on chemical or photo crosslinking of the material. Cell parameteres were evaluated on the molecular level for variety of parameters, including viability, activity, proliferation, stress markers expression, at last ability to adapt artificial environment to the cell functional niche with extracellular matrix markers expression, and proteoglycans.

The innovation of the presented study consists in the developing a unique protocol for detailed cell functionality evaluation during the organ printing procedures. In fact, based on the conducted study, it was proved the safety of the encapsulation methods. Moreover, based on the cell parameters post-encapsulation, there was suggested the optimal time for tissue maturation for application of the fabricated structures in organ printing, but also in other fileds, like developmental and pathological biology, or drug screening. Eventully, a novel way of simple blocks assembly into 3D complex structures was developed and proved to be safe for cell parameters.

At last, for the future research in organ printing, a detailed study over a cell behavior and functionality has to be performed for every fabrication method, what will improve the organ production process drastically.

Chapter 1.

General Introduction

1.1 Tissue engineering: general terms

1.1.1 Short history and definition of tissue engineering

Tissue engineering (TE) as independent field of science was formed around 40 years ago, however the first historical note about tissue engineering can be found in Genesis I: 1: “The Lord, breathed a deep sleep on the man and while he was asleep he took out one of his ribs and closed up this place with flesh. The Lord God then built up into a woman the rib that he had taken from the man”[1]. Moving through the ages many references of TE applications were found. Recently, a women mummy was found aged around 3000 years which had a wooden toe prosthesis that replaced the amputated one [2]. In India in 600 B.C. there was a first written reference about the rotational flaps application for reconstruction of amputated noses [3]. In Italy in 15-16th centuries many talented surgeons tried to improve the indian first version of rhinoplasty. Since that time, rhinoplasty procedure was drastically improved, however, the main principle remains the same as it was invented thousands of years ago.

Around 30 years ago, the term tissue engineering was mainly referred to the use of prosthetic devices and the surgical manipulation of tissues. The first experiments in TE though were conducted in 1970th in Boston, city that may be considered as tissue engineering hometown. Unfortunately, first experiments were without a practical success but they gave valuable theoretical conclusion that with a proper combination of material and cells it can be possible to

generate a viable tissue. Based on this conclusion, couple of years later in Massachusetts Institute of Technology a group of scientists developed a novel skin draft by using collagen matrix and dermal fibroblasts. However, the real inception of current tissue engineering field started in mid-1980s by two talented scientists Dr. Joseph Vacanti and Dr. Robert Langer, when they came up with the idea of designing scaffolds for *in vivo* cell delivery. The results were unexpected and hardly explainable but they lay to the groundwork of the extensive research in the field of tissue engineering. Even though, in 1988 during the meeting organized by National Science Foundation Tissue Engineering field was first introduced and described within the article of keynote presentation, till today the article that was published a little while after in 1993 in Science considered as the most-cited paper that describes tissue engineering discipline. In this paper Dr. Vacanti and Dr. Langer define Tissue Engineering as an "interdisciplinary field that applies the principles of engineering and life sciences toward the development of biological substitutes that restore, maintain, or improve tissue function or a whole organ" [4].

Since the time those first small, but so valuable experiments were conducted, many scientific groups focused their attention on tissue engineering field and drastic progress was achieved.

Thus, after many years of research scientists define the main goal of tissue engineering as production of suitable scaffold that would mimic natural tissue or organ for different applications like replacement or regeneration of tissues which were damaged due to trauma or disease; in vitro 3D models for drug screening and pathologies investigations.

1.1.2 Progress, current state and problems of tissue engineering

During the first meeting in 1988 tissue engineering field was discussed as an alternative method for some injuries treatment by manipulating with prosthetic materials combined with existing tissues. The actual organ or tissue production using the basic concept of combining materials with cells wasn't even considered at this memorable meeting, but since that time a lot has changed and significant progress was made in the field. One of the greatest scientists who made a priceless contribution in the field of tissue engineering is Dr. Anthony Atala and his group. At present his group is focused on growing tissues and organs of more than 30 parts of the body. Back in 2006 in the Lancet journal Atala published his first results of human bladder transplantation in 7 patients and their post-operative control [5]. The results were very promising, all patients recovered from the surgery and were able to improve the quality of their lives significantly. Since that publication many more successful bladder transplantations were made. Great success was also made in some other areas like skin regeneration [6, 7, 8], cartilage and bone tissue engineering [9, 10], corneal regeneration [11] and in many other fields.

Even though some tissues can be regenerated and grown back, there are still many unsolved issues in tissue engineering. Heart, liver, kidney and brain tissue engineering attracts the attention of many scientific groups, but the results are still on the intial stage. Some improvements were already done, but the day of engineered functional heart or kidney transplantation is not today. Brain engineering is even more complicated, brain work and organization is not completely understood by itself, what makes brain regeneration research even harder. However, heart seems quite well understood and well-studied organ, but its restoration and regeneration is not that easy as well, because of its structural complexity.

Each direction of tissue engineering like neural, cartilage or heart faces specific set of challenges that need to be solved, like cell source, scaffold modelling and proper biocompatible material selection, cell seeding and growth factors effect, following cell matrix analysis and mechanical testing, and finally animal testing before implementation on patients [2].

1.1.3 Tissue engineering approaches: advantages and open questions.

Figure 1.1 represents two main approaches that generally used in tissue engineering. A major approach for *in vitro* tissue reconstruction has been called "top-down" which is mainly focused on the seeding cells of interest on top of the synthetic or natural polymeric scaffold, such as agarose [13], alginate [14], collagen [15], hyaluronic acid [16, 17], silk fibroin [18, 19, 20], poly (glycolic acid) (PGA) [21], and many others, following cells penetration through the scaffold from the top to the bottom. The idea, cells would homogeneously populate the scaffold and self-organize by mimicking *in vivo* conditions. The success of this approach has translated several engineered tissues to the clinical stage. However, despite many developed improvements in surface pattering or even use of biomimetic scaffolding, such as decellularized ECM templates, top-down strategies often have some limitations such as thick scaffolds vascularization, cell seeding density, large-scale tissues reconstruction, and finally, limited design of the intricate microstructural features of tissues [14, 21].

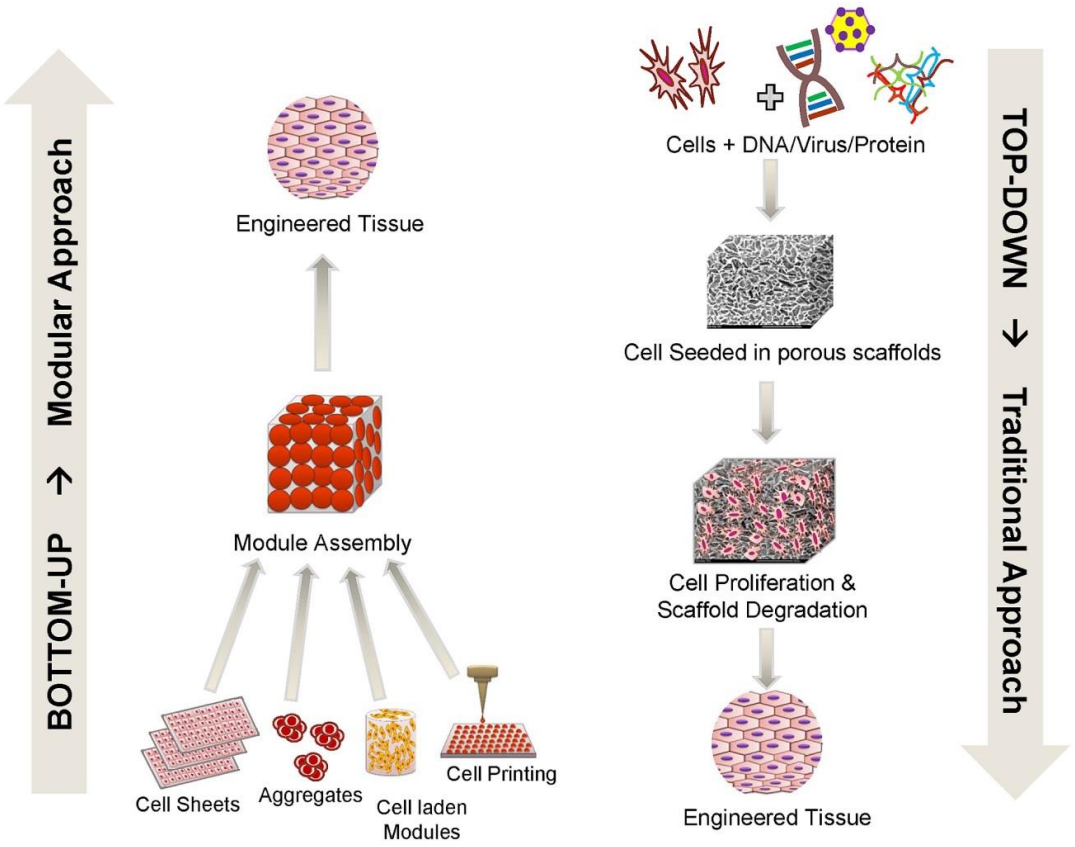

Figure 1.1: Tissue Engineering Approaches. Image adapted from R. Tiruvannamalai-Annamalai et al. [12].

Bottom-up approach is based on the initial production of small cell-laden building blocks, which can be beads or capsules [12, 22], cell sheets or aggregates [23] or any other cell-laden structure and following assembly of these building units into more complex structures. This approach was invented to overpass the limitations of top-down approach, like weak control over scaffold composition, or vascularization. With bottom-up approach, building blocks can be prepared with different cell types and after guided to assemble in complex 3D structures by the variety of methods, like 3D bioprinting [5, 12, 27], magnetic [24], robotic [25] or acoustic self-assembly [26], stacking cell sheets and others in the precise order, mimicking in vivo organ structure.

1.2 Organ printing: challenges, steps and current state.

Organ printing technology can be defined as biomedical application of rapid prototyping or layered additive biofabrication by using capable to self-assemble cell-laden building blocks or cell aggregates [27, 28, 29, 30]. The fundamental principal of organ printing technology implicates tissue capability for fusion to closely placed cell aggregates or building blocks. This principal was taken from natural embryonic development, where fusion is very common event during the layers formation and body parts development [31].

The ultimate goal of organ printing is large scale fabrication of 3D vascularized functional living organs for clinical transplantation and in vitro implementation for drug screening as well as platform for disease diagnostics [22, 24, 26, 29, 32]. Organ printing technology still has a lot of challenges, but with research and advanced improvements this developed technology will allow production of 3D functional living organs suitable for clinical implementation. Rapid prototyping is already well established and includes many methods such as stereolithography, selective laser sintering (SLS), fused deposition modeling (FDP), ballistic particles manufacturing (BPM) and others [29, 33, 34, 35, 36].

The simplest way to describe the principles of organ printing is to use analogy of printing technology. In order to print a book it is necessary to have next essential components: written text, a printing press, movable type, paper and ink. So as with organ printing, it is necessary to have CT scan or MRI scan of the desired organ (Figure 1.2), that will be so called “blueprint”, a “bioprinter” or robotic dispenser, a cartridge or container for dispensing biomaterials mixed with living cells or cell aggregates, biodegradable biomimetic hydrogel to support the printed structure or “biopaper”, and self-assembling cell aggregates or single cells in hydrogels “bioink” [27, 29, 30, 37, 38, 39, 40].

Organ printing composed of three main steps (Figure 1.2) [37]. Proper parameters and material selection for each of this step are essential for success in the 3D structure fabrication. Dr. Mironov defined 10 top challenges in organ printing technology [29, 30]. Below all these challenges are described in terms of organ printing steps: pre-processing, printing and post-processing [30].

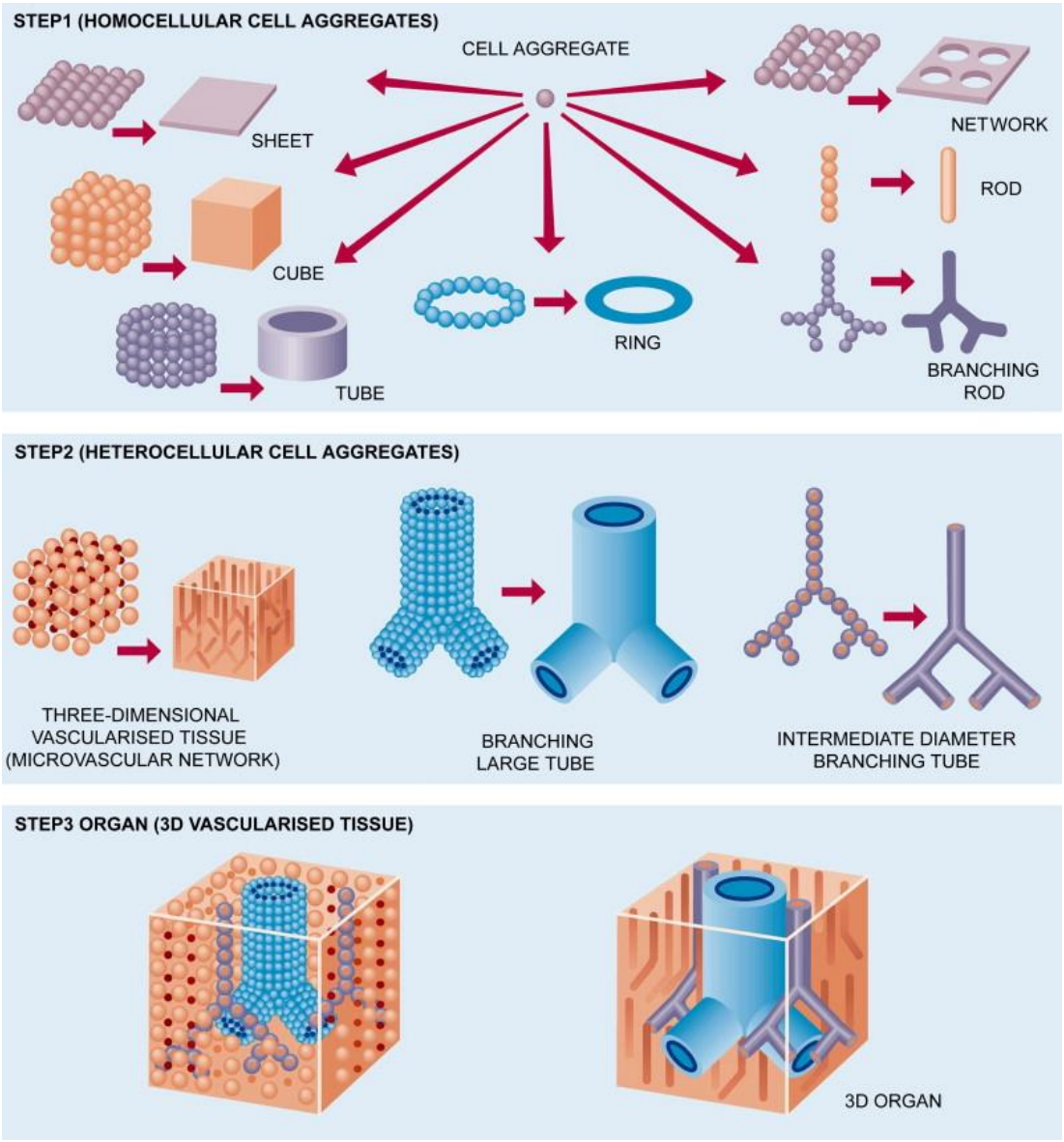

Figure 1.2: Organ printing process composed of three main steps. Image adapted from Mironov et al [37].

1. Pre-processing is challenged by design, theoretical modeling and *in silico* tissue self-assembly of the desired organ. This is the first, and the most important set of challenges, without a precise design and theoretical modelling of cell behavior after printing, all the following steps will be useless. Initially obtained with computer tomography scanning picture of the organ can't be used directly for organ printing. In silico tissue self-assembly will calculate and predict cells behavior, and which changes might happen during the organ maturation, such as cell fusion, shrinkage, matrix degradation by cells activity and many other parameters that have to be taken under control.

2. Printing step or direct cell encapsulation and controlled placement in defined order is challenged by the proper selection of biopaper, bioink and bioprinter, which in biological terms refer to the proper selection of biomaterials, cell source and encapsulation or printing conditions. Bioink refers to the cell-laden building blocks [41, 42, 43]. As far as the fundamental principal of organ printing based on tissue fusion process, the building blocks has to be located and prepared in the way that would stimulate and guide tissue fusion [40]. Thus, cells functionality, so as materials properties (biopaper) will play here a critical role. Biopaper can be defined as biodegradable, biomimetic hydrogels specifically designed for the bioprinting process with tissue fussion-permessive properties [31, 44, 45]. At last, bioprinter will have a crucial role on future 3D bioprinted organ. Bioprinter may affect significantly cell viability and vital characteristics during the following maturation step. Cell entrapment in 3D condition is stressful by itself, plus an effect of some encapsulation steps might affect cells viability, ability to proliferate and differentiate and many other characteristics might be affected, thus bioprinter selection so as direct encapsulation process has to be deeply evaluated before organ production.

3. Post-processing, or organ maturation in bioreactors is important for future organ functionality, such as heart muscle contractions, or bone strength, neural signaling in brain tissue and so on [31, 38, 46, 47]. To obtain a

desirable behavior of printed organ it has to be placed in conditions that would mimic in vivo, like pressure, growth factors supply, stress resistance and others. At last, during the maturation process, so as before implantation or printed organ implementation its main parameters have to be evaluated in non-invasive monitoring. Viability, vascularization, main organ function have to be perfect, otherwise implantation of not properly prepared organ may cause severe complications [48].

Even though organ printing technology faces many challenges, this is still feasible. In just a decade a dramatic success was made, meaning in the following decade even more will be accomplished. Many groups are working on these challenges and slowly move in the right direction to overpass these complications and finally be able to print functional living organ.

1.3 Cell encapsulation

1.3.1 General introduction.

In 1933 Bisceglie made a simple experiment, he enclosed tumor cells in polymer membrane and implanted them into pig's abdominal cavity. Results showed, that cells survived long enough, to make a conclusion that immune system didn't damage or destroy them [49, 50, 57]. Three decades later Chang introduced cell encapsulation as promising method for protecting cells from immune aggressiveness by encapsulating them in ultrathin polymeric membranes, and subsequently evoked term "artificial cells" [51]. This idea was widely applied in 70-80th for diabetes control in small animals by immobilizing xenograft islet cells. Since then, a dramatic progress was made in understanding materials science, immunology, genetics and pharmaceutical technology that are so crucial for successful cell encapsulation [49]. Microencapsulation found many applications in different fields, such as therapeutic treatment for diabetes, cancer, hemophilia and renal failure [50, 52, 53], stem cell research [22] and others [54, 55, 56]. Around a decade ago, cell encapsulation received enormous scientific attention as the main method for the second step of organ printing technology, as it described above.

Cell encapsulation methods consist in the entrapment of cells in microcapsules or microbeads starting from a suspension of cells in polymeric solution that can be solidified by chemical or physical methods [50-57]. Generally cell encapsulation involves fabrication of three-dimensional (3D) scaffolds, with either seeded cells on top or with cells directly encapsulated with aim to use this fabricated 3D structure for healthy replacement of damaged tissues, or for guidance and support for tissue recovery.

Cell microencapsulation is a technology that has tremendous potential in the field of tissue engineering and regenerative medicine for regeneration,

restoration but also for transplantation and substitution of damaged or diseased tissues and organs.

1.3.2 Methods for cell encapsulation

With microencapsulation methods cells can be entrapped in various controllable forms such as beads, sheets, or fibers [52, 57]. In the recently published review Gasperini [52] described main cell encapsulation strategies that are widely used. Table 1 summarizes and compares several cell encapsulation techniques according to the final scaffold size and shape, but also the scalability of these methods and type of gelation mechanism applied for encapsulation.

Name	Control of size	Minimum Size (d in µm)	Size dispersion	Best gelling mechanism
Extrusion	Medium	80	Medium/ Low	Fast/ Ionotropic
Lithography	Very good	50	Low	All
Emulsion	Low	10	High/ Medium	Thermal
Microfluidic	Very good	50	Low	All
Bioprinting	Very good	100	Low	All (more complex with thermal)
Superhydrophobic surfaces	Very good	1000	Low	All

Table 1.1: Cell encapsulation strategies [52-66].

1.3.2.1 Extrusion methods and state of the art.

The simplest and the most applicable method for cell encapsulation is extrusion [52, 56, 57, 58, 59]. This method is based on gravitational dripping properties of liquids. The suspension of pre-polymer solution mixed with cells extruded through the syringe or a needle. On the top of the needle drops form and when they reach a critical mass they fell freely in the collecting bath with the crosslinking solution. The final size of beads fabricated with extrusion methods depend on many factors, such as ionic concentration of the crosslinking bath, the surface tension of the drop, and the diameter of the pendant droplet neck [22, 52, 60]. Generally, the beads size is around 1mm, and the shape of the beads is not perfectly spherical, but rather droplet-like shape.

Many extrusion methods were advanced for obtaining the control over the final scaffold or bead size and shape, but also for improving cell viability and functionality [61, 62, 63]. For example, wet spinning, was modified extrusion method for final fabrication of fibers instead of beads. This method allows production of fibers, by extruding pre-polymer solution directly into the collecting bath with crosslinking solution without an air gap between the needle and a bath.

One else example of extrusion method modification is for generation of smaller size beads with controllable shape [52, 62]. The idea for production of smaller beads is to break down the extrusion jet before the drop will reach the critical mass and fells by itself. One of the applying methods is coaxial air flow [54, 62]. This method applies a compressed gas that directed through the extruding droplet and it causes the drop detachment faster than the droplet critical mass is reached. In the same mechanism beads can be produced but implying another liquid instead of gas.

Another advanced and precise method of small beads formation is vibrational encapsulation [65]. This system is based on the concept that liquid jet extruded from the orifice of the needle will be broken down into the equal

size droplets by applying vibration to the nozzle. By manipulating with flow and vibration parameters it is possible to obtain beads size around 100 μm.

At last, by applying an electrical charge to the extruding needle it is also possible to obtain smaller beads with controlled size, by so-called bio-electrospraying method [22, 52, 60, 62, 66]. The extruding droplet reacts to the presence of electrical charge by accumulating ions of opposite sign on its surface. As the result, ions accumulation creates stress that force droplet to detach from the needle and drop into the crosslinking bath [66].

1.3.2.2 Lithography-based methods

Lithography methods include two subtypes: stereolithography and photolithography [41-43, 50, 52, 55, 56, 62, 67, 68, 69]. Stereolithography is based on the hydrogels production using replica moulding. At first, replicas produced by spin-coating or pouring and following UV crosslinking. Next, replicas filled with cells suspended in prepolymer solution and exposed to UV light hydrogel crosslinking [67].
Photolithography is another widely applied method for cell encapsulation and based on using photo-mask that placed on top of the photocrosslinking material mixed with cells [68]. Photo mask can be designed to produce a hydrogels in variety of sizes and shapes. But also, the hydrogels can be produced with different cell types by mimicking tissue/organ complexity. This strategy is widely used for 3D model fabrication for diseases investigation or general science. There are several important requirements for fabrication of patterned biocompatible cell-laden hydrogels by photolithography [41, 42, 43, 68, 69]. First requirement is proper photocurable material amenable to polymerization caused by photosensitive free radicals. Another important requirement is photoinitiator (PI), that must not only initiate the reaction, but also eliminate the reaction as soon as UV light exposure is stopped, but most importantly for

tissue engineering application, it has to have low cytotoxicity. A separate attention must be paid for combination of factors like UV time exposure during photopolymerization, and PI concentration, both these factors can affect cell viability. At last, a photomask is important as well, it has to be made in the way to protect unwanted areas from UV light, and those that exposed, has to be permeable for UV rays and initiate the crosslinking.

Polymer networks can be synthesized using various chemical methods, such as photo-, chemical, mechanical- or thermal-initiated polymerization. Advances in materials science made it possible to design and synthesize polymer networks with molecular-scale control over the structure such as crosslinking density and with tailored properties, such as biodegradation, mechanical strength, and chemical and biological response to stimuli.

1.3.2.3 Emulsion-based methods

Fabrication of spherical capsules by emulsion-based method found a wide application in pharmaceutical industry [53, 70, 71]. This strategy is based on the mixing of two liquids that are immiscible (for tissue engineering application one of the liquids is hydrogel precursor), the surfactants applied to the mixture will stabilize the emulsion and allows preparation of smaller droplets. After the suspension reaches the equilibrium precursor droplets undergoes sol-gel transition and become solid [26].

1.3.2.4 Microfluidics-based methods

Microfluidics methods are based on the manipulations with small volumes of liquids in microenvironments as microchannels on chips [52, 54, 70, 72-78]. Droplets fabrication mechanism has similarity with emulsion encapsulation system, but this process happens in microenvironments and

applying flow of liquids to control the shape and size of produced microdroplets. Droplets that fabricated by microfluidics can be considered as bottom-up manufacturing, whereas the classical emulsion approach is top-down. The generation of microfluidics droplets happens through injecting the mixture of hydrogel precursor and cells into a microchannel and the droplets form when it reaches the continuous phase of non-miscible solution coming from the other inlets.

1.3.2.5 Bioprinting-based methods

3D bioprinting idea was taken from the paper printing technology. Like industrial printing technology had a revolutionary effect on people education, politics, religion and language across the globe, 3D printing affects dramatically science and research. Using 3D printing technology archeologists reproduce replicas of ancient and rare artifacts or some fossils for art, education and exhibitions. This technology allows design and work with three-dimensional spatial models [27]. But one of the most important applications 3D bioprinting found in organ or tissue fabrication.

3D bioprinting is layer-by-layer additive robotic positioning of biological materials mixed with cells and growth factors, with spatial control over the placement of functional components with aim to produce a 3D functional organ or tissue substitute. As showed in Figure 1.3 [27] ioprinting is complex procedure that composed of important steps, only proper performance of which can result in a successful organ/tissue fabrication. The main challenge of 3D bioprinting is reproduction of complex micro-architecture of extra-cellular matrix (ECM) components and multiple cell types in sufficient resolution to recapitulate biological function.

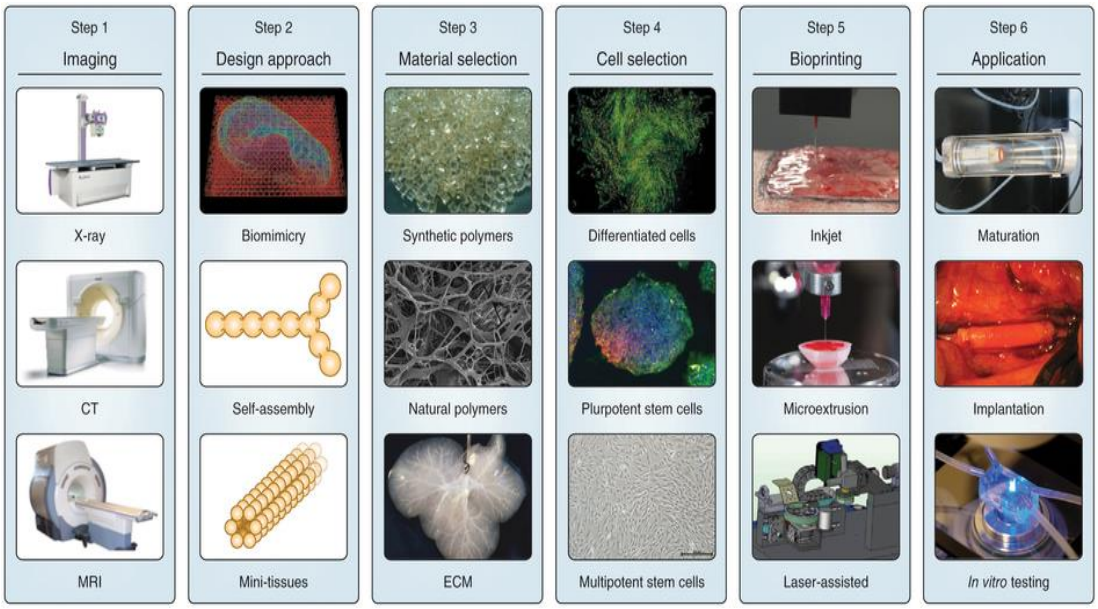

Figure 1.3: Bioprinting steps from the initial 3D computer modelling to the tissue printing and maturation. Images adapted from Atala et al [27].

There were developed many biofabrication technologies such as organ printing or directed tissue self-assembly, solid scaffold-based biofabrication, embedding and molding technology, cell sheet technology, digital and inkjet bioprinting and many others [27-28, 32, 39, 40, 79, 80].

1.3.2.6 Superhydrophobic surfaces based methods

This strategy based on the simple principle of some materials hydrophobicity [69, 81]. By placing a drop of water on the hydrophobic surface it will remain in the droplet shape. Thus, cells mixed with water-based hydrogel precursor can be dripped on the superhydrophobic surface and crosslinked or dried through the contact with air or any other desirable surrounding conditions, and the surface contact will allow to keep the shape of drops [52].

1.3.3 Material selection for cell encapsulation

Cell encapsulation process starts from the suspension of buffer-based pre-polymer solution with cells, so called the sol flowing phase. After applying chemical, physical or biochemical stimuli liquid pre-polymer solution undergoes a transition to gel form, so called non-flowing phase. All the stages of sol-gel transition have to be well adjusted for cell viability, means they have to be as close as possible to the cell physiological conditions [52, 82, 83, 86, 87]. Over the years of materials studying and application of cell encapsulation for organ printing technology, list of desirable materials properties become well-formed and clear. Materials for cell encapsulation must have suitable crosslinking mechanism for successful encapsulation process, biocompatible but most importantly it has to support cells viability, activity, proliferation and main functions [22, 24, 43].

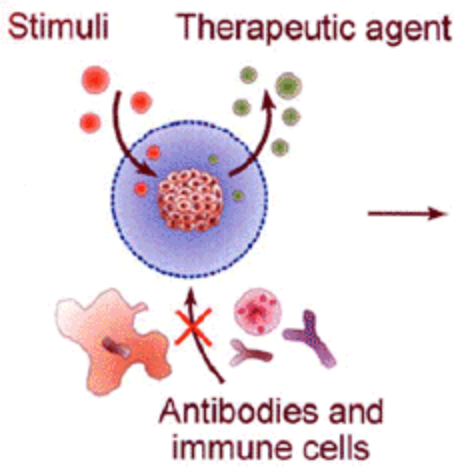

Figure 1.4: Cell microencapsulation: nutrients, oxygen and stimuli diffuse across the membrane, whereas antibodies and immune cells are excluded. Image adapted from Gorka O. et al [50].

Another crucial requirement is suitable short-term stability together with mechanical, physical properties. But also, it has to have a proper porosity

characteristics, depends on the future application [84]. It has to be supportive for inflowing nutrients, oxygen and growth factors, and outflowing toxic waste products and cells activity products, for example insulin for diabetes treatment encapsulated cell delivery [82]. But, crucially it has to protect cells against antibodies and immune cells penetration, for cell protection inside the beads [84]. The ideal bead/ hydrogel schematically presented in Figure 1.4.

Materials currently used in the field of tissue engineering for regeneration and repair are mainly naturally derived polymers, such as alginate [14, 82, 83, 102], gelatin and its modifications [86, 90], collagen [15, 87], silk fibroin [18, 19, 20, 88], hyaluronic acid [16, 17, 89]; but there are also synthetic polymers that are widely used for some applications, such as PGA, polyethylene glycol (PEG) [21, 91, 92]. Both of the material types have its advantages and disadvantages. Natural polymers have similar to human extra cellular matrix (ECM) composition and structure [93, 94, 95, 96]. They are also very biocompatible and supportive for cells growth and activity. Whereas synthetic polymers have good repeatability characteristics and good control over gelation, degradation processes. Another advantage of synthetic polymers, that they can be easily modified or tailored to reach desirable mechanical or physical properties, which is complicated with natural polymers [27]. However, synthetic polymers generally have poor biocompatibility characteristics, toxic metabolites and loss of mechanical properties during degradation.

The most commonly used and well described synthetic polymers with neutral properties are polyethylene glycol (PEG) [91, 92], poly (hydroxyethyl methacrylate) (PHEMA) [97, 98, 99], and poly (vinyl alcohol) (PVA) [99, 101]. PEG hydrogels are non-toxic, non-immunogenic and number one used FDA approved for biomedical application. PEG hydrogels can be covalently crosslinked through covalent bonding using variety of methods. Photo initiated crosslinking using acrylate-terminated PEG monomers is the most applicable method for PEG hydrogels formation. Cell-laden PEG hydrogels are inert, since

they are prevent protein adsorption. Because of easy manipulation and inertness properties, PEG polymers were modified in different ways for cell application to improve adhesion and proliferation, for example peptide sequence was incorporated into PEG structure to induce degradation, and cell adhesion [43].

PHEMA is another hydrogel that has been extensively studied and used in biomedical applications such as contact lenses and drug delivery. PHEMA hydrogels have good mechanical properties, optical transparency, and stability in water. PHEMA hydrogels are easily modified as well, to modulate the properties for different applications [97, 98, 99]. At last, PVA is another synthetic polymer. PVA hydrogels are stable, with crosslinks through the repeated thawing-freezing procedure or chemically crosslinked [99, 101].

Another group of polymers are naturally derived, such as collagen, silk, hyaluronic acid (HA), agarose, alginate, or gelatin and their modifications [13-20, 43]. Depending on their origin and composition, these materials can be applied for different applications. An advantage of natural polymers over synthetic is their natural low toxicity and biocompatibility.

Collagen and other mammalian cell derived protein-based polymers are effective matrices for cellular growth because they contain many cell-signalling domains present in vivo ECM. Collagen hydrogels can be easily obtained through the thermal crosslinking at 37°C degree, however they have relatively weak mechanical properties. Thus, many modifications were done with collagen that improved their mechanical characteristics, and crosslinking process.

HA is glycosaminoglycan (GAG) that is composed of repeated disaccharide units, and most abundant in wound healing and in joints, however it is still can be found in all cells types, but in less amount.

Ali Khademhosseini group hypothesized and proved the idea of using GelMA for micropatterened 3D hydrogels fabrication. As it was earlier

described, cell entrapment in GelMA hydrogels showed good results in cells long-term viability, and high proliferative potential [103, 104]. Thus, his group made an advanced study over 3D hydrogel binding surface, cells elongation and migration within the GelMa hydrogels. And they demonstrated that GelMA allows rapid cell adhesion, cell phenotype elongation, high proliferation potential, and migration in 2D and 3D. GelMA is promising material for variety of applications in tissue engineering [90, 105].

Another advanced research over GelMA application was made within Ali Khademhosseini group, by mixing GelMA with the FDA approved and described above PEG polymer [105]. By mixing these two polymers they wanted to obtain highly biocompatible, non-toxic, mechanically stable and easily manipulated hydrogel for cell encapsulation and micro patterned 3D hydrogels fabrication. Thus, they synthesized a mixed of PEG/GelMA hydrogel that is inexpensive, easily produced, and most importantly biologically and mechanically tunable.

1.3.4 Cell source for encapsulation

Organs and tissues are complex and composed of many different cell types and in various combinations. Immune rejection complications after transplantation makes cell source one of the main challenges for successful organ printing. Patient's embryonic cells (ECs) will the best cell source for any tissue engineering application, because of its potential to differentiate in any cell type of the body [106-114]. However, in many countries ESCs therapy is not an option because of the ethical reasons, as well as for adults autologous ECs are out of reach. An advance solution to this problem was found by the Japanese professor Yamanaka and his Nobel Prize for discovery of induced pluripotent stem cells [115, 116]. These reprogrammed stem cells mimic ESCs, but not identically, in terms of morphology, proliferation, gene expression, surface markers and teratoma formation [5, 117]. Many groups today work on different

protocols for induction of pluripotent stem cells [118, 119, 120, 121, 122, 123]. These cells can solve both complications: differentiation potential and immune inertness. In many cases less potent autologous stem cells can be a suitable source for tissue engineering, exception will be perfect when patience cells are damaged or patient doesn't have enough cells for therapy. Mesenchymal [124, 125], adipose [126, 127], blood, bone marrow derived stem cells [128, 129] are the most commonly used source for adult autologous transplantation and tissue engineering. The variety of stem cells that can be used for tissue engineering purposes is presented in Figure 1.5.

Any cell type chosen for cell encapsulation as building blocks for organ printing, has to have a high proliferation potential, to reach sufficient amount of cells for transplantation. Precise control over differentiation and proliferation in vitro and more importantly *in vivo*, is crucial for cell encapsulation. As it was mentioned above ECs and iPSCs are capable of teratoma formation which has to be eliminated and controlled. Too slow proliferation rate may result in the loss of viability and as a result cell death, whereas too high rate may cause hyperplasia and apoptosis. Timing for cell proliferation important as well, initial high cell proliferation rate is important to reach a proper cell density. But after some time the rate has to be equal to in vivo conditions to achieve cellular homeostasis, albeit without hyperplasia. This can be controlled with growth factors delivery, in some cases viral transfection is used for control over cell proliferation and senescence.

Thereby, cell selection faces next set of challenges: well-understood and characterized, easily reproducible cell source; proper cell type combinations which would closely mimic natural conditions; strict control over cells differentiation and proliferation.

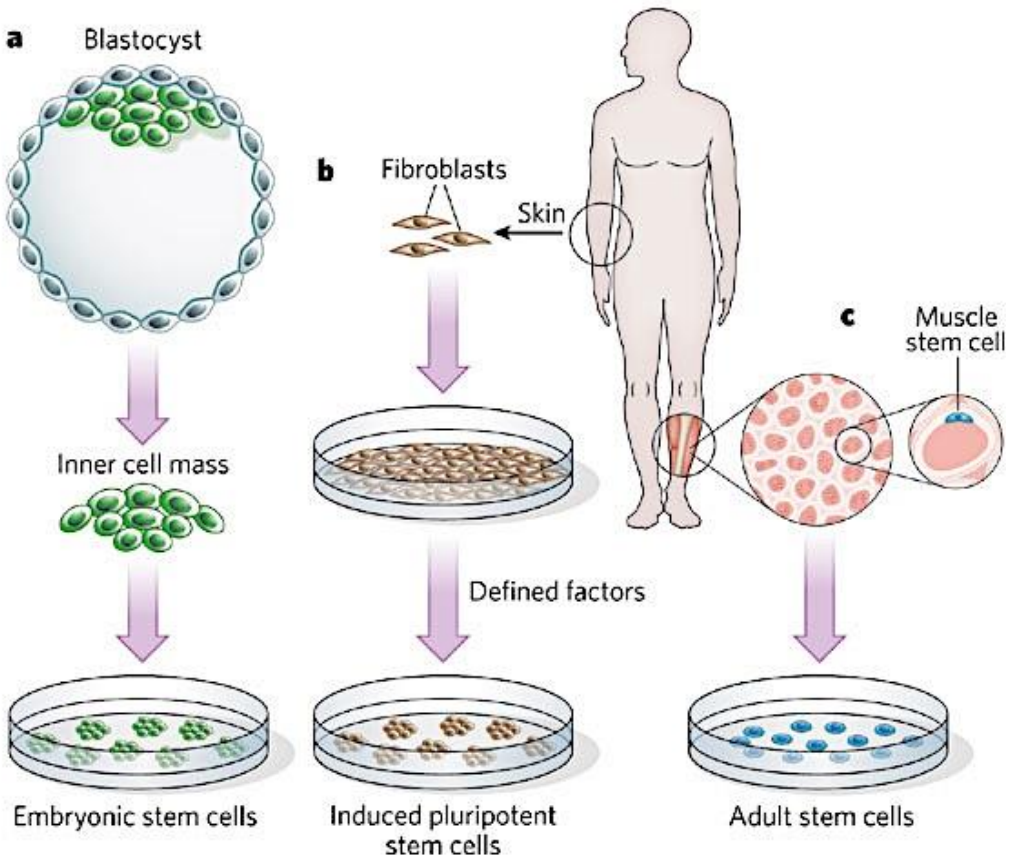

1.5: Stem cell source for tissue engineering applications. Image adapted from Lutolf et al [130].

1.4 Building blocks assembly techniques for 3D tissue engineering.

Human tissues and organs are complex, some of them like skin, or bladder are relatively simply organized, with small variety of cell types composed in the formation of these organs, whereas heart, kidney, and least understood brain are very complex, many different cells compose these organs and participate in the proper functioning. For example brain is composed of over 1 billion of different types of neurons, and 10 to 50 times more of glial cells, that act as servants for proper neural work (Figure 1.6) [131, 132].

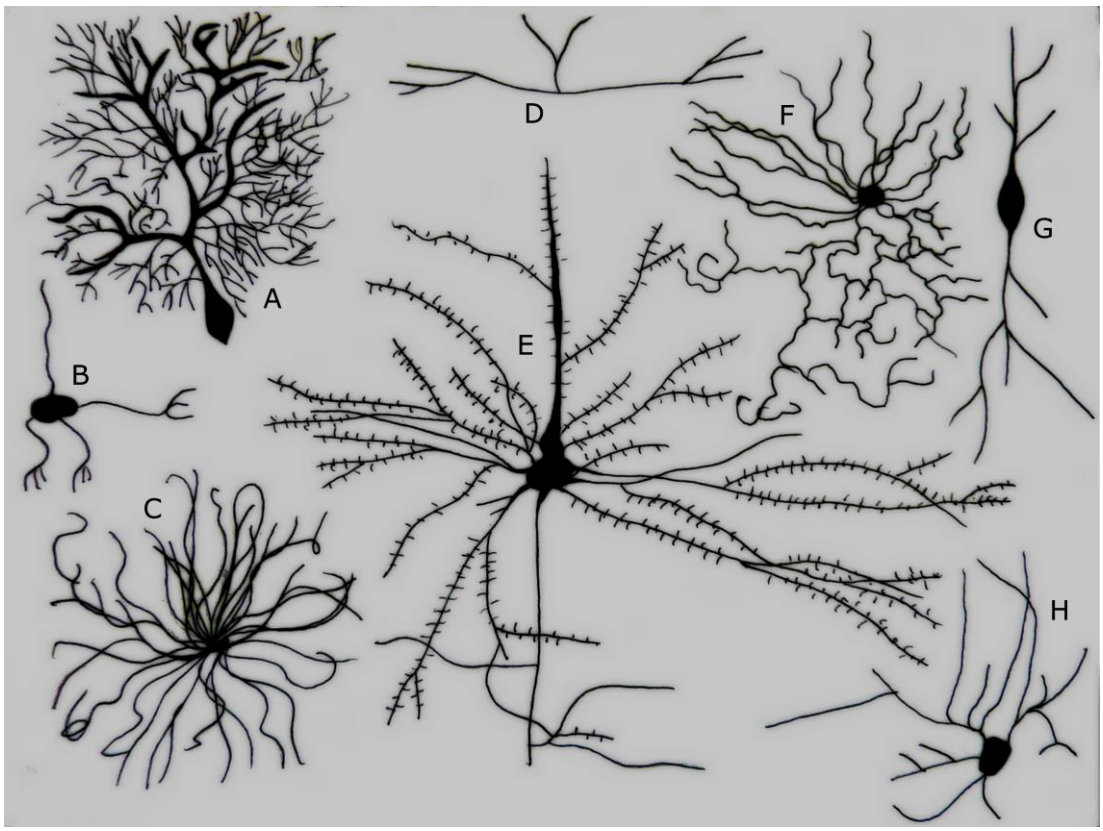

Figure 1.6: Different Types of Neurons. A. Purkinje cell B. Granule cell C. Motor neuron D. Tripolar neuron E. Pyramidal Cell F. Chandelier cell G. Spindle

neuron H. Stellate cell. Images adapted from Ferris Jabr; based on reconstructions and drawings by Cajal [131].

The complex tissue organization makes tissue engineering field is very challenging. As it was described above in section 1.4 there are many ways to fabricate cell-laden hydrogels in different shapes and sizes for variety of applications. However, many of them are capable of producing small size hydrogels, and more importantly they are limited to encapsulation of the poor variety of cell types into one hydrogel, which in many cases will be a serious limitation for tissue/organ fabrication [33, 34, 35, 36, 133, 134, 135, 136, 137].

Thus, properly prepared and laden with different cell types hydrogels have to be assembled in more complex structure that would mimic in vivo tissue in size and complexity.

Assembly of cell-laden building blocks found an emerging application in tissue engineering and regenerative medicine, but also for drug screening on complex 3D models fabrication. Assembly approaches are focused on enabling rapid and scalable fabrication of engineered tissue substitutes with controllable and predefined geometrical, biological features and complex architecture [33, 34, 35, 36]. The assembly idea was taken from the nature where assembled and repeated units are quite common, for example nephrons in kidney, lobules in liver, DNA assembly from nucleotides and protein splicing and assembly from RNA units. Inspired by nature, many research groups developed different approaches for cell-laden hydrogels assembly, such as acoustic, magnetic, robotic, or even bioprinting can also considered as technique for hydrogels assembly by direct printing of them, some of these approaches illustrated at Figure 1.7.

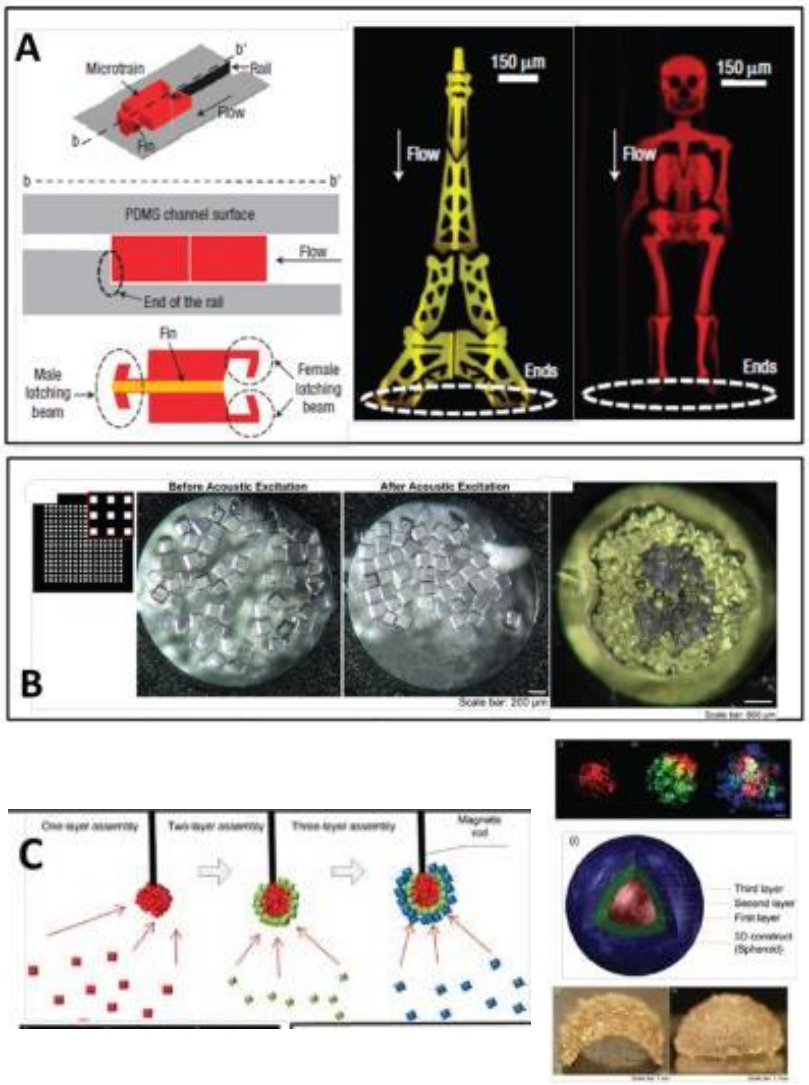

Figure 1.7: Directed assembly methods in literature for microscale hydrogels. A) Microfluidics assembly; B) Acoustic assembly; C) Magnetic assembly; Images adapted from Gurkan et al [33].

1.4.1 Magnetic and paramagnetic assembly

Magnetic fields have already found an application for cell sorting and isolation, in vivo imaging, and 3D cell culture [33]. Recently, magnetic field found an application for construction of 3D tissues. Hydrogel manipulation strategies using magnetic fields appear to be various, contactless and

inexpensive. There are some ways of producing hydrogels or building blocks with magnetic properties. The most common and originally proposed was loading hydrogels with magnetic nanoparticles of different kind, such as gold, iron oxide or bacteriophage. However, magnetic nanoparticles are potentially dangerous because of tissue cytotoxicity. Thus, new approaches that do not require nanoparticle presence are in great demand. Tasoglu and his group developed a new method for magnetic assembly by loading hydrogels with free radicals and vitamin E. These easy modifications allowed to perform guided self-assembly of materials with heterogeneous properties such as porosity, mass density and stiffness into the 3D structures [24, 34, 133, 134].

1.4.2 Acoustic assembly

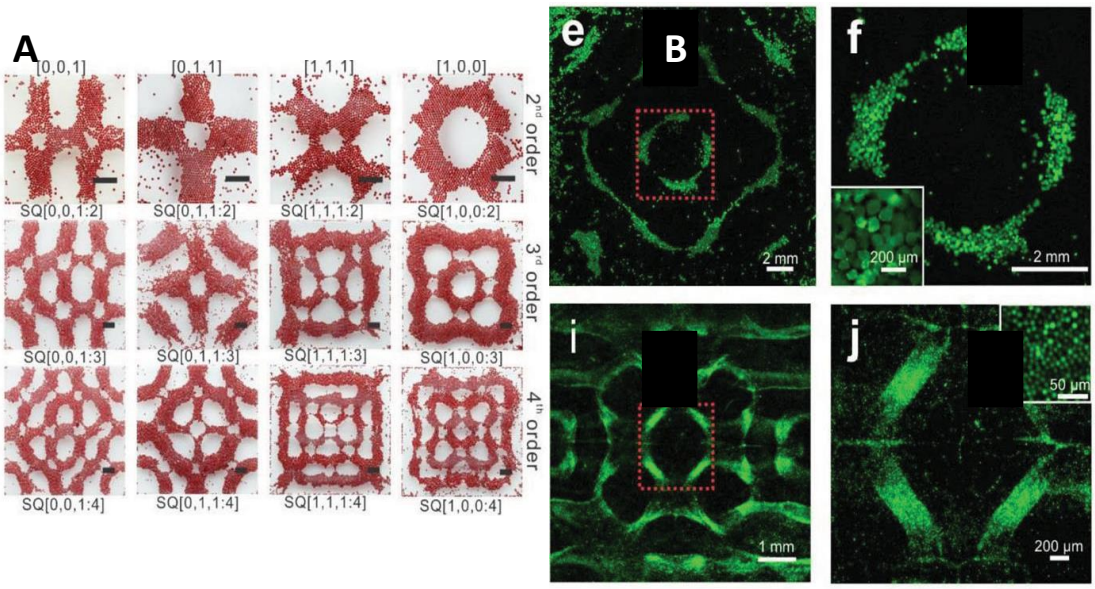

Figure 1.8: Building units assembly using acoustic waves. A) Diversity of structures created by liquid-based templated assembly. B) Liquid-based templated assembly for tissue engineering. Images adapted from Chen et al [26].

Acoustic fields have been used for in vivo imaging in medicine for quite some time, lately it has been applied in many other fields like particle

microcentrifugation, aggregation and trapping, cells manipulations like sorting and separation, and droplet concentration and mixing [26, 33, 135, 136].

Recently, acoustic field was applied for hydrogels assembly in bottom-up tissue engineering technology. This approach is based on the acoustic waves properties to organize cells or hydrogels of different size and weight on different layers of places. This approach shows high cell biocompatibility and versatile final structure manipulation as it shown in Figure 1.8 [26].

1.4.3 Robotic assembly

In the present world more and more fields are becoming mechanized, means industry is trying to use machines instead of humans work. This allows fabrication of many products in large-scale and in short time. Tissue engineering technology as well tries to mechanize the process of tissue/organ fabrication in many different ways. One of them is hydrogels self-assembly using micro-robots [36, 137].

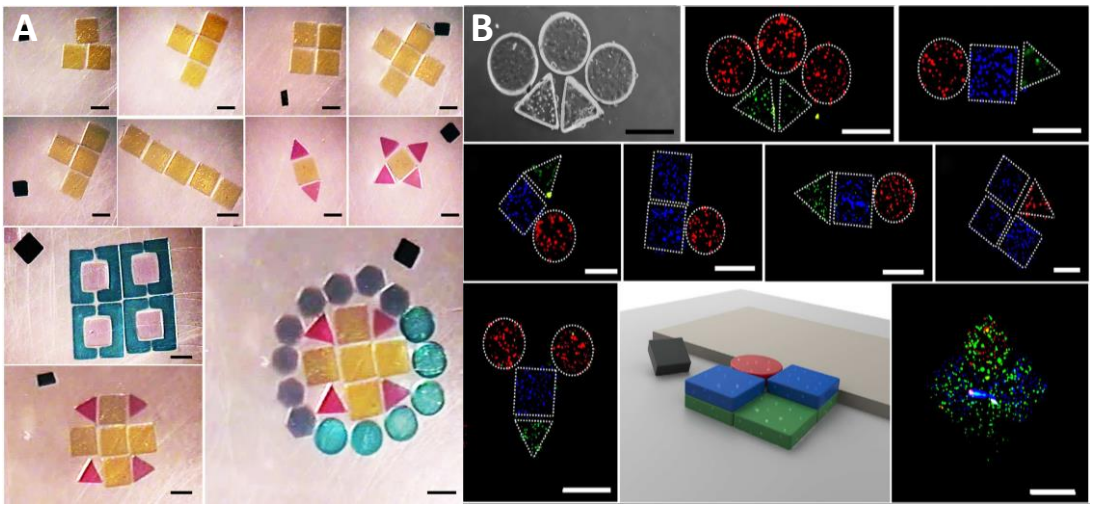

Figure 1.9: Micro-robotic assembly of versatile in shape and size hydrogels: A) Two-dimensional micro-robotic coding of material composition.

B) Spatially coded constructs for tissue culture. Images adapted from Tasoglu et al [36].

Magnetic levitation described in the above chapter is easy and cheap method for tissue assembly, however it has low precision over the assembly process. Microfluidics assembly, or multilayered crosslinking methods have a high precision over the assembly process, but just few of them might have a precision of ten microns in the hydrogels assembly, and definitely none of them can perform reassembly of the building blocks. Dr. Tasoglu and his team developed a versatile method to guide and manipulate assembly of building blocks into 2D and 3D complex functional structures using untethered magnetic micro-robots. The process of micro-robotic assembly presented in the Figure 1.9. This approach offers high precision over the 2D and 3D assembly, but also it allows application of a combination of soft and rigid materials together.

Chapter 2.

Research strategies and objectives

2.1 Thesis rationale

In the previous chapter there was introduced the concept of tissue engineering, its main approaches, advantages and open questions. After, there was presented a concept of organ printing with particular attention to its second step, cell encapsulation. There were described many methods for scaffolds or beads fabrication with focus on their complexity, proper cell type and material selection. At last, there was described in details a review on the cutting edge technology of building blocks assembly methods for complex 3D structures fabrication.

The final objective of the presented research work was detailed analysis of the organ printing strategies impact on cells viability, functionality and ability to maintain homeostasis in artificial conditions during the encapsulation process with following self-assembly into 3D complex structures (as the second step of organ printing), and during the tissue maturation period (as the third step of organ printing).

Cell encapsulation is the main method for the second step of organ printing, hence there were developed variety of different ways to produce cell-laden units. However, all of them are complex and multistep, thus might be harmul for cell behavior and functionality during the encapsulation process, but most importantly it might affect the cell behavior during the maturation process. Based on the possible cell functionality affectors such as heat, shear stress, chemicals and UV light exposure in the applied methods, we designed a protocol for detailed evaluation on the molecular level of the cells stress state, viability and functionality after encapsulation within short and long-terms [22].

Furthermore, different tissue engineering applications have set of crucial and unique requirements for fabricated structures that have to be met. Based on this knowledge, we evaluated the optimal maturation time referring to cells activity and functionality for variety of applications, such as organ printing, drug screening and 3D disease models. At last, we developed a simple contactless method for self-assembly of fabricated building blocks into 3D structures to mimic the tissue complexity, and evaluated its effect on cell behavior parameters.

In the presented research work, different techniques and materials were used to evaluate the most favorable and safe conditions for functional 3D living microtissues fabrication.

In the next section materials, structures and setups introduced and decribed.

2.1.1 Building units fabrication

2.1.1.1 Materials

To reach the main goal of the presented work there were used two natural polymers: alginate, gelatin methacrylate, and one synthetic polymer polyethylene glycol (PEG). For the levitational assembly part there were also used manufactured beads modified for cell application.

Alginate

One of the most commonly used materials for cell encapsulation is alginate, due to its easy ionic crosslinking, biocompatibility and mechanical, physical properties. Alginate is a polysaccharide that is extracted from the different types of seaweed, but also it produced by two types of bacteria, Pseudomonas and Azotobacter [52].

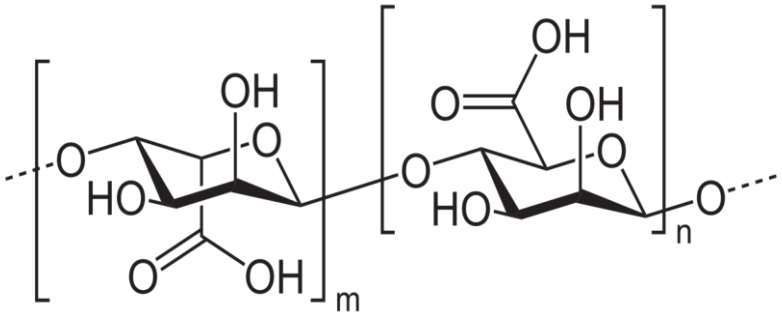

Figure 2.1 Sodium alginate structure. Image adapted from Lee at al [82].

Alginate composed 2 copolymeric blocks of (1,4)-linked β-D-mannuroic (M block) and α-L-guluronic (G block) acids as it showed in Figure 2.1 [52, 82]. The crosslinking process of sodium alginate happens upon the contact with multi-valent cations (Ca^{2+}), they bind adjacent sodium alginate chains forming ionic interchain bridges (Figure 1.4.3)

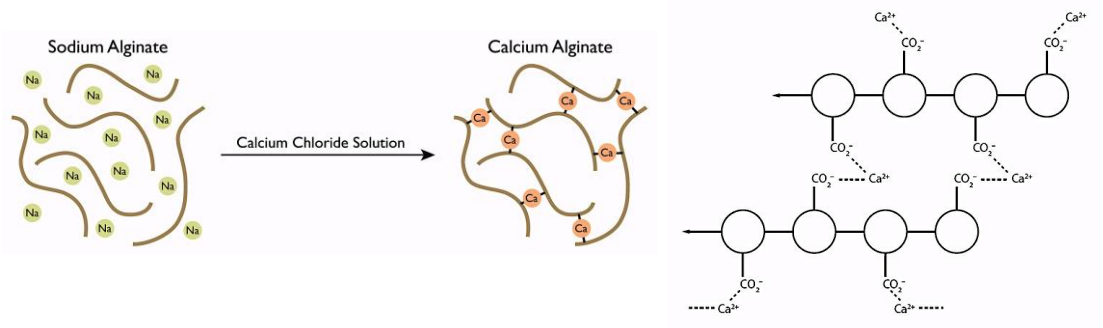

Figure 2.2: Sodium alginate sol-gel transition upon the contact with Ca^{2+} cations.

Alginate is lack of cell adhesion motifs, though a lot of research was done in tailoring alginate with RGD peptides sequence, which is crucial for cell adhesion and differentiation [102].

Alginate characterized as a material with a wide range distribution of pore size (5-200 nm), which depends on the initial sodium alginate percentage composition of M and G blocks. G blocks are responsible for bigger pore size as

well as for hydrogels rigidity and mechanical properties. But also, there was found a strong correlation between the alginate permeability and crosslinking ions; higher the concentration of cations, creates tighter alginate structure, especially on the outer part of hydrogel which is in direct contact with crosslinking solution.

The other very important characteristic of alginate, it's the ability to dissolve in vivo condition, as a result of bivalent ions exchange with monovalent ions from the body liquids. It will gradually dissolve calcium alginate, and transform it back to sodium alginate which is not degradable in vivo.

Alginate has become one of the most studied materials for cell encapsulation, and widely used. It was adjusted and modified for many different applications, such as immunoprotection of pancreatic islets, treatment of brain tumours, treatment of anemia and cryopreservation [52, 82, 102].

Gelatin methacrylate (GelMA)

The profound attention in photolithographical cell encapsulation received naturally-derived polymer gelatin, modified with methacrylate sites [103]. As it presented in Figure 2.3, gelatin was chemically modified with methacrylic anhydride, to obtain functional sites for photo crosslinking. Gelatin methacrylate (GelMA) is a photopolymerizable hydrogel comprised of modified natural ECM components, what makes it biocompatible and promising material for tissue engineering application.

Gelatin is inexpensive, denaturated collagen that can be derived from a variety of sources, it contains natural cell binding sites, such as RGD, and at the same time rich in MMP-sensitive degradation sites [103]. Chemical modification with methacrylic anhydride makes GelMA light polymerizable into a stable at 37°C hydrogel.

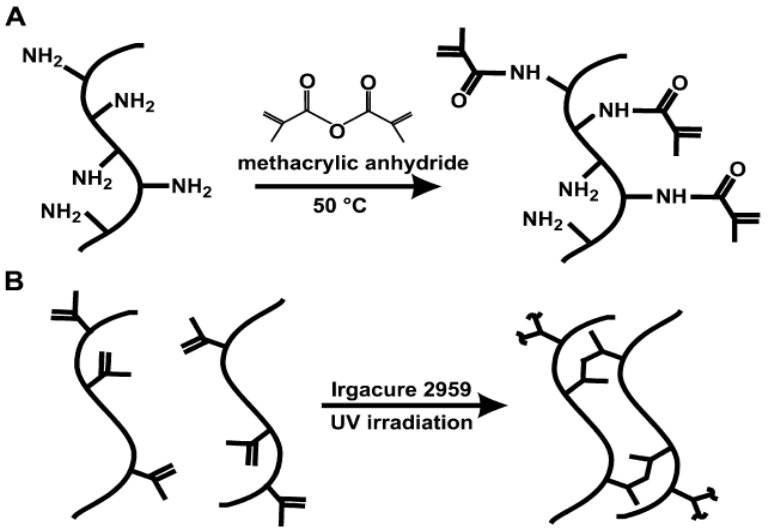

Figure 2.3: Synthesis of methacrylated gelatin. Gelatin macromers containing primary amine groups were reacted with methacrylic anhydride (MA) to add methacrylate pendant groups (A). To create a hydrogel network, the methacrylated gelatin was crosslinked using UV irradiation in the presence of a photoinitiator (B). Images adapted from Nichol et al [103].

Polyethylene glycol (PEG)

Polyethylene glycol s a polyether compound with many applications from industrial manufacturing to medicine. The structure of PEG is (note the repeated element in parentheses): $H\text{-}(O\text{-}CH_2\text{-}CH_2)_n\text{-}OH$.

PEG hydrogels are non-toxic, non-immunogenic and number one used FDA approved for biomedical application. PEG hydrogels can be covalently crosslinked through covalent bonding using variety of methods. Photo initiated crosslinking using acrylate-terminated PEG monomers is the most applicable method for PEG hydrogels formation. Cell-laden PEG hydrogels are inert, since they are prevent protein adsorption. Because of easy manipulation and

inertness properties, PEG polymers were modified in different ways for cell application to improve adhesion and proliferation, for example peptide sequence was incorporated into PEG structure to induce degradation, and cell adhesion [34, 43, 91, 92].

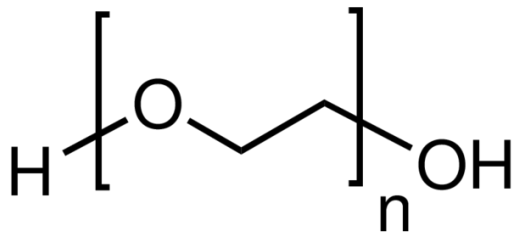

Figure 2.4: Polyethylene glycol structure.

2.1.1.2 Cell encapsulation methods

Electrohydrodynamic jetting

A custom-designed electrically insulated holder was placed under a biological hood. Sterile 3 mL syringe was filled with cells suspended in the alginate solution, connected to a polytetrafluoroethylene tube and placed on the pump set to a fixed flux of 0.05 mL/min. The other side of the tube was connected to a stainless steel needle and placed in the holder under the hood. The positive cathode of a generator (ES30, Gamma High Voltage Research Inc, USA) was connected to the needle while the anode was connected to a metallic plate placed under a Petri dish containing the sterile calcium chloride solution and placed below the needle at a distance of 5 cm. Once the flux of solution was established and the generator was switched on (V=8kV), droplets of alginate solution containing cells were ejected from the needle directly to $CaCl_2$ solution. After 10 minutes the beads were washed three times with full cell culture media and redistributed in 6-well tissue culture plates to perform the experiment [60].

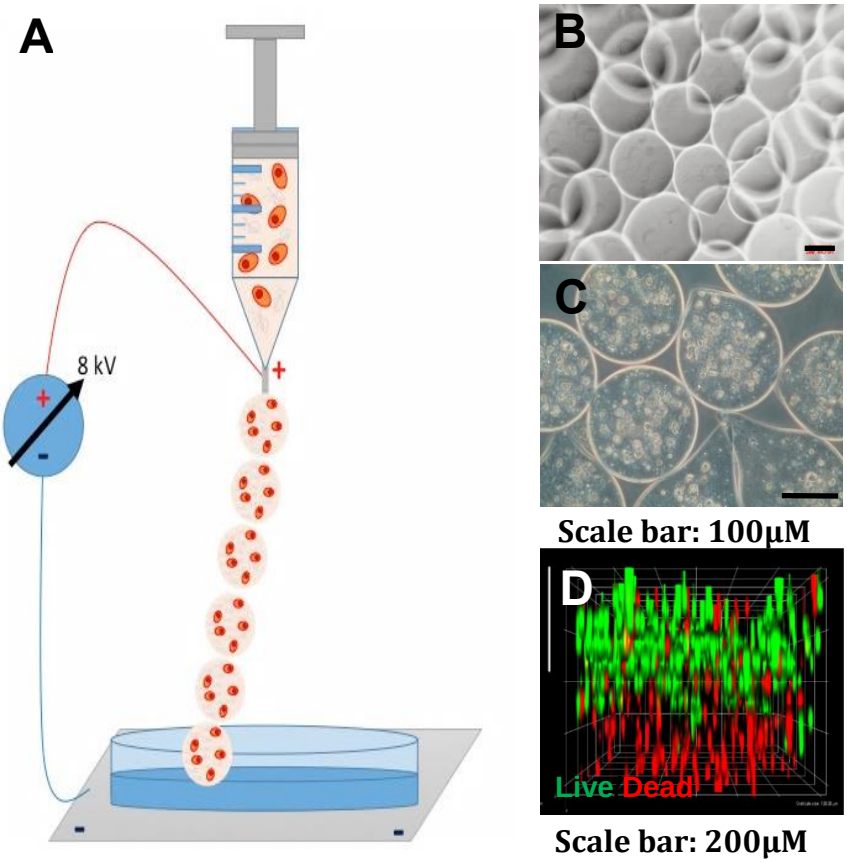

Figure 2.5: Electrohydrodynamic jetting encapsulation system. A. Encapsulation scheme; B. Beads view without cells; C. Beads with cells; D. Live/Dead analysis of cells encapsulated in the beads.

Photolithographic crosslinking system

Photolithography is another widely applied method for cell encapsulation and based on placing a photo-mask on top of the photocrosslinking material mixed with cells [34, 41, 42, 43, 68, 90, 104, 105, 106]. Photo mask can be designed to produce a hydrogels in variety of sizes and shapes. But also, the hydrogels can be produced with different cell types by mimicking tissue/organ complexity. This strategy is widely used for 3D model

fabrication for diseases investigation or general science.

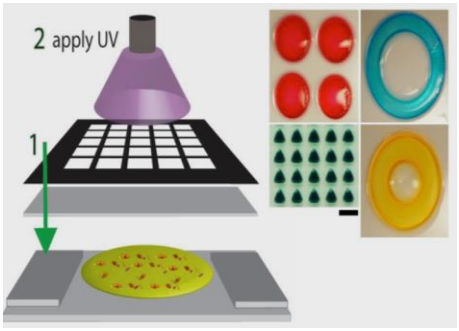

Hydrogel Fabrication Process

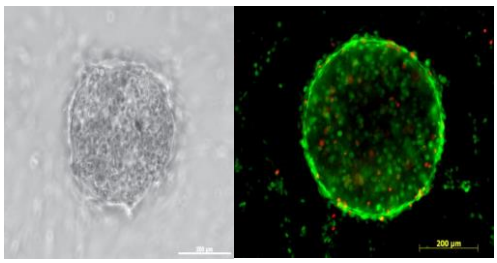

Scale bar 200 μm

Encapsulated Fibroblasts

Figure 2.6: Photolithographic encapsulation system [34]. Photolithographic encapsulation system. A. Encapsulation scheme; B. Hydrogel view with encapsulated cells; C. Live/Dead analysis of cells encapsulated in the hydrogel.

There are several important requirements for fabrication of patterned biocompatible cell-laden hydrogels by photolithography [42]. First requirement is proper photocurable material amenable to polymerization caused by photosensitive free radicals. Another important requirement is photoinitiator (PI), that must not only initiate the reaction, but also eliminate the reaction as soon as UV light exposure is stopped, but most importantly for tissue engineering application, it has to have low cytotoxicity. A separate attention must be paid for combination of factors like UV time exposure during photopolymerization, and PI concentration, both these factors can affect cell viability. At last, a photomask is important as well, it has to be made in the way to protect unwanted areas from UV light, and those that exposed, has to be permeable for UV rays and initiate the crosslinking.

2.1.1.3 Magnetic levitational assembly

Magnetic levitation is contactless and nanoparticle-free approach for tissue self-assembly [24, 34, 133, 134]. This method is based on the idea of levitating subjects in paramagnetic suspension. Salt ions of gadolinium (Gd^{3+}) and magnesium (Mn^{2+}) or radicals have paramagnetic properties. Cells were encapsulated in photo-crosslinkable polymers of gelatin (GelMA) and polyethylene glycol diethacrylate (PEGDA) and levitated in the media suspension with ions of Gd^{3+} salt. This approach shows high scaling potential, good cell viability and functionality, but also easy to manipulate and guide the hydrogels assembly makes it very promising for bottom-up tissue engineering.

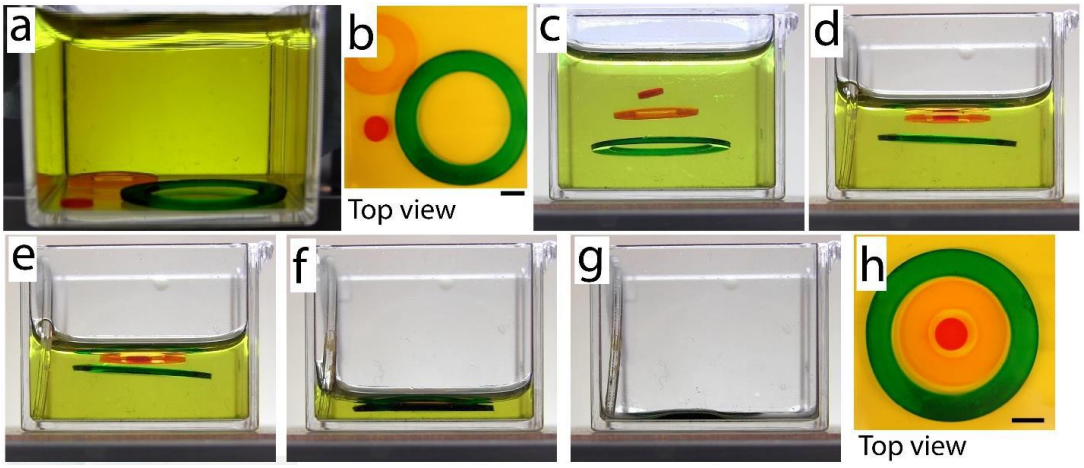

Figure 2.7: Paramagnetic levitational assembly of PEGDA hydrogels. A-H) Concentric assembly of two hollow-disks and a solid-disk PEG gel. Images adapted from Tasoglu et al [34].

2.1.2 Cells

In this work two main cell lines were used: m3T3 and hSHSY5Y.

2.1.2.1 NIH3T3

NIH 3T3 mouse embryonic fibroblast cells come from a cell line isolated and initiated in 1962 at the New York University School of Medicine Department of Pathology. 3T3 refers to the cell transfer and inoculation protocol for the line, and means “3-day transfer, inoculum 3 x 10^5 cells.” Using this protocol, the immortal cell line begins to thrive and stabilize in cell culture after about 20-30 generations of in vitro growth. The cell line has since become a standard fibroblast cell line and one the most commonly used cell models for tissue engineering methods testing.

2.1.2.2 SHSY5Y

SH-SY5Y is a human derived cell line used in scientific research. The original cell line, called SK-N-SH, from which it was subcloned was isolated from a bone marrow biopsy taken from a four year-old female with neuroblastoma. SH-SY5Y cells are often used as *in vitro* models of neuronal function and differentiation. The cells typically grow in tissue culture in two distinct ways. Some grow into clumps of cells which float in the media, while others form clumps which stick to the dish. SH-SY5Y cells can spontaneously interconvert between two phenotypes in vitro although the mechanisms underlying this process are not understood. SH-SY5Y has a dopamine-β-hydroxylase activity and can convert glutamate to GABA. It will also form tumors in nude mice in around 3–4 weeks. The loss of neuronal characteristics has been described with increasing passage numbers. Therefore it is recommended not to be used after passage 20 or verify specific characteristics such as noradrenalin uptake or neuronal tumor markers.

2.2 Outline and objectives

Organ printing as promising direction of tissue engineering tends to fabricate precisely designed with controlled shape and composition 3D tissue, which after a short maturation process would be capable of performing its main function and be ready for implantation. To reach this goal the process of tissue fabrication has to be evaluated in detailes from different aspects, fabrication methods, materials selection, at last, cells viability and functionality.

In general all tissue/organ fabrication methods are multistep and complex, thus they might affect cells viability and functionality during the fabrication process. There were developed and studied variety of methods for tissue fabrication, with detailed and precise research in materials or methods, but not that much attention was paid to cell molecular mechanisms stability after encapsulation process, and culturing in artificial 3D environment.

Thus, the overall objective of the presented work was evaluation of the effect of organ fabrication methods on cell parameters, such as viability, activity, proliferation and ability to maintain homeostasis in artificial 3D environment.

The main objective was reached with following aims.

Chapter 3 – AIM1

To evaluate the effect of EHDJ encapsulation system on cells behavior.

Cells were encapsulated in alginate beads by EHDJ method and cultured up to 4 weeks to evaluate the short- and long-terms effect on cell parameters. At defined time points cells encapsulated in the beads were analyzed on their main characteristics. It was shown, that cells are mildly stressed first week after encapsulation, however towards the 4^{th} week of culturing in the beads, cells completely recover of stess, moreover they start to proliferate and adapt the alginate bead environment to their own microenvironment, beneficial for their growth and functionality.

Chapter 4 – AIM 2

To evaluate the most favorable encapsulation time for variety of applications.

Cells were encapsulated in alginate microbeads by EHDJ method and cultured up to 4 weeks, at the established time points, cells were released from the beads and reseeded in tissue culture plates for following experiments. This work is targeted for the last step of organ fabrication, maturation. At this stage, cells have to replace the material used for fabrication and be able to produce ECM and maintain 3D structure without an artificial matrix. Results showed that most suitable for tissue maturation is to keep cells in the beads for 21-28 days to achieve the highest rate of their functionality in organ printing application. For drug screening application though, it was suggested to use cells that were encapsulated for 7-21 days.

Chapter 5 - AIM 3

Fabrication of building units with photolithographic encapsulation system, evaluation of cells parameters, and following assembly of fabricated building blocks into 3D complex structures.

For this part, cells were encapsulated in GelMA/PEG hydrogels or seeded on top of the beads and analysed for viability and activity. Building blocks were assembled by magnetical levitation into 3D structures in a contactless manner with high efficiency in short time. Presented results show an easy and fast method for fabrication of controlled multishape building blocks and their efficient assembly into more complex structures.

Chapter 3

Assessing the impact of electro hydro-dynamic jetting on encapsulated cells viability, proliferation and ability to self-assemble in 3D structures.

The main part of the presented in this chapter work was published in Tissue Engineering: Part C journal.

Liaudanskaya V., Gasperini L., Maniglio D., Motta A., Migliaresi C. Assessing the impact of electro hydro-dynamic jetting on encapsulated cells viability, proliferation and ability to self-assemble in 3D structures. Tissue Engineering: Part C (2014).

3.1 Abstract

In this chapter, systemic approach is propose to investigate the impact of electrohydrodynamic jetting (EHDJ) encapsulation on viability, proliferation, and functionality of the encapsulated cells. EHDJ consists in applying a high-voltage electrical field between a target substrate and a jetting needle, which is fed with a suspension of cells in a polymeric solution undergoing a sol-gel transition upon contact with the target. The viability, proliferation, and self-assembling ability of SHSY5Y human neuroblastoma cell line encapsulated in 2% alginate microbeads were analyzed by confocal microscopy and DNA quantification assays. In addition, the expression of stress (*HSP70B'*), apoptotic (*CASP3*), necrotic (*HMGB1*), hypoxic (*HYOU1*, *GAPDH*), adhesion (*NCDH*) and extracellular matrix (*COL1A1*) markers was measured with RT-qPCR. After an

initial upregulation of the *HSP70B*' expression within 24 h, its expression decreased to the negative control level together with a decrease in the expression of *CASP3*. Any increase in necrotic or hypoxic marker expression was not detected, while a slight upregulation of *NCDH* was observed in the first days after encapsulation, followed by its downregulation and stabilization to the control level. Furthermore, cell-laden beads started to self-assemble in three-dimensional (3D) constructs from the 3rd week after encapsulation. The results indicated that the EHDJ encapsulation method had a mild effect on cells, which after a week, fully recovered their proliferation rate and ability to self-assemble into 3D constructs.

3.2 Introduction

Cell encapsulation methods consist in the entrapment of cells in microcapsules or microbeads starting from a suspension of cells in polymeric solution that can be solidified by chemical or physical methods [64]. The technology has already found several applications, such as for the long-term encapsulation of insulin-producing cells for the diabetes treatment [82], chondrocytes phenotype retention [138], stem cells research [32]. Recently, cell encapsulation has been investigated for neural regeneration and for the treatment of the central nervous system malignancies [139, 140].

In regenerative medicine, cell encapsulation has received attention for the reconstruction of tissues or organs, following an early work of Mironov [29] who introduced the concept of organ printing. The procedure consists in the layer-by-layer deposition of encapsulated cells that are assembled in 3D structures [37, 38] to reproduce the organ/tissue architecture. 3D cell-laden structures may also be a suitable model for the fundamental science, drugs screening, as well as platform for diseases diagnostics [29, 37, 38, 39, 40].

Many methods have been proposed for cell encapsulation, such as microfluidics, emulsion, stereo/photolitography and extrusion [64]. These methods require a fine tuning of several parameters and an accurate selection of the encapsulating materials to keep cells alive, active, and capable of carrying out their main functions, such as the ability to self-assemble [44] or to produce biomolecules [141]. In the previous years, cell encapsulation has been proposed for applications in different fields, like bioprinting or skeletal tissue engineering. Agarose, gelatin, chitosan, collagen, polyethylene glycol, hyaluronic acid, alginate and other materials have been considered for the encapsulation of cells [31, 83-84].

Viability/activity of encapsulated cells has been already investigated [64, 85, 142, 143]. Examples are the evaluation of the heat shock protein 60/70

expression in bovine aortic endothelial cells (BAEC) printed by laser pulses [64]; the analysis of gene expression on some house-keeping, non- and blood-specific genes in bio-electrospraying assay of whole human blood [143]; the determination of the immune response on the presence of allogeneic/xenogeneic hepatoma cells encapsulated in the beads and transplanted in rats [85].

One still open issue is whether encapsulated cells keep their original functionality, gene expression profile and ability to self-organize in tissues/organs.

In this study cells were encapsulated in alginate by electrohydrodynamic jetting (EHDJ) technology [64, 141, 144].

Alginate is a natural polymer derived from the cell wall of brown algae, that quick crosslinkings upon contact with calcium containing solutions and can dissolve *in vivo* due to the calcium substitution [82, 83]. Behavioral parameters of SHSY5Y neuroblastoma cell line, selected as a model, encapsulated by EHDJ in alginate microbeads were assessed in the short-term from 3 hours up to 7 days, and in the long-term up to 4 weeks. Cell viability, activity and proliferation, as well as ability of cells to self-assemble, and gene expression of stress state-related markers (*CASP3, HMGB1, HYOU1* and *HSP70B'*) were evaluated in this study. Up-regulation of *CASP3* (caspase-3) gene–late apoptosis executor, indicates the induction of apoptosis in cells [145, 146, 147, 148]; *HMGB1* (high mobility group box protein 1) is a marker that is specifically produced in necrotic conditions [145, 149, 150, 151, 152, 153]; *HYOU1* (HYpOxia-Up-regulated 1) is a hypoxia inducible gene [154, 155, 156, 157], and the house-keeping gene *GAPDH* (GlycerAldehyde-3- Phosphate DeHydrogenase) is also overexpressed in hypoxic conditions [158, 159, 160]. *HSP70B'* (Heat Shock Protein 70B') is specifically produced by cells in stress conditions [161, 162, 163]. Cell adhesion, motion and communication were evaluated by *CDH2* (N-CaDHerin) expression [164, 165, 166, 167]. Finally, the ability to produce

extacellular matrix was analysed with *COL1A1* (COLlagen 1A1) expression [168, 169, 170]. The expression of all above genes in the samples were compared to the negative control (cells grown in tissue culture plate (TCP) till 85-90% confluence) and to the positive control (with induced hypoxia, apoptosis, necrosis and heat shock) [171, 172, 173, 174]. Gene expression level was normalized to the house-keeping control gene *RPS18* (40S ribosomal protein S18) expression [175].

This paper, therefore, presents a systemic investigation of the influence of electrohydrodynamic jetting (EHDJ) encapsulation on cells, with reference to the duration of encapsulation and cell viability, their ability to self-assemble, proliferate, and the expression of stress-related and some other vitally important genes.

3.3 Materials and methods

Materials

Alginic acid sodium salt from brown algae (alginate) and calcium chloride dehydrate were purchased from Sigma-Aldrich (USA). Calcein-AM, Propidium Iodide (PI), Phosphate buffer saline without calcium and magnesium (PBS), Dulbecco's modified eagle medium (DMEM) were purchased from Invitrogen (USA). The encapsulation system consists of a generator (ES30, Gamma High Voltage Research Inc., USA), a pump (NE-300, New Era Pump Systems, USA), a polyetrafluorethylene tube and a gauge 33 stainless steal needle (outer diameter: 0.210 mm, inner diameter: 0.108 mm Hamilton, Bonaduz/Switzerland). SHSY5Y human neuroblastoma cell line (ATCC® CRL-2266™, UK), Sonicator (UP400S Heilscher, Germany), Quant-iT PicoGreen dsDNA Assay Kit (Invitrogen, catalog number: P11496), 0.05% Triton-X 100 in PBS, RNeasy Plus Mini Kit (QIAGEN, catalog number: 74134) have been used.

Encapsulation process

Hydrogel preparation and sterilization.

Alginate powder was dissolved in PBS for 8 hours at room temperature under mild stirring to obtain an alginate solution at the desired concentration (2%, 2g/100 ml). Under a biological sterile hood, a syringe filled with solution was connected to a pump to be filtered overnight through a 0.22 μm filter. The sterile solution was immediately used after filtration. The crosslinking solution consisted of calcium chloride dehydrate dissolved in distilled water at a concentration of 400 mM, filtered through a 0.22 μm filter under sterile conditions.

Cell culture.

SHSY5Y human neuroblastoma cell line was expanded in 25-175mm tissue-treated culture flasks as monolayer (passages 12-16) at 37°C under 5% of CO_2 in high glucose Dulbecco's Modified Eagle Medium (DMEM) with 10% fetal bovine serum (GIBCO), 2mM Glutamine and 1% penicillin-streptomycin mixture (Sigma, USA). DMEM medium was changed every third day. The cells were cultured to 90-95% confluence before encapsulation [176].

Preparation of the alginate suspension with cells.

At 90-95% confluence cells were detached and moved to a 15 ml vial. Cells inside the vial were stirred at 1000 rounds/min for 10 minutes and the surnatant was removed. Cells on the bottom of the vial were resuspended in PBS and stirred again to remove any residues of medium containing cations that could crosslink the alginate solution. Cells were dispersed by vibration inside the buffer and an aliquot of the solution was taken to count the number of cells using a Cellometer Auto T4 (Nexcelom, USA) and Trypan Blue 0,4% (Life technologies, USA) as contrast agent. Cells were stirred again, and after removing the surnatant the alginate solution was added to obtain an alginate suspension containing 5 millions cells for milliliter. Medium, PBS, Trypsin/EDTA and the alginate suspension used were warmed to 37°C.

Cell encapsulation by electrohydrodynamic jet method.

Cell encapsulation was performed by following a protocol already published [60]. In brief, the encapsulation system was placed under the biological hood, a sterile 3 ml syringe was filled with cells suspended in the alginate solution, connected to the polytetrafluoroethylene tube and placed onto the pump. The pump was set at the fixed flux of 0.05 ml/min. The other side of the tube was connected to the stainless steel needle. The electrical potential was established by connecting the positive cathode of the generator to the needle,

and the anode to the metallic plate under the Petri dish. The Petri dish containing sterile calcium chloride solution was placed below the needle at a distance of 5 cm. Once the flux of solution was established and the generator was switched on (V=8kV), droplets of alginate solution containing cells were ejected from the needle directly to $CaCl_2$ solution. After 10 minutes the beads were washed three times with DMEM and redistributed in 6-well tissue culture plates to perform the experiment.

Cell release.

To perform part of *in vitro* evaluations accordingly to the time points of the experiment, cells were first released from the beads. The hydrogel was dissolved by removing the DMEM media containing Ca^{2+} cations with a short wash in PBS at room temperature, followed by a 15 minutes incubation in PBS at 37°C to favor the ion exchange with the surrounding buffer. After that, the samples were centrifuged and cells were collected for the experiment.

In vitro evaluation

Cell viability.

Cell viability was estimated by fluorescence visualization (confocal microscopy) of samples stained with calcein/propidium iodide. Samples were observed 3 hours, 1, 3, 7, 14, 21 and 28 days after encapsulation following standard protocols. In brief, samples were incubated for 20 min at 37°C in a solution of calcein (1 µl of stock solution for 1 ml of DMEM). After that the supernatant was removed, the beads were washed with a $CaCl_2$ solution and collected from the bottom of the vial after centrifugation (500 rpm for 1 min). The procedure was repeated again at room temperature for 5 min with a solution of propidium iodide (100 µl for 1 ml of $CaCl_2$). To validate the results a positive control was prepared by inducing the cell death with a 5% H_2O_2 treatment overnight.

Cell proliferation.

DNA extraction was performed by placing the cells extracted from the beads in a solution of 0.05% Triton-X in PBS, followed by sonication for 10" (cycle: 1, amplitude 40%). After that, DNA was extracted and PicoGreen was used for the quantification. Fluorescence intensity of PicoGreen – DNA complex was measured in 96-well plates on a plate reader (485 nm excitation and 538 nm emission; Safire, Tecan, Austria). A calibration curve was built up using the DNA standard provided with the assay to correlate fluorescence intensity to the concentration of DNA.

Gene expression.

Gene expression analysis was performed using quantitative reverse transcription polymerase chain reaction (RT-qPCR). Cells were released from the beads and total mRNA extraction (3 replicates for each group) was performed according to the protocol for the QIAGEN mRNA extraction kit. mRNA was resuspended in a final volume of 30 µl with RNAse-free water and its yield was quantified by standard spectrophotometry. Reverse transcription using 1 µg of total RNA was performed with SuperScript III Reverse Transcriptase (Invitrogen, UK) and oligo-dT primers, according to the manufacturer's protocol, in a 20 µl volume. Transcribed cDNA was diluted 1 to 20 times till a final volume of 100 µl in RNA-free water was obtained. Primers were selected from online primers bank PrimerBank [177]. *GAPDH* primers were designed (Table 3.1). Reactions were set up in 10 µl volumes, which included 2 µl cDNA, 0.2 µl of each primer, 5 µl of KAPA and 2,6 µl of RNA-free water. Amplification and detection was carried out using a CFX96 Touch™ Real-time PCR machine (BioRad, UK), using the default universal cycling conditions recommended by the manufacturer. Measurements were performed in triplicate for statistical analysis.

RPS 18_f	5'-ATCACCATTATGCAGAATCCACG-3'
RPS 18_r	5'-GACCTGGCTGTATTTTCCATCC-3'
GAPDH_f	5'-TCGGAGTGAACGGATTTC-3'
GAPDH_r	5'-GCCAGAGTTAAAAGCAGCCCT-3'
CASP3_f	5'-GAAATTGTGGAATTGATGCGTGA-3'
CASP3_r	5'-CTACAACGATCCCCTCTGAAAAA-3'
HMGB1_f	5'-TATGGCAAAAGCGGACAAGG-3'
HMGB1_r	5'-CTTCGCAACATCACCAATGGA-3'
HYOU1_f	5'-GAGGAGGCGAGTCTGTTGG-3'
HYOU1_r	5'-GCACTCCAGGTTTGACAATGG-3'
HSP70B'_f	5'-GATGTGTCGGTTCTCTCCATTG-3'
HSP70B'_r	5'-CTTCCATGAAGTGGTTCACGA-3'
NCDH_f	5'-AGCCAACCTTAACTGAGGAGT-3'
NCDH_r	5'-GGCAAGTTGATTGGAGGGATG-3'
COL1A1_f	5'-CCACCAATCACCTGCGTACAGAA-3'
COL1A1_r	5'-GGGCAGTTCTTGGTCTCGTCAC-3'

Table 3.1: Primers sequence for RT-qPCR [177].

Statistical analysis

All statistical analysis was performed with GraphPad Prism 6 software. Statistical analysis for more than two groups was carried out using one-way ANOVA with Tukey's post-hoc tests. $P<0.05$ was considered significantly different. Gene expression of SHSY5Y line in tissue culture plate (at passage 16)

was set up as a control, and equal to 1. For gene expression analysis the ddC_T approach was applied [166]. Targeted gene expression was calculated by the fold change related to the control group.

3.4 Results

The study was performed up to 4 weeks at different time points: 3 hours, 1, 3, 5, 7, 14, 21 and 28 days. During that time cells self-assembly, viability, proliferation and gene expression were investigated.

Cell encapsulation

The parameters for the encapsulation process and beads characteristics were already investigated and published [60]. Beads with diameter of about 200 μm, were made using 2% alginate with 8kV and a G33 stainless steel needle (I.D.:0.108 mm) (Figure 3.1A).

Cells self-assembling and migration

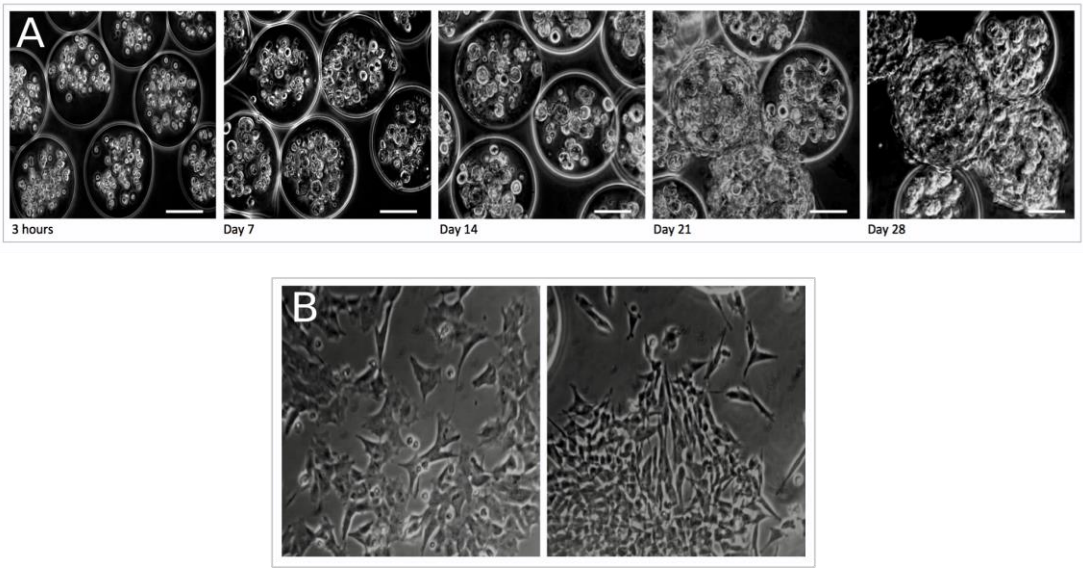

Figure 3.1: Beads with diameter consistently stable, about 200 μm were made using 2% alginate ejected under 8kV from G33 stainless steel needle (I.D.: 0.108 mm) to $CaCl_2$ solution for crosslinking. (A) Optical microscope images represent cell behavior inside the beads at different time points: 3 hours, 7, 14, 21 and 28 days after encapsulation. Scale bar is 100μm. (B) Phenotypic transition in cells encapsulated in the beads and migrated outside.

Cell the morphology, organization and distribution of cells inside the beads starting from 3 hours after encapsulation up to 4 weeks presented in the Figure 3.1A (Zeiss optical microscope). In the first week cells were small, round-shaped and homogeneously distributed at the center of beads without visual changes up to the 7th day. Toward the 14th day, cells started to proliferate and move to the border of the beads. After 2 weeks cells partially moved outside the beads, adhering to their surface as well as to the tissue culture plate. Toward the 28th day after encapsulation, most of the beads were gathered in groups and overpopulated by cells. The beads were distorted and partially degraded in many cases. Cells that were migrated and attached the TCP surface, made clusters with fibroblast-like phenotype from the center to outside (Figure 3.1B).

Cell viability

Calcein/propidium iodide staining and following fluorescence visualization (Confocal microscopy) were used for the cell viability evaluation. Images showed homogeneous distribution of the cells encapsulated in the beads. Absence of dead cells was observed 3 hours after encapsulation, and few 1-3 days after (Figure 3.2A). Some dead cells were observed at days 5 and 7. During the following 2 weeks few beads with only dead cells were observed, but in general there were few dead cells in the beads. At the end, at 28th day no dead cells were detected. Results were compared with to the positive control samples (necrotic cells).

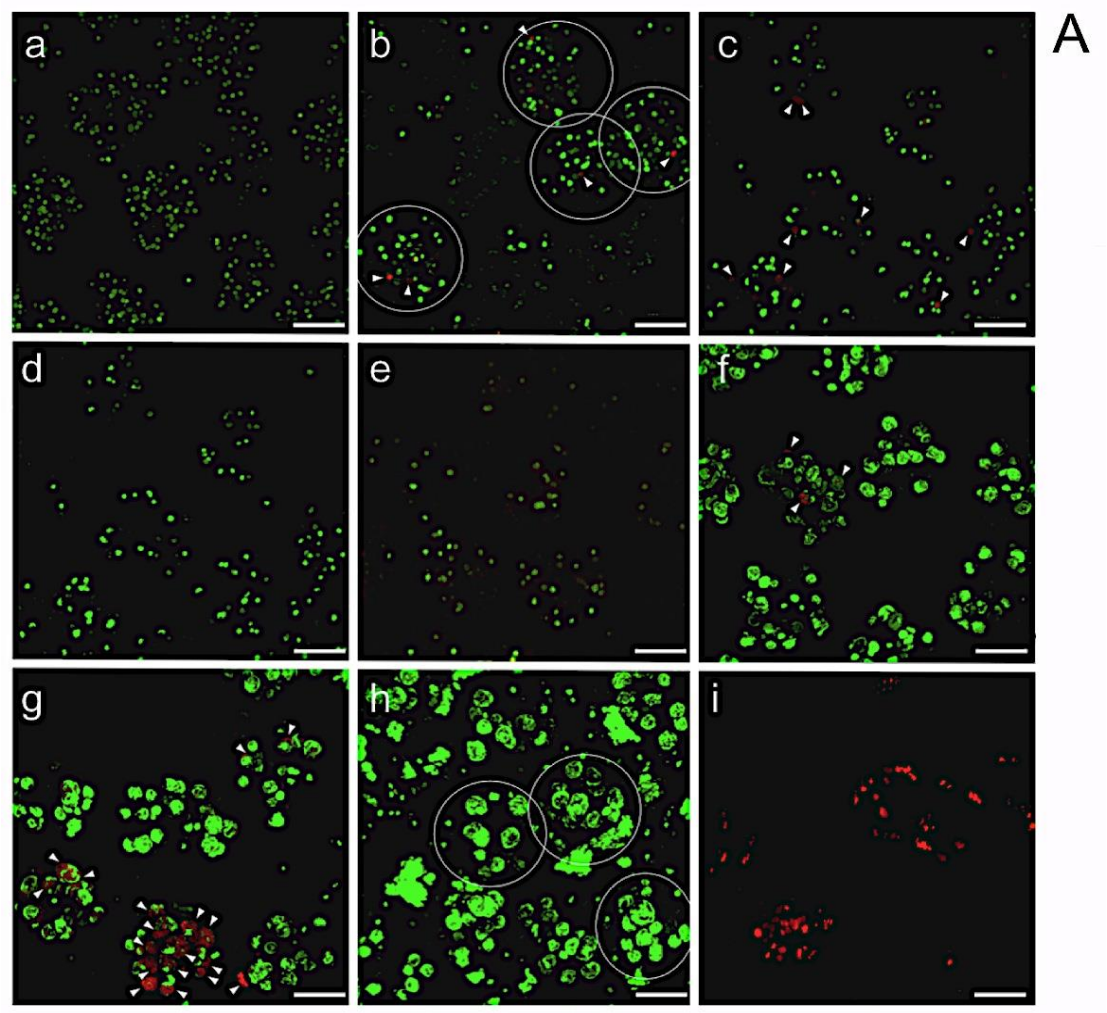

Figure 3.2: (A) Live/Dead analysis with confocal microscopy of SHSY5Y cells encapsulated by EHDJ method in 200 µm 2% alginate beads: a) 3 hours; b) 1; c) 3; d)5; e) 7; f) 14; g) 21; h) 28 days; i) positive control (necrosis induced with 4% H2O2 overnight). Scale bar is 100µm.

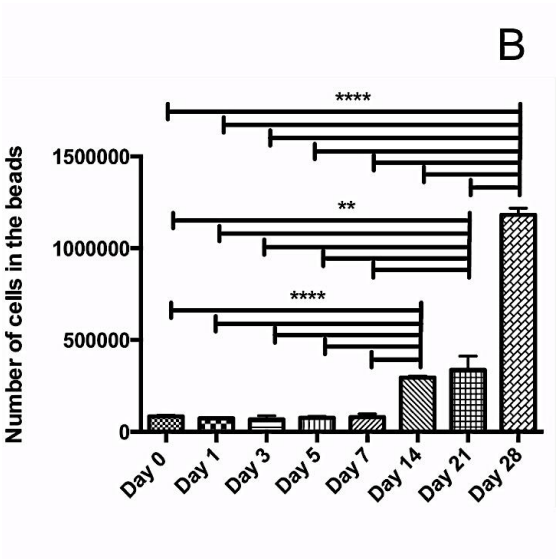

(B) Cell proliferation in the beads analyzed with DNA quantification assay within 4 weeks of encapsulation. Circles represent the beads border. Dead cells are evidenced by arrows except than in i). Error bars represent Mean±SD (n=3). **p<0.01, ****p<0.0001.

Cell proliferation

Cell viability test results were confirmed with followed DNA quantification assay. 10% decrease in cell number was detected 24 hours after encapsulation (however not statistically significant), and no variations in cell number up to the 7th day (Figure 3.2B). After the first week cells number started to increase and tripled from the 3rd to the 4th week of encapsulation.

Stress markers expression within the alginate beads

The results of RT-qPCR have been summarized in Figure 3.3.

The expression of the targeted genes was compared to cells grown in tissue culture plate till 85-90% confluence (culture negative control), and as positive control, cells with induced hypoxia, apoptosis, necrosis and heat shock were used [171, 172, 173, 174]. One week after encapsulation 20 to 80 times increase in *HSP70B*' expression was detected, with the highest level after three hours (no statistical differences from the positive control) (Figure 3.3A).

However, afterward, a stable decrease in *HSP70B'* expression was observed with complete normalization to the negative control level at day 21 after encapsulation. Along with *HSP70B'* overexpression, a two fold increase of *caspase-3* gene (no difference with the positive control sample) was detected in the first days after encapsulation, followed by stabilization to the negative control level during the next time points, with slight increase again at day 14. Necrotic marker *HMGB1* expression was detected on the negative control level, without statistically different variations during the experimental time points, except at day 14 when it was slightly up-regulated and at day 5 when it was down-regulated. Both hypoxic markers *HYOU1* and *GAPDH* expression wasn't elevated during the whole encapsulation time. However, *HYOU1* expression during the first 3 weeks was significantly below the negative control level, whereas the *GAPDH* expression was comparable to the negative control samples. In the first 24 hours double up-regulation of *N-cadherin* expression was detected, followed by a significant down-regulation at the next time points, stabilization to the control level at days 14 and 21 and by down-regulation again at day 28.

Eventually, *collagen1A1* expression was decreasing within 3 days of encapsulation, and after the significant increase in the expression was observed up to the 14th day, followed by down-regulation till the last experimental time point (Figure 3.3E).

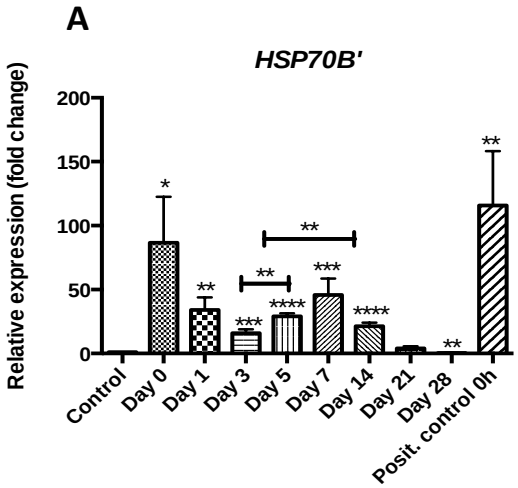

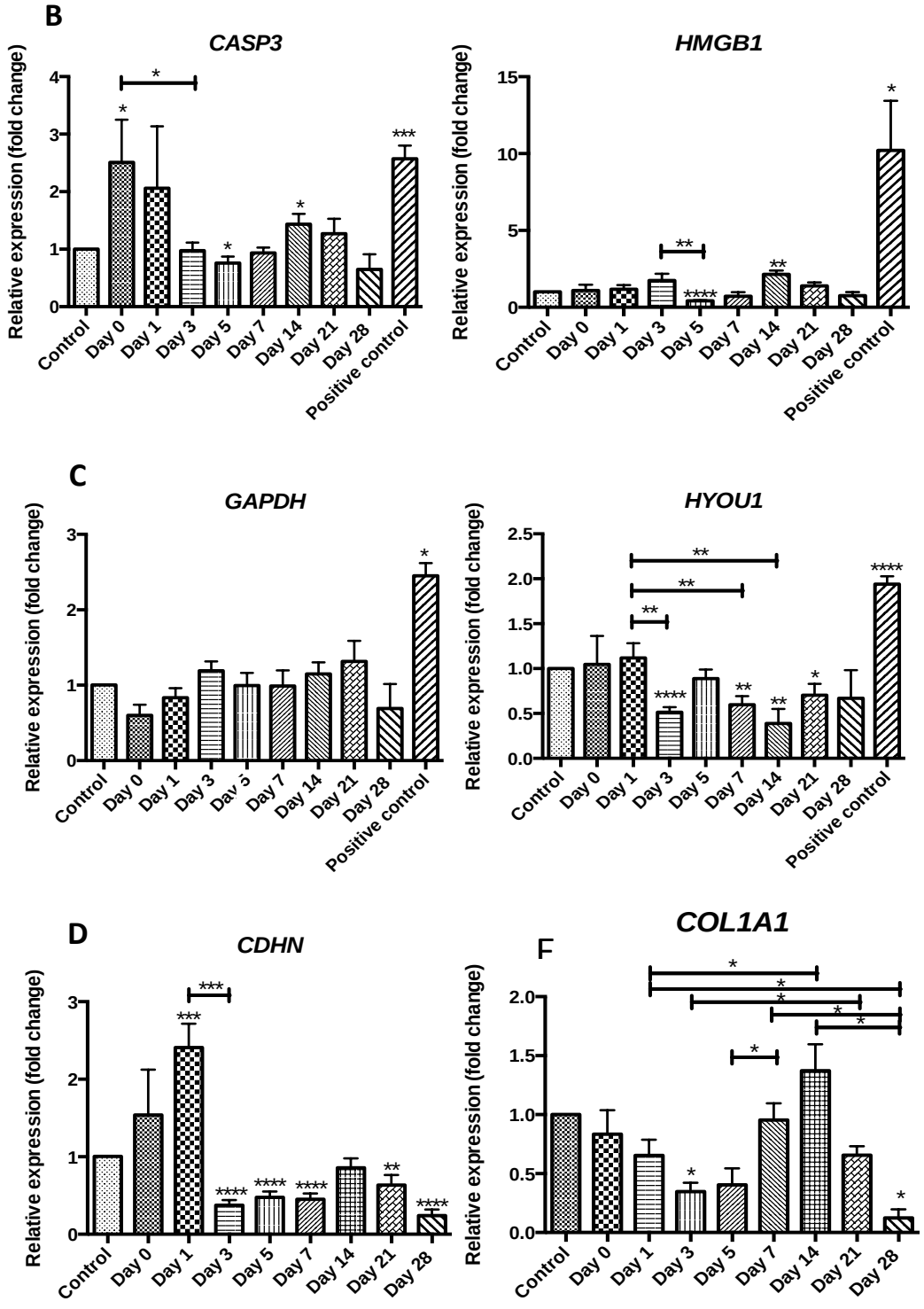
B
CASP3
HMGB1
C
GAPDH
HYOU1
D
CDHN
F
COL1A1
Relative expression (fold change)
Control
Day 0
Day 1
Day 3
Day 5
Day 7
Day 14
Day 21
Day 28
Positive control

Figure 3.3: RT-qPCR analysis of stress/apoptotic/necrotic markers in SHSY5Y cells encapsulated in 2% alginate beads by EHDJ method and evaluated at 8 time points. Expression of all targeted genes in studying samples were compared to the negative control samples (cells grown in tissue culture plate) and to the positive control samples (with induced hypoxia, apoptosis, necrosis and heat shock) [171, 172, 173, 174]. A) Expression level of *HSP70B'*- stress marker; B)*CASP3, HMGB1* – apoptotic/necrotic markers; C)*HYOU1,GAPDH* - hypoxia markers; D)*CDH2* – adherence marker; E)*COL1A1* – extracellular matrix marker. Error bars represent Mean±SD (n=3). *p<0.05, **p<0.01, ***p<0.001, ****p<0.0001.

3.5 Discussion

Methods of cell encapsulation are complex and can damage cells, change their ability to self-assemble or other vital characteristics. A deep and systemic analysis is essential to control cells functionality and activity after processing.

In particular, referring to EHDJ encapsulation, heat, oxygen or nutrition deficiency, shear stress, as well as high electrical fields can lead to changes in cell behavior, such as decreased proliferation rate and activity, inability of cells to communicate and self-organize, changes in cell molecular mechanisms (cancer metastasis, or autophagy), or to stress accumulation. Eventually, as a consequence of stress exposure, cell death can be triggered by two different mechanisms: apoptosis or necrosis (Figure 3.3) [158, 178, 179]. Generally necrosis is the result of severe trauma or injury, whereas apoptosis, or programmed cell death, happens as the result of normal cell cycle, or it can be enhanced by some mild outer stimuli, like hypoxia, heat or the presence of some molecules [145, 179]. Several methods have been developed for apoptosis/necrosis evaluation, based on the microscopic evaluation of phenotypic changes, nuclei fragmentation, detection of molecular markers, like phosphatidylserine (PS) presence, different caspases and *HMGB1* expression or cytochrome c release; some of these methods are mentioned in Figure 3.4.

In this study apoptosis/necrosis detection was performed at the molecular level; methods based on microscopic observations after immunostaining were not efficient and informative due to the interference of the alginate matrix.

Before or in some cases even after the activation of programmed or acute cell death pathways, heat shock proteins (HSP) are produced for protection [161, 162, 163, 180, 181]. The HSP family is composed of proteins that are increasingly expressed in response to stresses (ex. Hsp70A, Hsp90), with some members of the family specifically expressed in particular stress conditions like

heat, hypoxia and heavy metals exposure (ex. Hsp60, Hsp70B', Hsp72) [159, 160, 161]. In literature there are reports about cell stress resistance due to the HSP over-expression and cell recovery [176, 182]. However, HSP over-expression generally points to the presence of stress with no indications about its nature. In addition to HSP, specific genes like, *HIF1α*, *HYOU1* and *GAPDH* are good markers for hypoxia detection [154, 155, 156, 157, 158, 159, 160, 161, 162, 183]. Caspase is the major family of proteases that is responsible for apoptosis propagation, with specific genes for each stage: *caspase 8,9* are early markers, whereas *caspase 3* and *7* are late apoptotic executors, the expression of which can directly point to the propagation of apoptosis [145, 146, 147, 148]. *HMGB1* over-expression is a good diagnostic marker to detect the presence of necrosis.

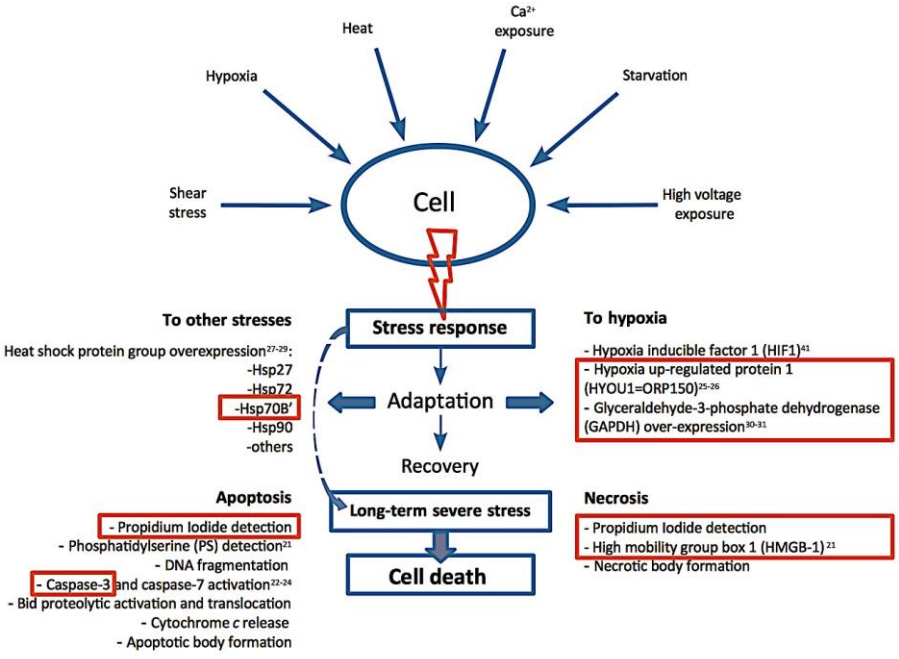

Figure 3.4: Theoretical model of cell response to stress exposure. In *red boxes*, factors that were evaluated in this article.

This study evaluated with a systemic approach the effect of EHDJ encapsulation on the cell characteristics like ability to self-assemble, viability, activity, proliferation and the expression of specific genes (stress, apoptotic and necrotic). *In vitro* evaluations were performed at different time points to check the short-term effect from 3 hours up to 7 days after encapsulation, and long-term up to 4 weeks. SHSY5Y human neuroblastoma cells at passage 16 were encapsulated in 2% alginate beads (200 μm diameter) applying 8kV to the extrusion needle.

Initially, short-term effect (stress molecules production and apoptosis propagation) of EHDJ encapsulation on the cell's behavior was analyzed. RT-qPCR analysis indicated 3 hours after encapsulation *HSP70B*' expression 80 times higher than in the negative control group (Figure 3.3A). HSP proteins main function is to protect cells against apoptosis, necrosis, hypoxia or other type of stresses. Stress accumulation leads to HSP family over-expression, that in turn, induces cell stress recovering, followed by cell stress resistance [176, 180, 181, 182, 184]. However, notwithstanding the expression of HSPs, under severe stress conditions cells can overpass the function of HSP and initiate programmed cell death propagation [176]. Cell viability analysis showed absence of cell death 3 hours after encapsulation, however investigation at the 1st and the 3rd day revealed the presence of some dead cells (Figure 3.2A). Cell viability results were confirmed at molecular level by the 2-2.5 fold increase of the expression of *CASP3* (*caspase-3*) gene in the first hours after encapsulation till the first day (Figure 3.3B). In the following days (3-7), *CASP3* expression decreased and stabilized to the negative control level, supporting the cell viability test. In fact at day 7 after encapsulation a decreased amount of dead cells was observed. Our experimental results agree with the results found in literature about the molecular mechanisms of cell stress protection and apoptosis propagation in stress conditions [176]. Cell death reaches the maximum level 24 hours after stress exposure following the caspase-3 cleavage

and activation [185]. DNA quantification test confirmed the results above and showed 10% decrease in cell number the first day after encapsulation (not significantly different) (Figure 3.2B). Up to the 7th day of the experiment there wasn't any significant variations in cell number. These results prove that the EHDJ encapsulation system has mild stress effect on the cells in first 24 hours, however they are able to recover in a short time and remains viable.

Long-term encapsulation can cause nutrition or oxygen deficiency that in turn can trigger stress accumulation and apoptosis propagation, as well as hypoxia followed by necrotic cell death. From the 5th day of the encapsulation, the level of *HSP70B'* increased again up to 50 times. However, after the 7th day *HSP70B'* expression declined in a clear trend with full recovery to the negative control level at day 21. At day 14, together with a slightly elevated *HSP70B'* expression, death-related markers level was also elevated. The cell viability test showed a moderate amount of dead cells (Figures 3.2A). Expression of hypoxic markers *HYOU1* and *GAPDH* was comparable to the negative control at later time points (Figure 3.3B,C). Up to the 4th week of encapsulation the expression of stress-related markers wasn't observed. Along with a decline in the expression of *HSP70B'*, cells regain their ability to proliferate and the results of DNA quantification test showed two fold increase in cell number between the first week and the second, and triplication towards the 4th week. Presumably, the initial *HSP70B'* overexpression led cells to the stress resistant state, protecting them against hypoxia or other impulses. This is supported by literature and the analysis about stress resistance development after HSP family overexpression in stress conditions [161, 162, 163]. Peculiarly, significant decrease was detected in *HMGB1* and *CASP3* expression at day 5, compared to the negative control. This can be explained by the absence of the physiological 1-5% cell death because of the lack of cell proliferation [145, 146, 147, 148]. A decreased level of *HYOU1* was observed at days 3 and 7. To understand whether *HSP70B'* overexpression has a real protective effect on the encapsulated cells,

further experiments with *HSP70B'* silencing need to be conducted. Obtained results suggest an absence of stress conditions and stable cell state inside the beads during the 3 weeks followed by the first week of stress recovering after encapsulation process.

At last, the cells ability to adapt in artificial environment was evaluated with two markers: *N-cadherin* and *collagen1a1* [164, 165, 166, 167, 168, 169, 170]. Double up-regulation of *N-cadherin* observed during the first days of the experiment can be the result of cells growing inside the beads. These results suggest cells released 24 hours after encapsulation will have favorable conditions for adhesion and self-assembly, in fact, this phenomenon was described in the literature earlier [185, 186]. However, considering that SHSY5Y cells used in the experiment are tumor cell line, there can be another explanation for this phenomenon. According to the literature review, overexpression of *N-cadherin* leads to metastatic cells flow and to increased level of trans-endothelial migration [167]. However, the chemistry of the material can lead to decrease in the ability of cells to adhere. This was observed from double down-regulation of *N-cadherin* expression toward the 7^{th} day of encapsulation. During the following weeks *N-cadherin* expression was varied, but within the control level. The initial decrease in the *collagen1A1* expression can be explained by the cell stress recovery up to the third day after encapsulation [168, 169, 170]. After cells recovered of stress the level of *collagen1A1* was increased within 2 weeks, followed by its downregulation. The expression pattern can be easily explained and compared with other cell parameters, the initial low level was the result of stress recovery, after that cells started modification of the alginate bead environment to their functional niche. Within 2 weeks cells produced sufficient amount of extracellular matrix, thus the expression of collagen1a1 wasn't necessary and its downregulated. By the time niche was modified cells started active proliferation and assembly (Figure 3.1A, 3.2B).

After 2 weeks cells started massive migration outside the beads, followed by its attached to the surface of the alginate beads and the tissue culture plate. Alginate lacks adhesion motifs and as a consequence, cell adhesion to its surface was weak. Even though beads were gathered in clusters overgrown by cells, they were not firmly adherent and could be detached applying shaking or pipetting. However, for organ printing application this technique can be applied in a very efficient way, where cells could be printed in very precise 3D structure on the top, or inside of different matrices, what will support cell migration and self-assembly even better.

3.6 Conclusions

In summary, SHSY5Y cells encapsulated by EHDJ method in 200μm 2% alginate beads are subject to mild stress conditions, whereby they are able to recover in a short time. In fact, our analysis showed that cells could be encapsulated up to 4 weeks without undergoing cell death or oxygen deficiency. Cells kept their ability to self-assemble in 3D constructs mimicking an *in vivo* morphogenesis. This is a positive phenomenon for tissue maturation in organ printing application.

This article provides a systemic approach for the evaluation of the effect of EHDJ encapsulation on cell behavior in short and long term (up to 4 weeks after encapsulation). In this study, we proposed a protocol for evaluation of the EHDJ encapsulation effect on the cell behavior. This protocol can be used not only for the EHDJ encapsulation method but also for other tissue engineering methods. To obtain a full picture of the effects of EHDJ encapsulation, further experiments are needed to evaluate tissue/organ maturation in post-encapsulation time [29, 37, 140].

Acknowledgements

Authors acknowledge the Centre of Integrative Biology (CIBIO) of University of Trento for providing SHSY5Y cell line, and Dr. Wei Sun for helping with RT-qPCR measurements and data evaluation.

Chapter 4

Homeostasis maintenance is critical parameter for application of cell encapsulation in tissue fabrication.

4.1 Abstract

Cell niche homeostasis plays a critical role in many body functions, such as tissue functionality, stem cell maintenance and differentiation, wound healing, cancer development and propagation, and many others. Thus, it's a crucial parameter to control in tissue fabrication process, application of knowledge about cell homeostasis and microenvironment can drastically improve tissue maturation and following post-transplantation adaptation. The main goal of this study was to evaluate post-encapsulation behavior of cells referring to their ability to maintain homeostasis and functionality such as viability with apoptosis-necrosis rate analysis, activity with Alamar Blue test, proliferation with DNA quantification assay, and ability to form niche with *N-cadherin* expression. The results were collected for 8 experimental groups: cells encapsulated in the beads for different time from 3 hours up to 4 weeks and compared to the control group. It was suggested based on the observed results that optimal time for beads maturation and niche formation is 4 weeks. Cells self-assembly into tight micro-clusters with high level of N-cadherin expression, high activity and proliferation potential, so as relatively low cell death level would be beneficial for tissue adaptation post-implantation.

Moreover, there was suggested a variety of applications for EHDJ produced beads, besides tissue fabrication for transplantation, such as 3D models for diseases molecular mechanisms understanding, cosmetics testing

and drug screening. Thus, it was proved that EHDJ encapsulation system is safe, easy in manipulation, and suitable for application in different fields.

4.2 Introduction

The idea of the body's ability to achieve an internal balance in the changing environments was first mentioned around 200 years ago, in 1920 by Walter Cannon this process was termed homeostasis [188]. Cell homeostasis is the capability of biological systems to maintain a relatively stable milieu in a fluctuating external environment [189]. Evolutionary cells of many organisms, including humans have learned how to survive and function even in extreme conditions, all because of cells adaptation and homeostasis maintenance. Cell niche homeostasis plays a critical role in many body functions, such as stem cell maintenance and differentiation, temperature balance, in cancer development and propagation, and many others [189, 190, 191, 192, 193, 194]. "Niche" or cell microenvironment according to Scadden's definition is specific anatomic location that regulates how cells participate in tissue generation, maintenance and repair. Cell niche or microenvironment is in the majority extracellular matrix, it can contain as well blood vessels, nerves or any other factors that would maintain cells viability, differentiation and functionality [192, 193, 194]. Thus, extracellular matrix (ECM) is the main component of the cellular niche and composed of proteins with supporting function, such as collagens, laminins, elastins and others; biomolecules, with nutrition and fate-controlling function, such as growth factors, small integrin-binding glycoproteins; at last proteoglycans, and water [93, 94, 95, 96]. ECM always undergoes slight modifications by cells activity. ECM plays a key role in cell activity like proliferation, adhesion, migration, differentiation, apoptosis and gene expression [94].

The general goal of regenerative medicine is focused on recovering, restoration or replacement of damaged or diseased tissues with in vitro fabrication of proper substitution [195, 196, 197, 198]. Application of knowledge about tissue homeostasis and cell microenvironment into tissue

fabrication process can drastically improve tissue maturation and following post-transplantation adaptation [196, 199]. One of the most commonly used technologies for tissue fabrication is organ printing, which is relatively new direction however it already received a profound attention as promising technique. Organ printing composed of three main steps according to prof. Mironov, the first step calls pre-processing, which is the tissue/organ design using computer tomography scanning or any other similar technologies to define precise tissue composition [29]. The next step is processing or direct cell encapsulation. Cell encapsulation techniques are widely used in tissue engineering as simple yet powerful tool for tissue fabrication [49, 50, 51, 52, 83]. At last, post-processing, or organ maturation, which is mainly focused on cells expansion inside the matrix and maintaining 3D tissue substitutes in bioreactors that would mimic *in vivo* microenvironments [27, 28, 29, 30]. The last step of organ printing, post-encapsulation is the most critical and important for tissue homeostasis maintenance. In many cases cell encapsulation process implies stem cells, because of its multi or pluripotency potential, what makes post-encapsulation maintenance is crucial for proper stem cells differentiation and self-renewal.

At present, many techniques and protocols were developed and applied for cell encapsulation, such as photolithography, microfluidic encapsulation, ink-jet and bioprinting [49-81], so as many materials were evaluated for above-mentioned applications [16, 17, 18, 19, 20, 21, 82, 84, 87, 88, 89, 90, 91, 92]. However, some work was already done [22, 42, 85, 143], on cell parameters evaluation during or post encapsulation, but still many aspects need to be addressed. Cell homeostasis and microenvironment maintenance post-encapsulation are critical parameters to control for successful tissue fabrication.

In recently published study a detailed analysis of cell viability, metabolic activity and cell stress level was made on cells encapsulated in the alginate beads by EHDJ encapsulation [22]. Study showed cells were subjected to a mild

stress, however they were capable to recover in short time, and maintain their main functions, like proliferation and ECM production.

Moreover, this study showed cells within 3 weeks modified artificial alginate environment into their functional niche, by producing ECM components, like *collagen1* and *N-cadherin*. However, the main goal of maturation process, the third step of organ printing, is formation of homeostatically stable, functional tissue, where artificial matrix used initially for tissue fabrication process, would be substituted by the cells ECM, including growth factors, and biomolecules important for proper tissue function [29, 30, 93]. Thus, maturation process can be considered as completed, when fabricated tissue can maintain its structure and stability by itself without external factors and support.

The main goal of this study was to evaluate post-encapsulation behavior of cells referring to their ability to maintain homeostasis and functionality such as viability: apoptosis-necrosis rate, activity and proliferation.

Thus, to be able fully evaluate cells state and capacity to maintain fabricated tissue structure they were placed in control conditions (TCP), and supplied with full media after being encapsulated up to 4 weeks. Without an artificial matrix (which has to degrade in fabricated tissue) cells were tested for their ability to maintain homeostasis and self-assembly ability, and some functionality parameters like cell death rate, proliferation and activity level. SHSY5Y human neuroblastoma cell line (neural progenitors) was used as a suitable model for encapsulation [200]. Cells at passages 12-16 were encapsulated by EHDJ encapsulation method in 2% alginate beads (beads size varied around 200μm) up to 4 weeks [22, 60]. Cells were released from the beads by dissolving the alginate in PBS and reseeded in TCP after they were washed with media to remove alginate residues at 8 time points: 3 hours, 1 day, 3, 5, 7, 14, 21 and 28 days after the encapsulation. Cells seeded in TCP without being encapsulated before were used as a control group. After reseeding cells

were subjected to a set of in vitro tests for evaluation of viability with apoptotic/necrotic detection kit, metabolic activity with Alamar blue assay, proliferation level with DNA quantification assay, at last adhesion, motion and cell-cell communication properties with *N-cadherin* expression at 4 time points: day 1, 3, 5 and 7.

4.3 Materials and methods

Materials

Alginic acid sodium salt from brown algae and calcium chloride dehydrate were purchased from Sigma-Aldrich (USA). Phosphate buffer saline without calcium and magnesium (PBS), Dulbecco's modified eagle medium (DMEM) were purchased from Invitrogen (USA). The encapsulation system consists of a generator (ES30, Gamma High Voltage Research Inc., USA), a pump (NE-300, New Era Pump Systems, USA), a polyetrafluorethylene tube and a gauge 33 stainless steal needle (outer diameter: 0.210 mm, inner diameter: 0.108 mm Hamilton, Bonaduz/Switzerland). SHSY5Y human neuroblastoma cell line (ATCC® CRL-2266™, UK), Sonicator (UP400S Heilscher, Germany), Quant-iT PicoGreen dsDNA Assay Kit (Invitrogen, catalog number: P11496), Apoptotic/Necrotic kit (PromoKin PK-CA707-30017); 0.05% Triton-X 100 in PBS; paraformaldehyde (PFA) 4%; antibody for N-cadherin (santa cruz rabbit sc-7939), DAPI (life technologies).

Encapsulation process.

Hydrogel preparation and sterilization.

Alginate powder was dissolved in PBS for 8 hours at room temperature under mild stirring to obtain an alginate solution at the desired concentration (2%, 2g/100 ml). Under a biological sterile hood, a syringe filled with solution was connected to a pump to be filtered overnight through a 0.22 μm filter. The sterile solution was immediately used after filtration. The crosslinking solution consisted of calcium chloride dehydrate dissolved in distilled water at a concentration of 400 mM, filtered through a 0.22 μm filter under sterile conditions.

Cell culture. SHSY5Y human neuroblastoma cell line was expanded in 25-175mm tissue-treated culture flasks as monolayer (passages 12-16) at 37°C under 5% of CO_2 in high glucose Dulbecco's Modified Essential Medium (DMEM) with 10% fetal bovine serum (GIBCO), 2mM Glutamine and 1% penicillin-streptomycin mixture (Sigma, USA). DMEM medium was changed every third day. The cells were cultured to 90-95% confluence before encapsulation [176].

Preparation of the alginate suspension with cells.

At 90-95% confluence cells were detached and moved to a 15 ml vial. Cells inside the vial were stirred at 1000 rounds/min for 10 minutes and the surnatant was removed. Cells on the bottom of the vial were resuspended in PBS and stirred again to remove any residues of medium containing cations that could crosslink the alginate solution. Cells were dispersed by vibration inside the buffer and an aliquot of the solution was taken to count the number of cells using a Cellometer Auto T4 (Nexcelom, USA) and Trypan Blue 0,4% (Life technologies, USA) as contrast agent. Cells were stirred again, and after removing the surnatant the alginate solution was added to obtain an alginate suspension containing 5 millions cells for milliliter. Medium, PBS, Trypsin/EDTA and the alginate suspension used were warmed to 37°C.

Cell encapsulation by electrohydrodynamic jet method.

Cell encapsulation was performed by following a protocol already published [60]. In brief, the encapsulation system was placed under the biological hood, a sterile 3 ml syringe was filled with cells suspended in the alginate solution, connected to the polytetrafluoroethylene tube and placed onto the pump. The pump was set at the fixed flux of 0.05 ml/min. The other side of the tube was connected to the stainless steel needle. The electrical potential was established by connecting the positive cathode of the generator to the needle, and the anode to the metallic plate under the Petri dish. The Petri dish

containing sterile calcium chloride solution was placed below the needle at a distance of 5 cm. Once the flux of solution was established and the generator was switched on (V=8kV), droplets of alginate solution containing cells were ejected from the needle directly to $CaCl_2$ solution. After 10 minutes the beads were washed three times with DMEM and redistributed in 6-well tissue culture plates to perform the experiment.

Cell release.

To reseed cells for in vitro evaluations cells were released from the beads and reseeded in 12-well plate tissue culture plates. The hydrogel was dissolved by removing the DMEM media containing Ca^{2+} cations with a short wash in PBS at room temperature, followed by 15 minutes incubation in PBS at 37°C to favor the ion exchange with the surrounding buffer. After that, the samples were centrifuged and cells were collected for counting. Cells were resuspended in 5 ml of full cell culture media. Cells were dispersed by vortexing inside the media and an aliquot of the solution was taken to count the number of cells using a Cellometer Auto T4 (Nexcelom, USA) and Trypan Blue 0,4% (Life technologies, USA) as contrast agent.

In vitro evaluation

The study was performed up to 4 weeks on 8 different groups: 3 hours, 1, 3, 5, 7, 14, 21 and 28 days after encapsulation. The reference group was cells in TCP without being encapsulation before. Samples were subjected to a set of tests at 4 time points: day 1, 3, 5 and 7. Table 4.1 represents the schematic schedule of the conducted experiment.

			In vitro evaluation day			
			Day 1	Day 3	Day 5	Day 7
Experimental group	Control	1	Apoptosis/ Necrosis rate Alamar Blue assay - activity DNA quantification- Proliferation N-cadherin expression	Apoptosis/ Necrosis rate Alamar Blue assay - activity DNA quantification- Proliferation N-cadherin expression	Apoptosis/ Necrosis rate Alamar Blue assay - activity DNA quantification- Proliferation N-cadherin expression	Apoptosis/ Necrosis rate Alamar Blue assay - activity DNA quantification- Proliferation N-cadherin expression
	3 Hours	2				
	1 Day	3				
	3 Days	4				
	5 Days	5				
	7 Days	6				
	14 Days	7				
	21 Days	8				
	28 Days	9				

Table 4.1: Scheme of the conducted set of experiments for evaluation of cells viability, apoptosis/necrosis rate, activity and adhesion ability post-encapsulation.

Apoptosis/necrosis evaluation.

Cell death type was evaluated using PromoKine apoptotic/necrotic kit. Briefly, cells were fixed with 4% PFA in the tissue culture plate at established time points. Samples were washed twice with 1X Binding buffer, and after were incubated for 15 min with solution of 5µl of FITC-Annexin V and of 5µl of Ethidium Homodimer III in 100 µl of 1X Binding Buffer (light protected). Next,

samples were washed twice with 1X Binding buffer and stained for 5 min with DAPI (light protected). After brief washing in PBS results were analysed with Nikon confocal microscope. Green light represented apoptotic cells, red color for necrotic cells, and blue for the nuclei, corresponding to the total amount of cells. The results were obtained in the view of confocal fluorescent images, and the total number of cells, apoptotic and necrotic cells were calculated with ImageJ cell counter plugin. After results were analysed with GraphPrism 6 software. All the samples were made in triplicates, and for each sample there was made 3 images for statistical calculation.

Cell proliferation.

DNA extraction was performed by placing the cells extracted from the beads in a solution of 0.05% Triton-X in PBS, followed by sonication for 10" (cycle: 1, amplitude 40%). After that, DNA was extracted and PicoGreen was used for the quantification. Fluorescence intensity of PicoGreen – DNA complex was measured in 96-well plates on a plate reader (485 nm excitation and 538 nm emission; Safire, Tecan, Austria). A calibration curve was built up using the DNA standard provided with the assay to correlate fluorescence intensity to the concentration of DNA.

Cell activity.

Cells activity was measured with Alamar Blue assay. Cells were incubated with 10% Alamar Blue solution in full DMEM media for 2.5 hours protected from light. After incubation, 100 µl of solution of each sample was transferred to 96-well plate (black) and measured with fluorescent plate reader machine (485 nm excitation and 538 nm emission; Safire, Tecan, Austria). After samples were washed with PBS solution and placed at 37°C in full DMEM media till the next time point assay.

N-cadherin expression with immunocytochemistry assay.

Reseeded cells were fixed with PFA 4% for 30 min, after samples were blocked and permeabilized with blocking buffer (1% BSA, 0,3 % TritonX in PBS) for 1 hour. Primary antibody to N-cadherin (sc-7939) was applied for overnight at 4C°. After PBS washing was performed 3 times for 10 minutes. Secondary anti-rabbit antibody was applied for 1 hour at room temperature with following 3 times washing in PBS. At last, DAPI solution was applied for 5 min. After, cells were washed twice with PBS. Results were analysed with the confocal microscope (Nicon).

Statistical analysis

All statistical analysis was performed with GraphPad Prism 6 software. Statistical analysis for more than two groups was carried out using one-way ANOVA with Tukey's post-hoc tests. $P<0.05$ was considered significantly different. All samples were prepared in triplicates for statistical difference validation.

4.4 Results

The results were analyzed within each experimental group at 4 experimental time points and compared to the reference group and within each other. All results presented in Figures 4.1-4.7.

Control group (1). There was observed a general low level of cell death rate, with decreasing level of necrosis from the first towards the last experimental time point. Control samples had high proliferation potential so as high activity level. Addition to that, control cells show high level of N-cadherin experission at all experimental times, and homogeneous cell population with epithelial like phenotypes, as it specific for SHSY5Y cell line (Figures 4.1-4.7).

3 hours group (2). The first experimental group, showed statistically similar to the control group results. The general cell death rate was on the same level, with slight increase of necrosis on the third day of culturing, similar cell number adhered to the tissue culture plates, and proliferated in the same pattern as the control group. There was found significant difference in the number of cells in suspension at day 7 after reseeding. At last, there was observed no differences in the cell phenotypes and grow patterns, so as in the level of N-cadherin expresion (Figures 4.1-4.7).

1 day group (3). Cells reseeded one day after encapsulation, showed significant increase in the cell death rate (both apoptotic and necrotic) within 3 days of culturing, however it gradually decreased towards the 7^{th} day of culturing. Cell proliferation level significantly slowed, but reached the control level at 7^{th} day of cultring. There was also obsereved an increasing amount of cells in suspension, especially the last day of culturing. At last, cell-cell communication was disturbed, by decreased amount of N-cadherin expression, though phenotypically cells were similar to the control group (Figures 4.1-4.7).

3, 5 and 7 days groups (4,5 and 6). The next set of experimental groups had similar pattern in all the conducted tests. All groups showed an increase in

cell death level, but only at the first and the last day of culturing, whereas in the middle cell death rate was on the control level. Next, proliferation rate was slower than in the control group, but had the same pattern. The 4th group had the highest amount of cells in suspension at day 7 after reseeding, and the lowest level of N-cadherin expression at this time. Group 5 had significantly lower amount of cells in suspension by the 7th day of culturing, and very high level of N-cadherin expression. At last, group 6 had the highest level of cells in suspension the first day after reseeding, and very low level of N-cadherin expression this time point, but amount of cells in suspension reached the control level by day 7 of culturing, so as the N-cadherin expression. There was also observed phenotypical shift to the mesenchymal-like in the groups 5 and 6 groups, but the growing pattern was the same as in the control group, homogeneous distribution on the surface of tissue culture plate (Figures 4.1-4.7).

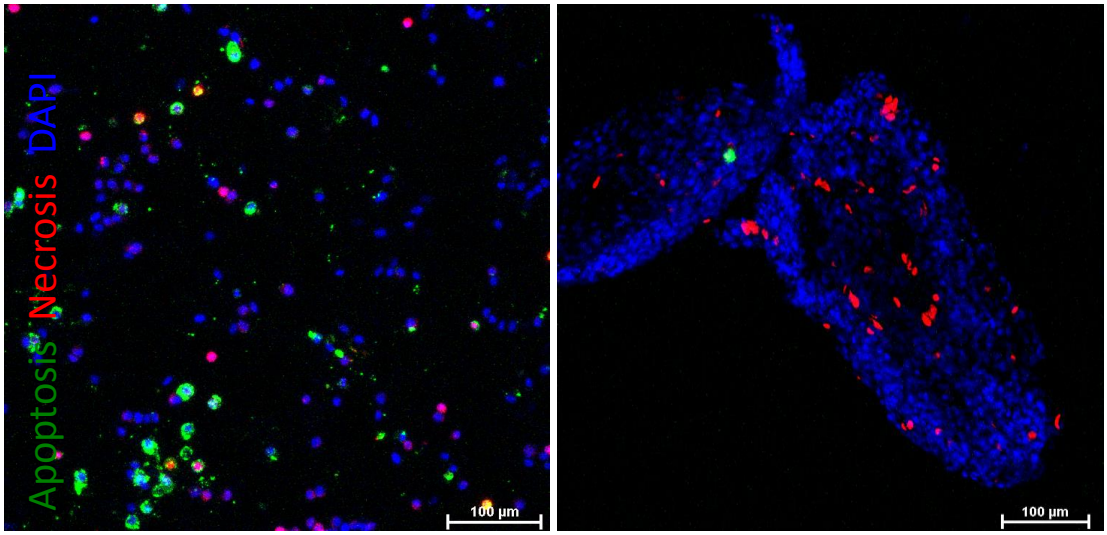

Figure 4.1: Apoptotic/necrotic cell death evaluation. Cells were stained with DAPI for detection of the total amount of cells. An example of Promikine kit stainings with experimental sample of Day 7.

14 days group (7). This group of samples had the lowest level of necrosis the first day after reseeding, but the highest apoptotic level among all the

experimental groups and samples, which completely recovered to the control level towards the 7th day of culturing. The total cell number was on relatively low level, but higher than in groups 4-6. There was observed very high amount of cells in suspension the first day (supports the high amount of apoptotic cells), but the amount of cells in suspension returned to the control level at next experimental point. The activity of this group was on relatively low level as well. There was observed from the first day the highest level of *N-cadherin* expression within all the experimental time. At last, cells had mesenchymal-like phenotypes and they started to grow in tigher groups (Figures 4.1-4.7).

21 days group (8). This group had the highest level of necrotic cell death, but it gradually decreased towards the last experimental day. The apoptotic cell death level was elevated as well the first day after reseeding, but it completely recovered towards the last day of culturing. This group as well had the quite low proliferation level, so as cell activity level was quite low, the level of cells in suspension was on the control level at all time points. There were also observed tight cells cluster with very high level of *N-cadherin* expression, at last cells had mesenchymal-like phenotype (Figures 4.1-4.7).

28 days group (9). At last, cells reseeded after 28 days in the beads had elevated level of cell death at all points, but first day. However, this group of cells had the highest proliferation rate, hence the activity level was very high as well. There was observed very high amount of cells in suspension first day reseeding, so as the last day, even with the highest level of *N-cadherin* expression at all experimental points. At last, cells were growing in very tight groups in multi-layers with overexpression of *N-cadherin* in this areas (Figures 4.1-4.7).

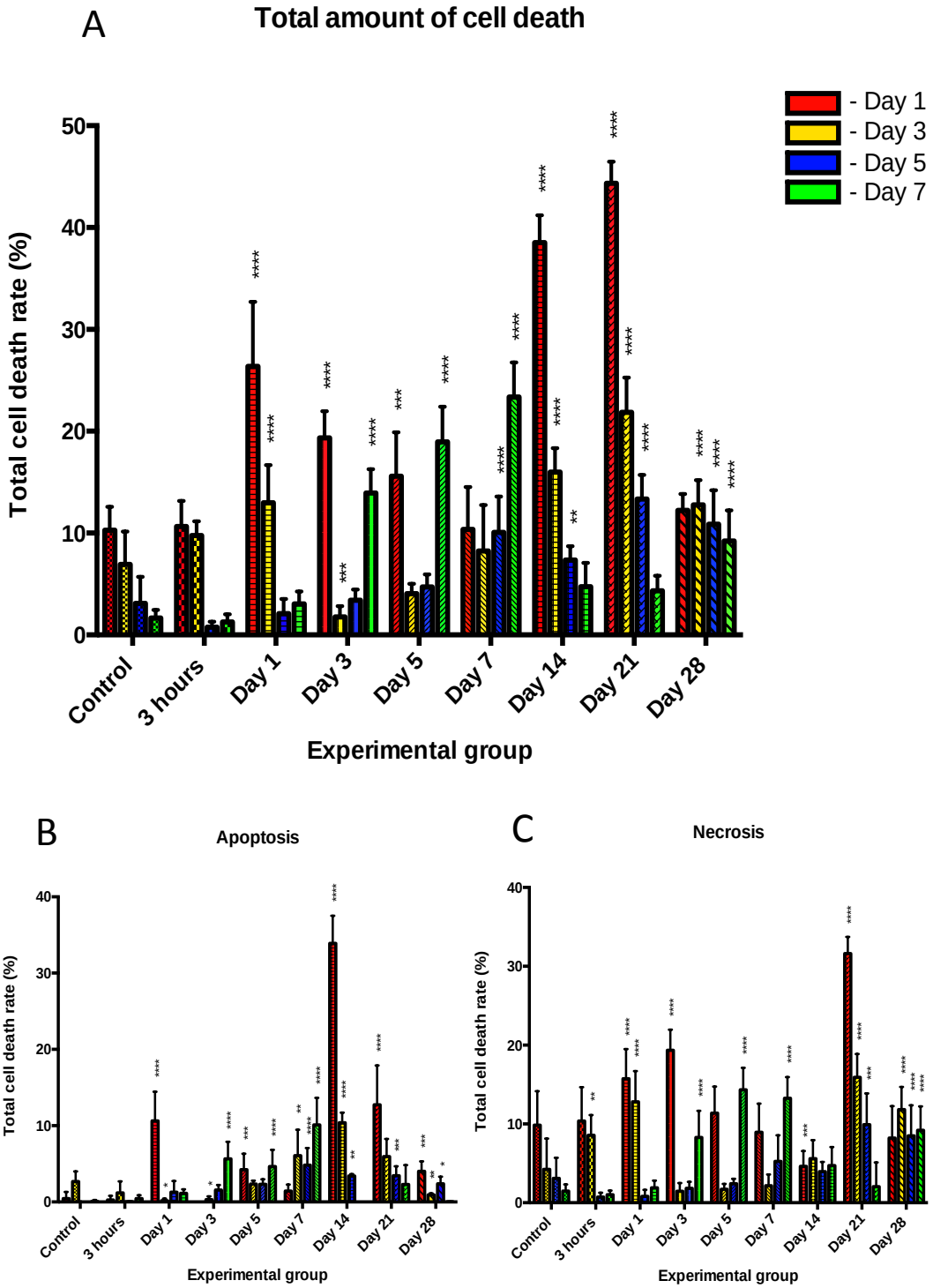

Figure 4.2: Cell death type and rate evaluation with PromoKine in 8 studying groups and the reference control group. Experimental and reference

groups were subjected to apoptosis/necrosis detection at 4 time points: day 1, 3, 5 and 7. The results were evaluated with confocal microscope, and following calculations with ImageJ cell counter plugin. A. Total amount of cell death; B. Apoptosis rate; C. Necrosis rate. Statistical analysis was performed comparing results of experimental groups to the control one within in vitro evaluation days: 1, 3, 5 and 7. Error bars represent mean±SD (n=3). *p<0.05, **p<0.01, ***p<0.001, and ****p<0.0001

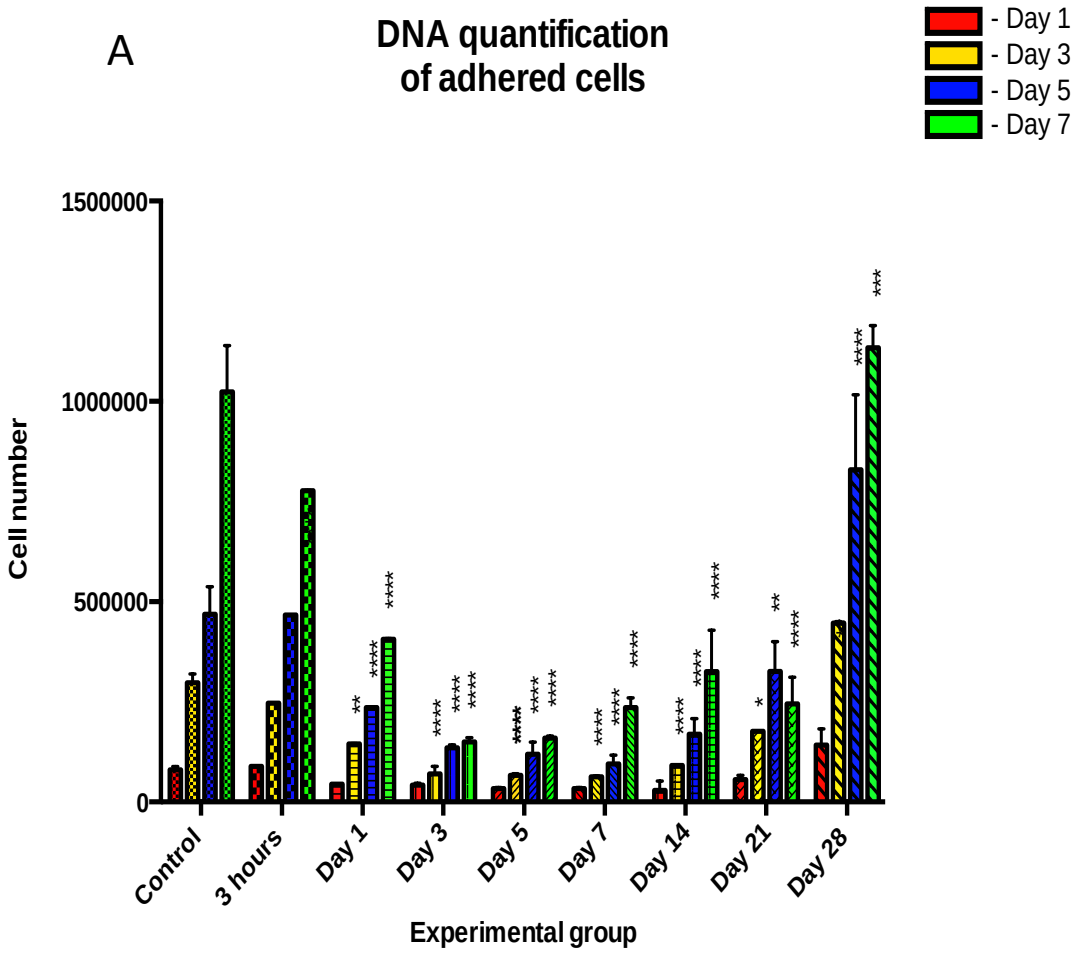

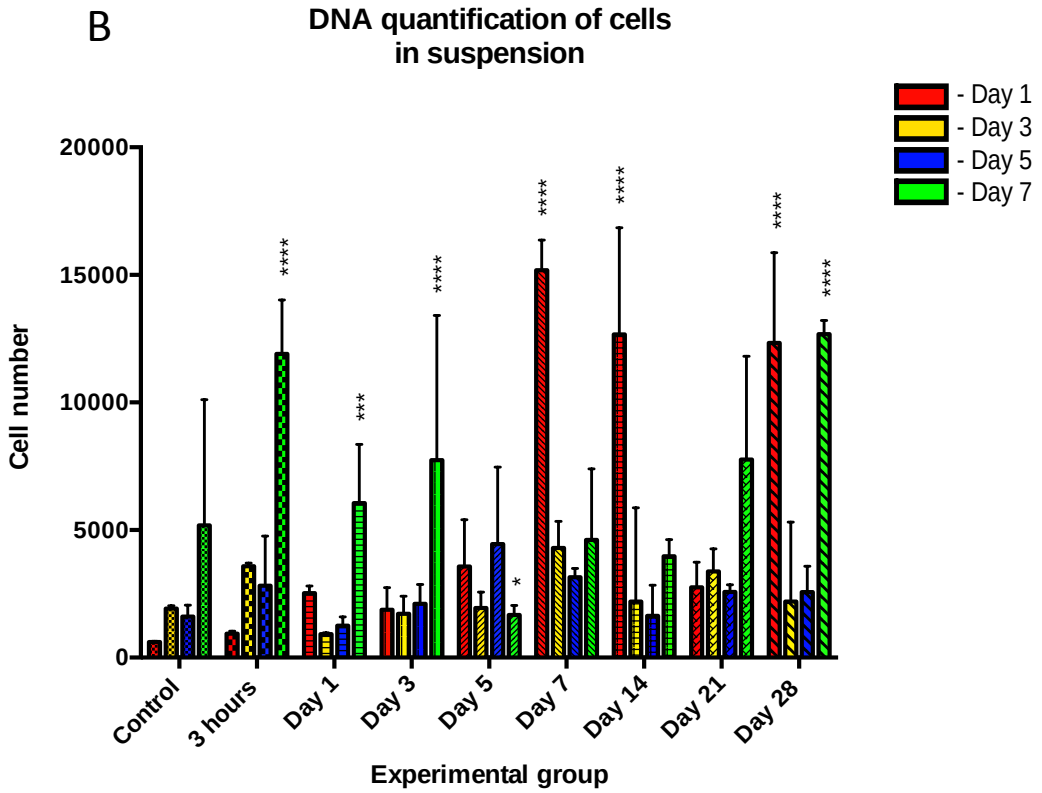

Figure 4.3: Cell proliferation rate measured with DNA quantification assay. All experimental groups and control were divided in 2 subgroups: cells adhered to the surface of tissue culture plate, and cell in suspension that were not able to adhere. Experimental and reference groups were subjected to DNA quantification test at 4 time points: day 1, 3, 5 and 7. A. Cells adhered to the surface of tissue culture plates; B. Cells in suspension. Statistical analysis was performed comparing results of experimental groups to the control one within in vitro evaluation days: 1, 3, 5 and 7. Error bars represent mean±SD (n=3). *p<0.05, **p<0.01, ***p<0.001, and ****p<0.0001

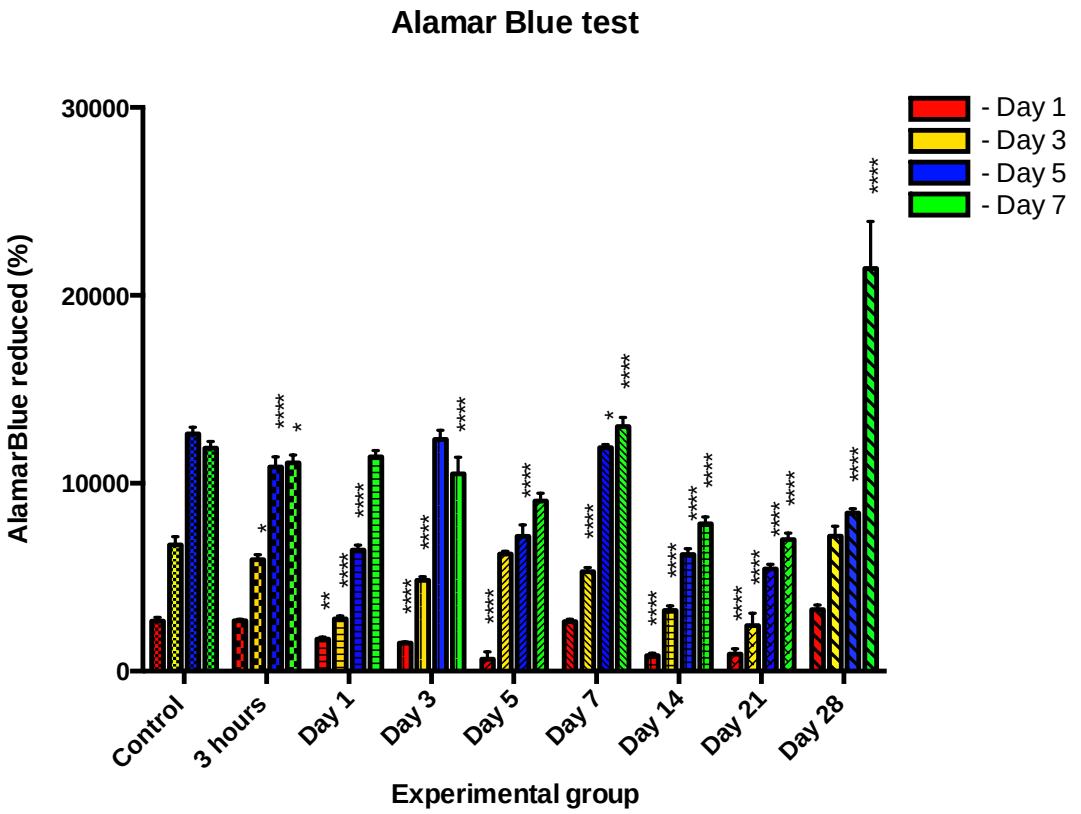

Figure 4.4: Cell activity rate measured with Alamar Blue assay. Experimental and reference groups were subjected to Alamar Blue assay at 4 time points: day 1, 3, 5 and 7. Statistical analysis was performed comparing results of experimental groups to the control one within in vitro evaluation days: 1, 3, 5 and 7. Error bars represent mean±SD (n=3). *p<0.05, **p<0.01, ***p<0.001, and ****p<0.0001

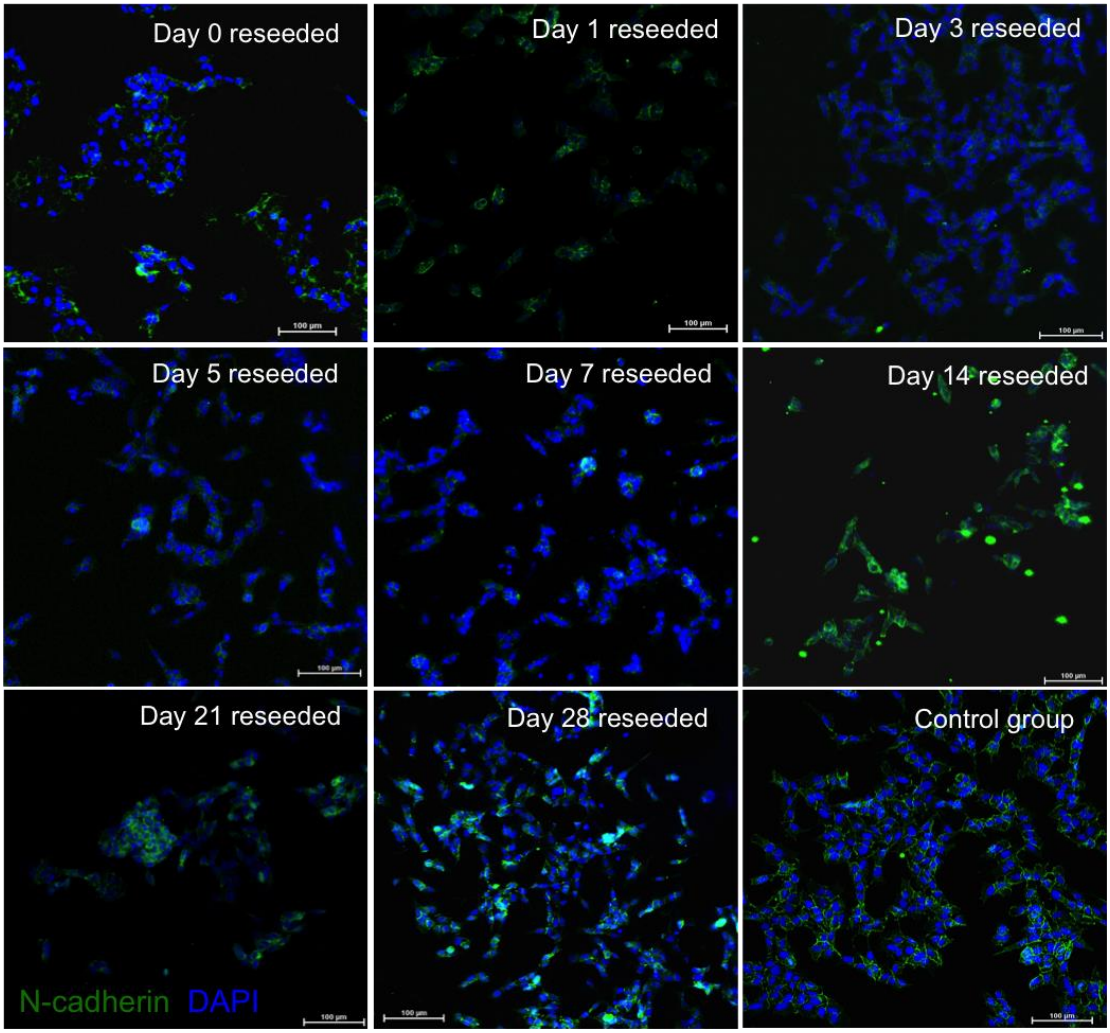

Figure 4.5: The ability to communicate and self-assemble in groups was evaluated with *N-cadherin*/DAPI expression at Day 1 on cells encapsulated in 2% alginate beads by EHDJ method, released and reseeded at 8 experimental time points in control conditions, and compared to the group of cells that were not encapsulated.

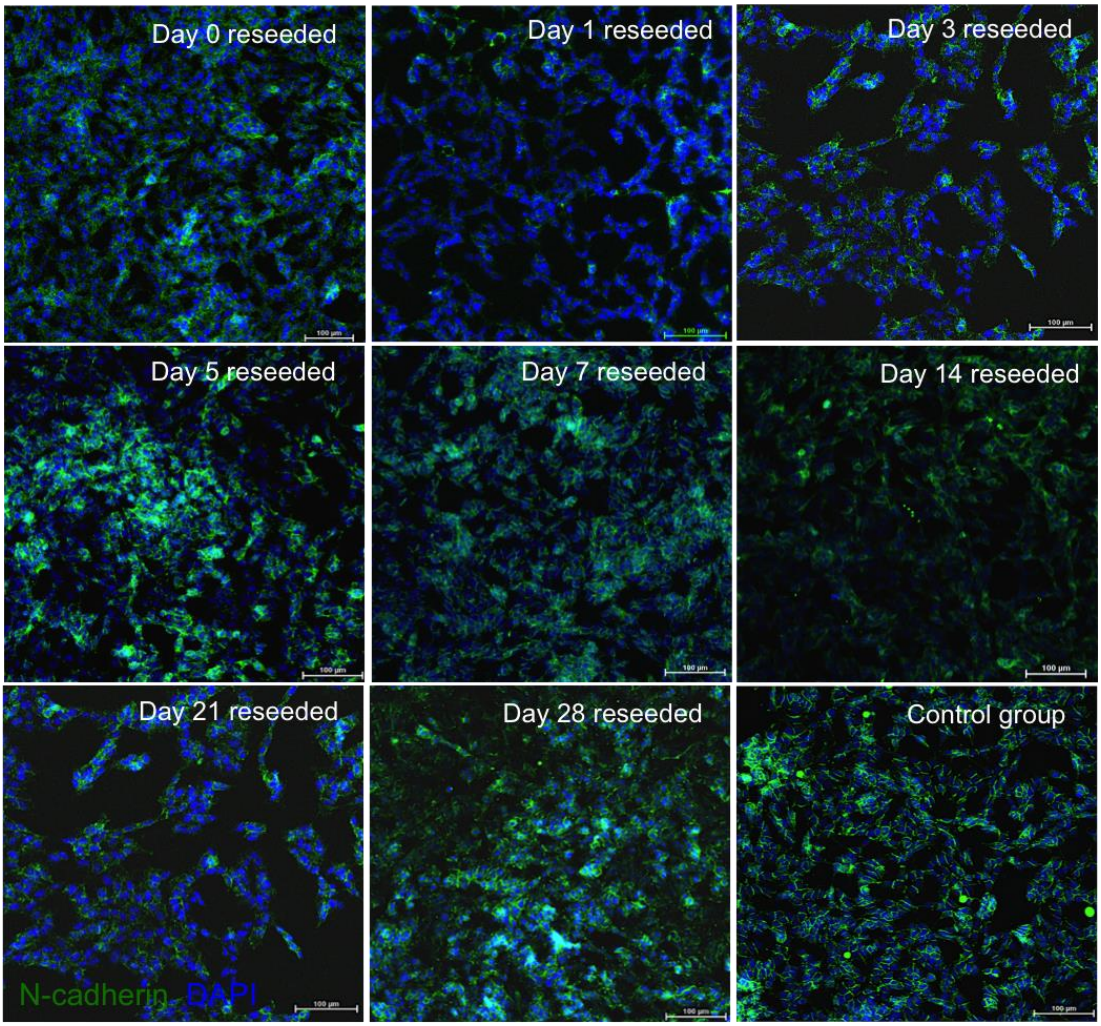

Figure 4.6: The ability to communicate and self-assemble in groups was evaluated with *N-cadherin*/DAPI expression at Day 7 on cells encapsulated in 2% alginate beads by EHDJ method, released and reseeded at 8 experimental time points in control conditions, and compared to the group of cells that were not encapsulated.

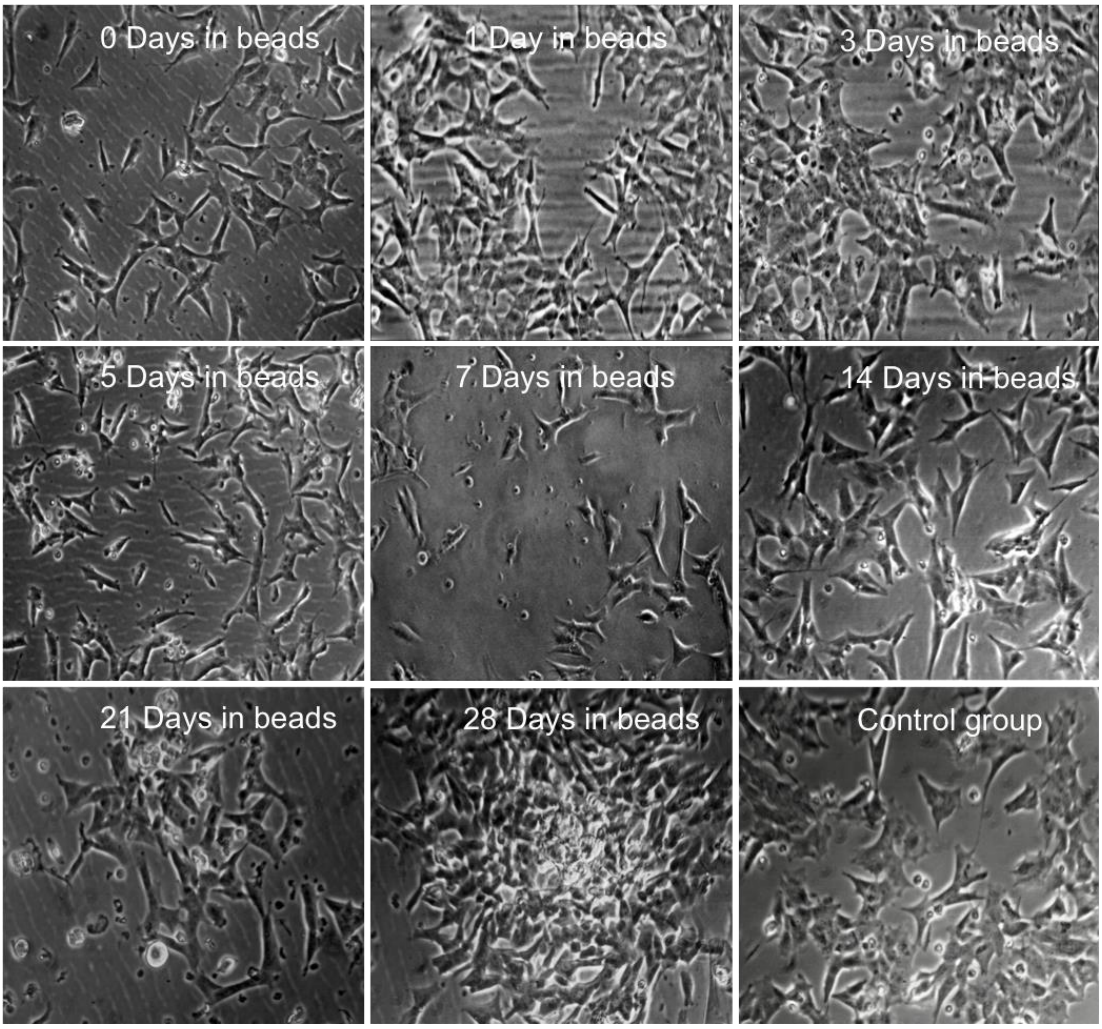

Figure 4.7: Phenotypic changes and growth patterns were evaluated with brightfield imaging of cells encapsulated in 2% alginate beads by EHDJ method, released and reseeded at 8 time points in control conditions and compared to the group of cells that was not encapsulated.

4.5 Discussion

Organ printing is complex multistep technology of tissue, organ fabrication. Dr. Anthony Atala recently published a review in Nature on bioprinting and the requirements for successful tissue production [27]. One of the main requirements is the cell source and its functionality [28, 29, 30]. According to this review, cells must have a high proliferation potential and activity, especially initially after implantation to reach the proper cell number and build the extracellular matrix that would support the tissue structure without an artificial matrix. Another key parameter for successful tissue fabrication is cell microenvironment maintenance [93, 94]. Control over cell microenvironment is crucial aspect for tissue engineering and regenerative medicine research [201]. By manipulating cell niche composition it is possible to affect cells behavior via biophysical, biochemical or other mechanisms [191, 192, 193, 194, 197]. Thus, tissue engineering has to combine the knowledge about cell microenvironment and surrounding physical forces with engineering methods for successful 3D tissue fabrication and its following maturation [199].

In the previous chapter, there was presented a detailed study of EHDJ encapsulation system effect on cells behavioral characteristics, that showed high level of cell viability, activity and proliferation potential [22]. After the tissue fabrication, maturation follows, thus the next step, was to evaluate the best encapsulation time in terms of most favorable cell parameters for tissue maturation, such as high proliferation potential, ECM matrix production and low death rate.

Thus, here is presented a deep study of cells behavior post-encapsulation by electrohydrodynamic jetting in 2% alginate beads for different time up to 4 weeks, and discussion over the most suitable cell conditions for successful tissue maturation referring to cells ability to maintain homeostasis by adapting artificial matrix to their functional niche.

The main application of EHDJ encapsulation system is for the second step of organ printing. The crucial requirement for this application is the production of 3D structures with viable functional cells capable of maintaining their homeostasis during the maturation process [27, 28, 29, 30, 31]. Eventually, by the time of transplantation cells encapsulated in artificial 3D conditions, have to modify surrounding environment to their functional niche by degrading the artificial matrix and replacing it with their own ECM and biomolecules important for homeostasis maintenance [93, 94, 95, 188-195].

As it was shown in the previous study [22], cells undergo mild stress during and 48 hours after encapsulation, but with elevated level of heat shock proteins expression (play a critical role in cells recovery during and after stress) cells fully recover by the end of the first week, and more importantly they become resistant to the following stress exposures. In the conclusion, based on the observed results it takes 1 week for stress recovery, and around 2 weeks to adapt an artificial alginate bead environment to their functional niche [202]. The niche adaption hypothesis was supported by the expression pattern of *collagen1A1* gene (Figure 3.4E), the main component of ECM. The first week after encapsulation the expression of *COL1A1* was decreasing (stress recovery time), but after 5 days it started to grow until day 21 when the niche supposedly was formed, and cells started its normal activity and proliferation. Thus, these results prove the importance of niche in cells adaptation after encapsulation, and indicates after the 3rd week of encapsulation cells highly active and most favorable for transplantation.

However, to prove the hypothesis of cells adaptation and recovery within 3 weeks, the following test experiment was performed, to evaluate cells behavior and stress state after being encapsulated and released from the artificial matrix within 4 weeks at 8 time points and placed in the minimum stress conditions. The results were compared to the control group, cells maintained in TCP without being encapsulated before.

The evaluation of cell behavior post-encapsulation in 8 experimental and control groups supported the above-mentioned hypothesis. Based on the obtained results within 9 groups, one group was considered as the most suitable for tissue maturation after encapsulation, 28 days in the beads. As it is shown in the Figures 4.1-4.7 all vital parameters for the last experimental group met the main requirements for tissue fabrication, as it was described above, high proliferation level, relatively low death rate, high migratory and communication potential, good self-assembly, so as high cell activity level. Group 9 had the highest proliferation rate and activity level, beneficial for achieving the proper cell number and ECM amount for functional niche formation. So as high level of *N-cadherin* expression from the first day after cells were placed in the control conditions. Another important parameter was noticed, is cells were tend to grow in tight junctions (Figure 4.7), keeping the memory of being closely placed in encapsulated artificial 3D environment. This group also had relatively low death rate for apoptosis and necrosis. All these parameters will be beneficial for fast and successful scaffold adaption after implantation; moreover it might decrease the risk of immune rejection or fibrosis propagation, because of homeostatic stability in the fabricated tissue. However, this group had relatively high amount of cells in suspension, first and last day of culturing (the same pattern was observed for many groups), this peculiar pattern can be explained by the ability of these cells to grow in two forms: adhered to the tissue culture plates and in suspension.

The other experimental groups 4-8 recovered after encapsulation stress, were not able to meet the tissue fabrication requirements, because of low proliferation level, low activity and high cell death rate. Thus, if perform fabricated tissue implantation before 4 weeks of maturation, it might cause a severe immune reaction, hence rejection or fibrosis of the implanted replacement. However, the disadvantages of these groups for organ printing

application, can be the advantage for application of these groups as 3D models for diseases investigation so as for drug screening.

3D models currently are highly demanded tools in many different fields, such as basic biology understanding, pathology mechanisms evaluation for cancer, schizophrenia, Alzheimer's and others [203-212]. Moreover, beauty companies need proper 3D models for cosmetics testing. Thus, here is considered another application of EHDJ encapsulation system for 3D models fabrication for disease molecular mechanisms understanding. The main requirement for this application will be functional and stress-less cell state, with stable proliferation level.

According to the obtained results, groups 4-8 will be the most favorable for 3D disease models application. Cells by the time of 2-3 weeks are already adapting alginate environment to their niche, thus they fully recovered and function in their normal regime. The level of N-cadherin is on the control level, whereas the proliferation and activity level is lower, mimicking in vivo conditions (cell proliferation rate in vitro is accelerated by growth media compare to in vivo conditions [211]). The death rate stabilizes to the control level after the first day of culturing. By encapsulating modified to a desirable disease type cells, within 2-3 weeks it is possible to achieve a good model for in vitro investigations.

Above described application of 3D model for disease molecular mechanisms understanding, logically brings the discussion to another application, drug screening [212, 213, 214, 215]. Many drugs today fail to reach market because of inability to meet necessary requirements during testing steps in vitro and in mice, in vivo. Thus, proper in vitro testing on human 3D fabricated tissue might significantly improve the process of drugs development.

Based on the above described application of EHDJ encapsulation system for 3D models fabrication, the drug screening can be conducted at any of 4-8 groups. As it was shown, these groups have viable, functional cells that mimic

3D in vivo tissue with relatively low and stable proliferation level and high activity what will be perfect for drug screening. Drug screening on 3D models have an advantage over 2D cultures, by proper design of 3D models it can perfectly mimic targeted tissue, including blood vessels, variety of cell types and tissue complexity, which is out of reach in 2D cultures. Over in vivo mice testing, 3D model can have a benefit as well, because it will mimic human tissue, which has differences from mice.

Thus, the second conducted study presented here, proved that EHDJ encapsulation system is safe, easy in manipulation, and suitable for organ printing application. The next set of experiments will be focused on tissue fabrication, its maturation, *in vitro* functionality testing and following *in vivo* implantation.

4.6 Conclusions

For successful 3D tissue fabrication, cell homeostasis and niche have be to deeply studied and controlled for every tissue engineering method. This chapter presents a detailed evaluation of EHDJ encapsulation system effect on cell behavior during the maturation process for organ printing application. The conducted study, supported the hypothesis presented in the previous chapter, cells recover from encapsulation stress within one week, and after they actively modify alginate bead microenvironment to their functional niche within 3 weeks, thus by the end of the 4th week fabricated microbeads were ready for implantation. Moreover, there was described a variety of possible applications for EHDJ fabricated beads, such as 3D models for pathologies investigation, so as for drug screening.

Acknowledgements

Authors acknowledge the Centre of Integrative Biology (CIBIO) of University of Trento for providing SHSY5Y cell line.

Chapter 5

Fabrication of complex 3D structures with photolithographic encapsulation and following magnetic levitational assembly.

This part of work was conducted during PhD internship under the supervision of Prof. Utkan Demirci at Stanford University School of Medicine, Canary Center at Stanford for cancer early detection, USA. The results of the conducted study resulted in 2 publications:

- Tasoglu, S., Yu, C.H., Liaudanskaya, V., Guven, S., Migliaresi, C., Demirci, U. (2015) Magnetic levitational assembly for living material fabrication. Advanced healthcare materials (in press).
- Namkoong B.*, Guven S.*, Ramesh S., Liaudanskaya V., Abzhanov A., Demirci U. Recapitulating cranial osteogenesis with neural crest cells in 3-D microenvironments. STEM CELLS (Submitted).

5.1 Abstract

Functional 3D micro tissue fabrication is critical for many fields, such as tissue engineering, *in vitro* models for developmental and molecular biology and others. Originally most of the body tissues are complex, composed of variety of cell types, with perfectly aligned microunits, like kidney or neural layers of grey matter and other unique tissue characteristics. Thus, creation of 3D micro tissues in vitro composed of functional micro units, each predetermined with its composition, functionality and shape to recapitulate body tissues is challenging. In this chapter presented a promissing and simple approach for creation of functional living structures with controllable structural, morphological, and

chemical features using photolithographic encapsulation system for fabrication of small building units and its following assembly into more complex 3D structures with magnetic-based levitational method. This strategy allows production of functional shape-controllable units with defined structure and composition and their alignment in a paramagnetic suspending media into complex 3D structure, mimicking natural tissue.

5.2 Introduction

3D micro tissue fabrication *in vitro* became very important to study cell and tissue physiology, moreover as tissue/organ replacements for regenerative medicine [201, 217]. 3D microenvironment has a dramatic effect on many cell growth parameters, such as diffusion of growth factors or other important proteins, stem cells differentiation; moreover, it might also have an impact factor for morphological changes over larger scale, such as morphogenesis and others [216]. It was also demonstrated that cellular microenvironment plays a crucial role in cell phenotype fate orientation, for example, phenotype can supersede genotype simply due to interaction with ECM [192]. Culturing cells in 3D gives a direction for recapitulation of *in vivo* cell growth.

Thus, 3D microtissues have a critical role in tissue engineering for transplantation, restoration and recovery of damaged tissues, but also as cancer models for molecular analysis *in vitro*, and as a tool for new drugs efficacy and toxicity screening [203-210, 212, 213, 214, 215].

There were developed several approaches for a successful 3D complex tissue fabrication such as top-down and bottom-up [12, 14, 15, 21, 27]. Top-down approach is widely used in TE, but it does not allow the production of geometrically well-defined complex constructs that may cause some difficulties such as vascularization of large scaffolds, and 3D spatial orientation of different cell types [12]. Bottom-up approach can overpass these problems. In the last decade bottom-up approach was deeply investigated and variety of methods were developed for successful 3D complex tissue fabrication such as extrusion- and lithography-based methods, bioprinting, magnetic, robotic and levitational assembly of cell-laden units, cell sheets or aggregates [24, 25, 26, 27, 34].

Photolithography, is one of the commonly used methods for micro tissues fabrication in bottom-up approach, initially it was developed for application in microelectronics, however around a decade ago it found an application in tissue fabrication. At present, photolithographic encapsulation

applied for fabrication of microengineered hydrogels that can be used for different purposes, such as 3D models fabrication for structural biology research, drug screening, self-assembly methods for tissue engineering and many others [67, 68, 69]. This technology became feasible in tissue engineering partly because of discovery and development of natural and synthetic photo cross-linkable biopolymers [41, 103, 104, 105]. Polymer crosslinking happens through exposure to UV light. Generally, thin masks are used to create a desirable final shape hydrogels. Masks have to be designed in black and transparent parts, in the way just transparent part will allow pass the UV light and crosslink the sensitive material. After UV exposure, not cross-linked material will be washed away, and just solid hydrogels will be left on the cover slip. The final resolution of fabricated hydrogels can be vary from sub microns to millimeters. When the average cell size is around 10 microns, thus this technology allow encapsulation of high cell densities in microstructures.

However, hydrogels produced with photolithographic system have simple composition that doesn't mimic the complexity of the natural tissues. Thus, small cell-laden units with controlled shape and composition have to be assembled into more complex ones. Techniques for aligning and assembling soft biological or non-biological components reliably in three dimensions (3D) are critical for several current micro/bio-manufacturing processes such as bottom-up tissue engineering and significant for a range of other applications including automated manufacturing lines and inspecting products for quality control [217]. In the last decade, there were presented many methods for micro-units assembly without guidance, such as fluidic force [218], magnetic force [35, 219-220], gravity [220] and guided assembly, like railed microfluidics [221], robotic assembly [24], acoustics [26], magnetics [35, 133] and others [222, 223, 224, 225].

Here is presented contactless and nanoparticle-free approach for tissue self-assembly, magnetic levitation. This method is based on the principle of

levitating subjects in paramagnetic suspension [35]. Salt ions of gadolinium (Gd^{3+}) and magnesium (Mn^{2+}) or radicals have paramagnetic properties, thus can be applied for cell-laden units levitation. However, paramagnetic suspension might have a toxic effect on cells, thus it has to be evaluated prior the tissue fabrication.

NIH3T3 mouse fibroblasts were encapsulated in photo-crosslinkable polymers: modified gelatin (GelMA) and polyethylene glycol diethacrylate (PEGDA), or seeded on laminin-coated beads, with following levitational assembly in the media suspension with ions of Gd^{3+} salt. Cells behavior parameters were evaluated with Live/Dead and Alamar Blue assays for viability, immunocytochemistry to ki67/collagen1/phalloidin to demonstrate cells proliferation potential, activity and functionality post-assembly.

The main goal of this chapter is to demonstrate powerful yet simple approach for creation of complex living microtissues with tunable features using photolithographic encapsulation system and magnetic levitational assembly, moreover, to evaluate the fabrication and assembly processes effect on the biological parameters such as cell viability, proliferation and activity. Presented approach allows fast fabrication of various shaped hydrogels or cell seeded microbeads and following alignment in a paramagnetic suspending media into functional 3D microtissues.

5.3 Materials and methods

Cell culture.

NIH3T3 Mouse fibroblasts cell line was expanded in 25-175-mm tissue-treated culture flasks as a monolayer at 37°C under 5% of CO_2 in high glucose Dulbecco's Modified Essential Medium (DMEM) with 10% fetal bovine serum (GIBCO), 2mM Glutamine and 1% antibiotic/antimicotic mixture (Sigma, USA). DMEM medium was changed every 3rd day. Cells were cultured to 90-95% confluency before encapsulation.

Hydrogel preparation.

GelMA (gelatin methacrylate) 5% (wt/v) prepolymer solution was prepared by first dissolving the photo-initiator (PI) 0.5% (w/v) in PBS. When the PI was dissolved completely foam-like GelMA 5% (wt/v) was added and dissolved at 80°C.

PEG (polyethylene glycol) 15 % (w/v), 19.7 % (w/v) and 50 % (w/v) PEGDMA 1000 (Polysciences Inc.) were prepared by dissolving PEGDMA into PBS. Then, 1 % (w/v) photo-initiator (Igracure 2959, Ciba) was added into the mixed solution. The mixed solution was placed into the 80° oven for 20 minutes to form prepolymer solution.

Encapsulation by UV crosslinking.

GelMA: 100 µl of cell suspension in prepolymer solution was placed on a cover slip and photo-crosslinking was performed with UV-light intensity of 2.6 mW/cm^2 for 15 seconds for GelMA (Omnicure S2000). 2 mm round with 150um thickness cell encapsulated hydrogels were obtained using UV photo mask. Cell-laden hydrogels were washed with PBS to remove any remaining prepolymer solution and submerged in cell culture media after placed in an incubator (5% CO_2, 37°C).

PEGDMA: 300 µl of 15% PEG prepolymer solution was pipetted onto 600 µm spacer, and exposed under UV light (2.9 W/cm2, 5 cm between the light source and prepolymer solution) for 30 seconds to achieve gelation. With the same parameters of UV light, for 19.7 % PEGDMA, 600 µl was pipetted, while for 50 % PEGDMA the volume of pipetted solution was 1.3 ml. Different shapes of photomasks were also used for different concentrations. Smallest disk shape (r=2 mm) photomask was for 15 % PEGDMA, medium donut shape (inner diameter r2=1.5 r) was for 19.7 % PEGDMA, and largest donut shape (inner diameter r3=1.1 r2) was for 50 % PEGDMA.

Hydrogels levitation

After UV crosslinking, three gels with different sizes and shapes were picked up carefully and placed into paramagnetic medium within a plastic reservoir (3.3 cm x 3.3 cm x 2.7 cm), and a 3 mm thick rectangular PMMA (3.3 cm x 5 cm) was covered to cap the reservoir. The plastic reservoir was connected to a syringe pump (WPI, Programmable Syringe Pump), serving as a medium pumping system used after achieving levitation. Cell-laden gels were assembled with the levitation set up in 50mM GD solution. The PMMA chamber was exposed to magnetic force created by two magnets (same poles facing each other), and the distance between the two magnets was 3 cm. During the levitation, the 50 % PEGDMA gel would be at the bottom layer, the 19.7 % PEGDMA gel would be at the middle layer, and the 15 % PEGDMA gel would be levitated at the top layer. After all the gels were levitated and achieved equilibrium in the middle of reservoir, the solution draining process was started. The flow rate of syringe pump was set as 3 ml/min. Under this flow rate, the force created during the withdrawing process would not affect the gels' position.

Beads coating with NIH3T3 cells.

Polystyrene divinylbenzene beads (manufactured) were coated with 20μg/ml laminin for overnight at 4C° to enhance cell adhesion. Laminin-coated beads were placed in advanced prepared 24-well plate coated with agarose. After the solution of 5 million of NIH3T3 cells in 1ml of DMEM was added to the beads and placed at 37C°, 5% CO_2. After 2 days beads were seeded with 5 million cells for the second time. Beads were incubated with cells in total for 5 days.

Levitation set-up of beads coated with NIH3T3 cells.

Cell-laden beads were assembled with the levitation set up in 50mM GD solution. Total time exposure to GD solution 10 min: beads assembly followed by drainage of GD solution. Assembled beads were collected on the cover slip on the bottom of the chamber. After assembly beads were crosslinked by embedding them in 5% GelMA (0.5% PI) and exposure to UV light with 2.6 mW/cm^2 intensity for 15 sec. After samples were submerged in cell culture media and placed in an incubator (5% CO_2, 37°C).

In vitro evaluations.

Viability assay.

Cell viability was evaluated by fluorescence visualization of samples stained with calcein/EthD-1. In brief samples were incubated for 20 min at 37°C in a solution of calcein/EthD-1 (2mM calcein and 2mM EthD-1). After that the supernatant was removed, the hydrogels were washed 2-3 times with a PBS solution. Cell counting was made with ImageJ cell counter plugin. Assembled and crosslinked cell-laden beads were submerged to viability evaluation with Alamar Blue assay every second day after the levitation. 10% solution of Alamar Blue in DMEM was added to samples for 4 hours. After 100 μl was taken in

triplicate and analyzed using fluorescent reader machine. Beads without cells crosslinked with GelMA were used as a BLANK for this assay.

Immunocytochemistry.

Levitated and crosslinked cell-laden beads/samples were fixed with PFA 4% for 30 min, after samples were blocked and permeabilized with blocking buffer (1% BSA, 0,3 % TritonX in PBS) for 1 hour. Primary antibodies for Ki67 (Abcam ab16667) and collagen I (Abcam ab6308) were applied for overnight at 4C°. After PBS washing was performed 3 times for 10 minutes. Secondary anti-mouse for collagen-1 and anti-rabbit for ki67 antibodies were applied for 1 hour at room temperature with following 3 times washing in PBS. At last, DAPI solution was applied for 5 min. After washed twice with PBS. Results were analysed with the confocal microscope (Leica).

Statistical analysis.

All statistical analysis was performed with GraphPad Prism 6 software. Statistical analysis for more than two groups was carried out using one-way ANOVA with Tukey's post-hoc tests. $P<0.05$ was considered significantly different.

5.4 Results and discussion

There was conducted a set of experiments to evaluate an appropriate GD salt concentration and time exposure that will be least harmful for cells but suitable for levitational assembly. NIH3T3 cells (10mln cells per 1ml of prepolymer solution) were encapsulated in 5% GelMA (gelatin methacrylate) hydrogels with diameter of 500μm and thickness of 150μm (Figure 5.1).

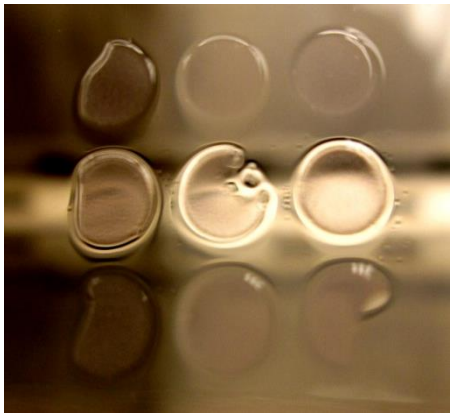

Figure 5.1: Example of GelMA hydrogels for GD salt toxicity evaluation.

Effect of GD at different concentration and time exposure on cell viability.

Initially, to understand the range in which GD salt will be safe for cells, the following set of experiments was performed. The results of conducted experiments are shown in Figure 5.2A-B.

1. Effect of different GD concentration on the cell viability (Figure 5.1A). 3 concentrations of GD salt were prepared: 10mM, 50mM, 100mM. Set of GelMA hydrogels was prepared straight before test. Hydrogel parameters with encapsulated NIH3T3 cells: d=500μm, thickness of 150μm. Samples were exposed to different GD salt concentrations for 10 minutes.

2. Effect of 50 mM GD salt exposure for different time on the cell viability (Figure 5.2B). Hydrogels were exposed to 50mM GD solution for 5 min, 15 min

and 60min. Set of hydrogels was prepared straight before test. GelMA hydrogel parameters with encapsulated NIH3T3 cells: d=500μm, thickness of 150μm.

Based on the first experiment GD concentration of 50mM was chosen as the best working concentration for the levitation and cells viability (Figure 5.2 A). With increase in GD salt concentration, there was observed an increased rate of the cell death. Exposure to 50 mM GD salt for 10 min showed around 95% cell viability. Based on the results of the next experiment, there was observed that exposure for 1 hour to 50 mM GD salt decreases the viability for almost 40% percent, which not desirable for tissue engineering application. Exposure to 5 and 15 min showed high level of cell viability and suitable for application in tissue engineering. Based on the levitational assembly of cell-free hydrogels prior the viability experiments, it was observed that 10 min is optimal time for all the assembly and gels retrieve.

All the following experiments for cell-laden hydrogels or building units were conducted using 50mM GD salt and time exposure 10 minutes.

Effect of 50 mM GD salt exposure for 10 minutes for long-terms cell viability, functionality and activity.

Levitational assembly was designed for implementation in numerous fields including regenerative medicine, cell-based pharmaceutical research and tissue engineering. The initial set of experiments proved to be safe for cells viability at proper GD exposure conditions, but for mentioned above applications long-term post-levitational effect on cells viability and functionality as important as immediate.

At first, cells long-term viability was measured every second day after GD exposure with Live/Dead assay. The results of treated samples were compared to the control group of cells encapsulated in GelMA hydrogels (in the same conditions as studying groups) but were not exposed to GD salt. Results are presented in Figure 5.2 C-D.

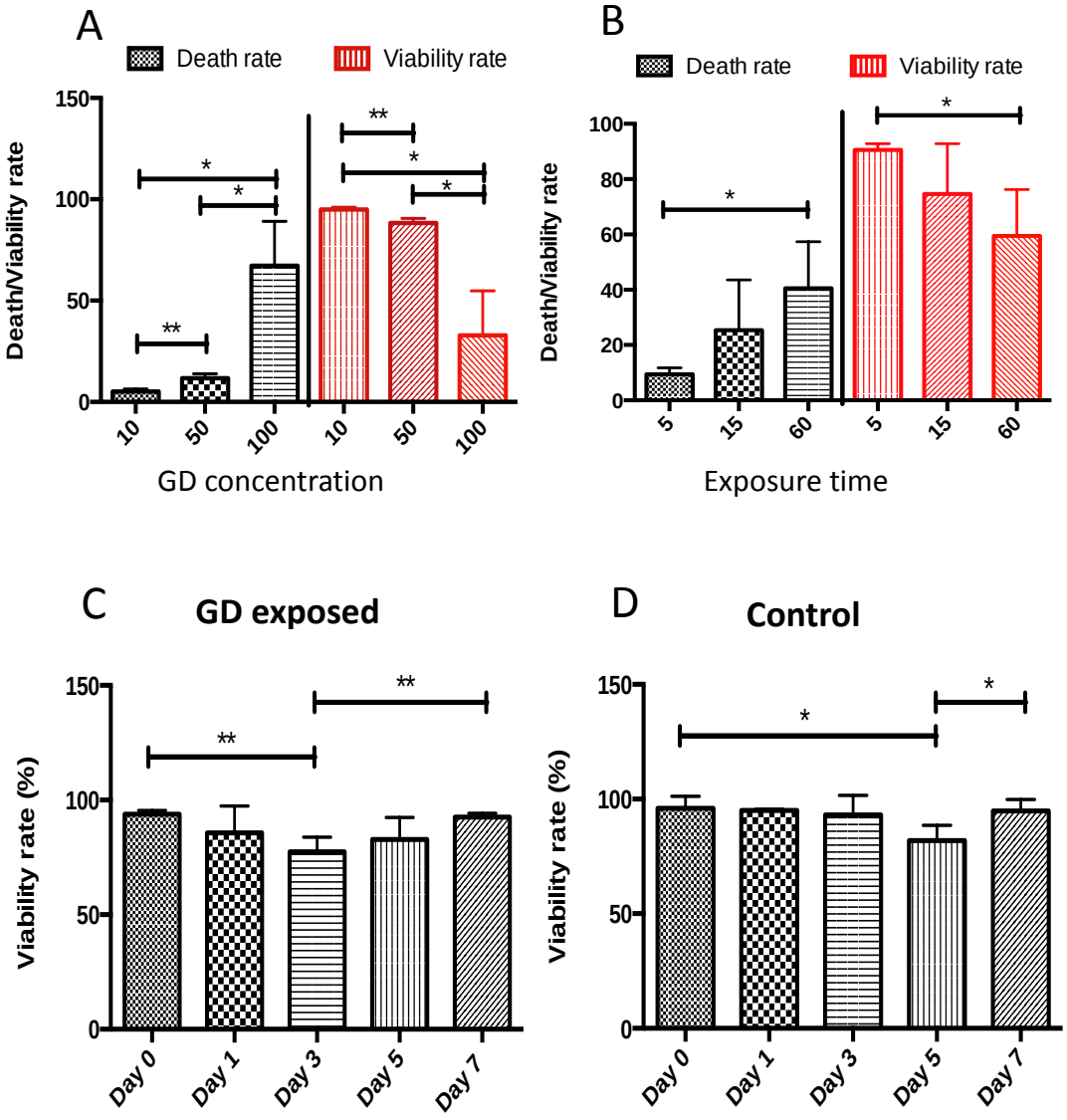

Figure 5.2: Cell viability after GD exposure: A) at different concentration; B) at different time. Long-term viability results of 50mM GD treated/not treated hydrogels for 10 minutes. Lines connecting individual groups indicate statistically significant difference. One-way ANOVA with Tukey's post-hoc tests, *p<0.05, **p<0.01.

Next, Gd salt exposed samples were evaluated for expression of cell functionality markers: ki-67 and collagen1, which are responsible for proliferation potential and extra cellular matrix production, respectively. Samples were evaluated for above mentioned markers expression every second day after Gd salt treatment. Results are presented in Figure 5.3.

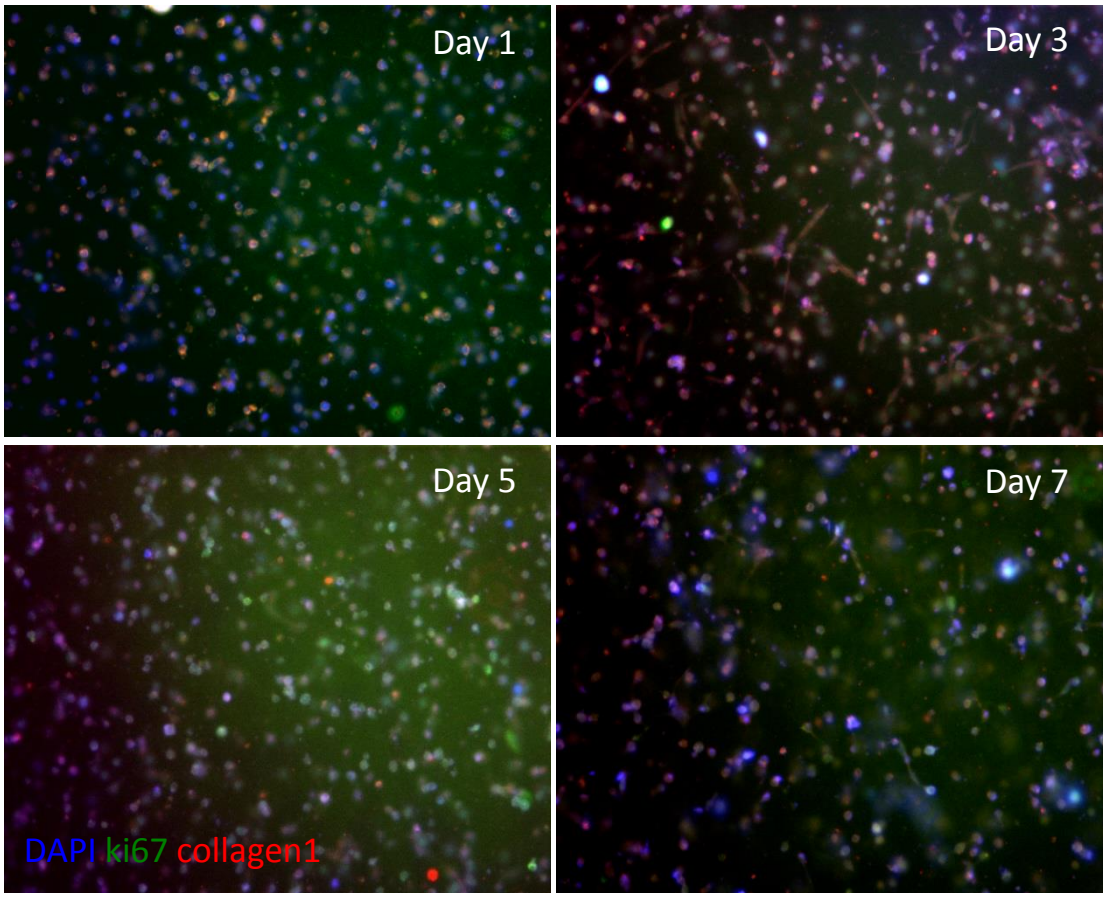

Figure 5.3: Long-term effect evaluation of GD exposure on cells proliferation capacity and ability to produce ECM with immunocytochemistry to ki67 and collagen type 1.

Conducted experiments demonstrated cells stay alive with no significant differences from the control group for up to 7 days after GD exposure (Figure 5.2 C-D), most importantly cells were expressing proliferation marker, and also

performed they main function, extracellular matrix production (Figure 5.3) and cell niche formation.

However, during the daily microscope analysis of samples there was noticed the difference in cell proliferation rate and behavior between studying and control samples. Cells in the control samples proliferated with higher rate than in GD treated samples. It was hypothesized that GD salt exposure might affect the cells proliferation rate.

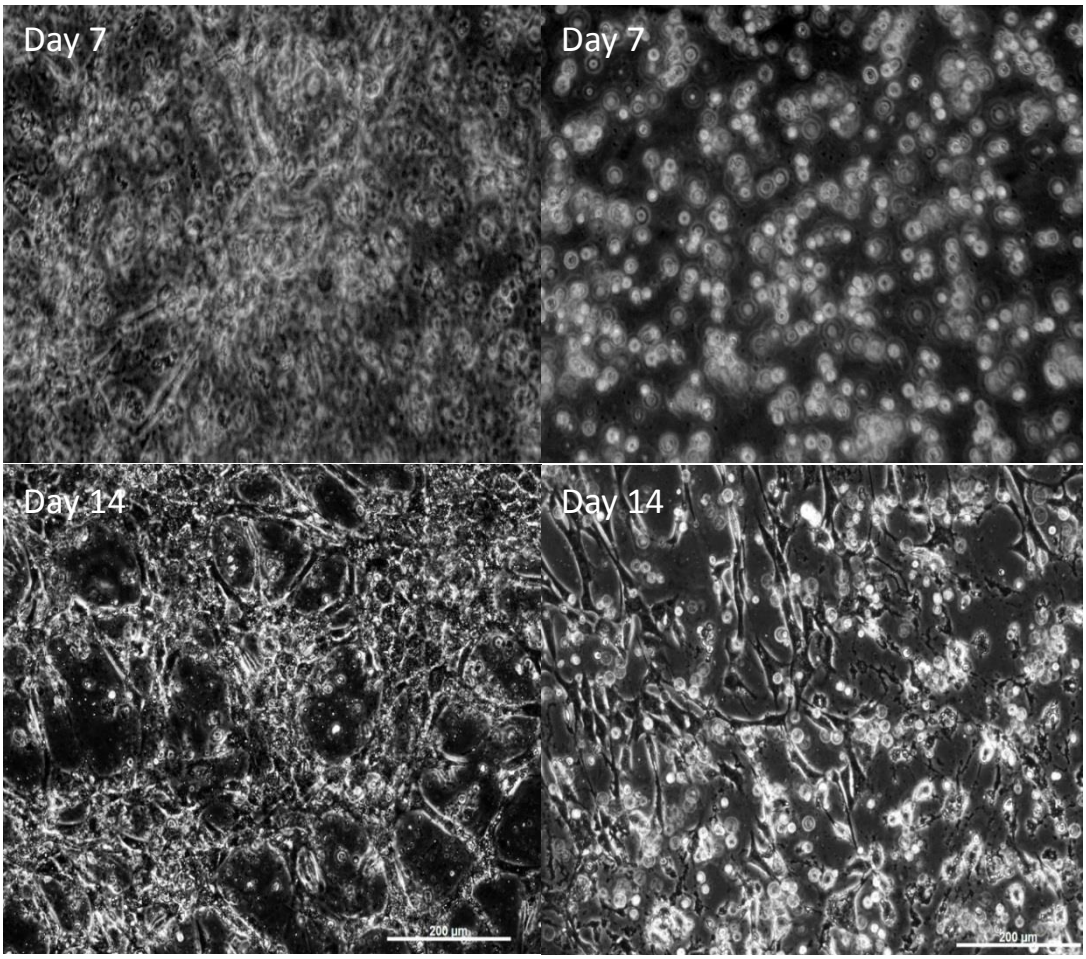

Figure 5.4: Brightfield images of not treated/treated with GD cell-laden 5% GelMA hydrogels at days 7 and 14.

Thus, the next experiment was conducted to evaluate the time needed for full recovery of cells after GD treatment. Gd treated samples were cultured in full media in CO_2 incubator and compared to the control with brightfiled microscope imaging daily, until the similar confluency has been, as it presented in Figure 5.4.

Hydrogels self-assembly by the levitation.

Donut-shape PEG hydrogels were prepared in three different concentrations 9,5; 10 and 10,5 (% w/v) as it was described in methods part above. And assembled in 50 mM GD in chamber placed between two magnets (Figure 5.5).

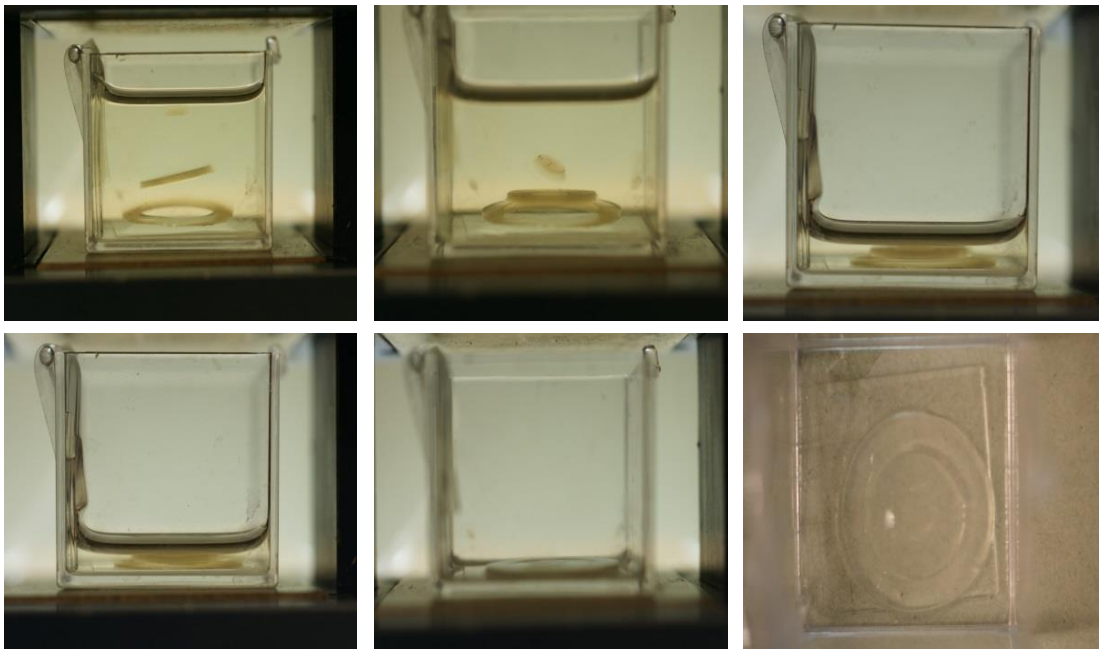

Figure 5.5: Levitational self-assembly of soft micro-components. Concentric assembly of two hollow-disk and a solid-disk PEG gels.

It took about 2-3 minutes to assemble hydrogels. To retrieve the assembled construct GD solution was drained using the syringe pump (5-7

minutes). To maintain the assembled construct secondary UV crosslinking with PEG was applied.

To analyze the effect of levitation on viability of assembled samples, live/dead test was made before the levitation and immediately after (Figure 5.6 A).

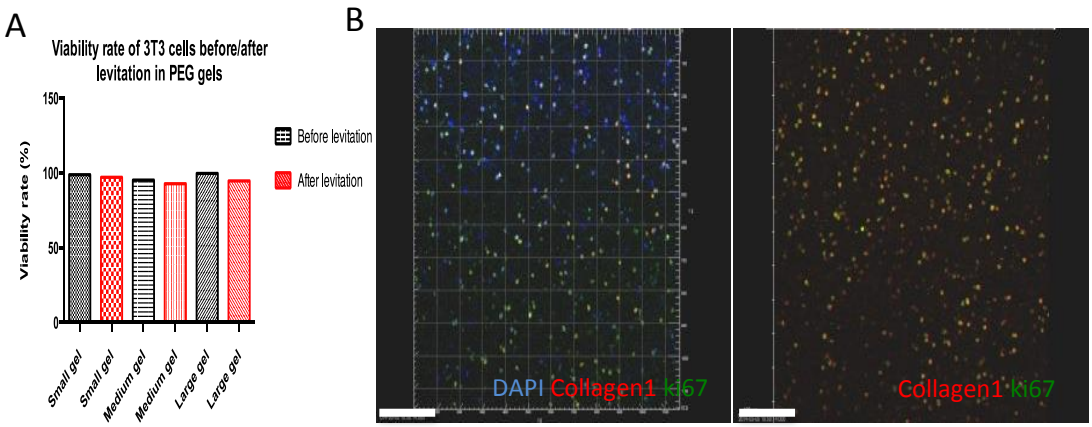

Figure 5.6: A) Live/Dead test before and immediately after the levitational assembly. B) Immunocytochemistry assay to ki67 and collagen type 1 markers.

Next, assembled hydrogels were maintained for 7 days in full media in CO_2 incubator and after analyzed for proliferation rate and ability to produce extracellular matrix with ki67 and collagen type 1 markers expression.

As it presented in Figure 5.5 the assembly was performed successfully, with precise alignment of hydrogels according to their weight and size. The Live/Dead assay of levitated/not levitated samples showed no significant differences. Also, we demonstrated the cells were functional with ki67 and collagen1 markers expression.

Levitation of manufactured beads coated with cells.

To demonstrate the broad application for levitational set-up with units in different size and shape, there were prepared cell-seeded beads (described in details in methods) and assembled with the levitational set-up (Figure 5.7).

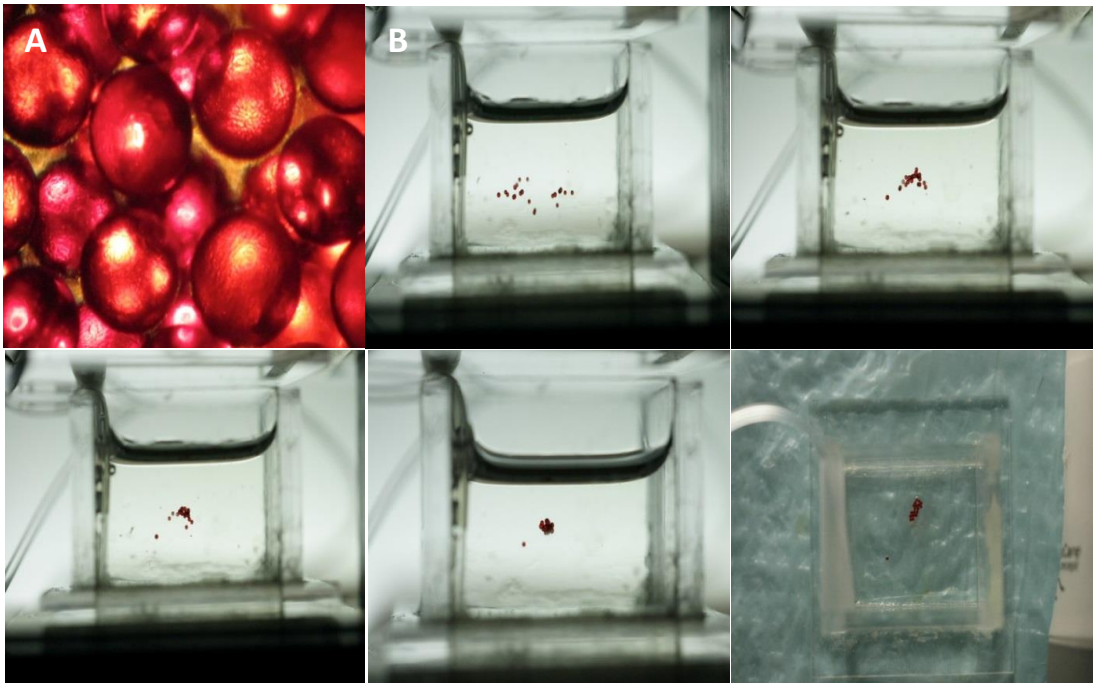

Figure 5.7: A) Cell-seeded beads before the assembly; B) Beads assembly process by the levitational set-up.

Cells were analyzed for viability and activity with Live/Dead kit, however the results were not conclusive. The beads size was large and its original color was red, which gave an artificial effect during the results evaluation with fluorescent microscope. Live/Dead kit wouldn't allow the quantification of the results. Thus, for viability evaluation of levitated beads Alamar Blue assay was used (Figure 5.8). For proliferation and activity evaluation samples were fixed at Day 1 and Day 7 and stained with antibodies for ki67 (proliferation marker) and collagen type 1 (ECM marker), phalloidin (cytoskeleton) and DAPI (nuclei)

for immunocytochemitry. The results were analyzed with the confocal microscope (Figure 5.8).

Viability assay showed cells were alive after assembly with the levitation set up, and also their activity was increasing to the 7th day after the levitation. IC results showed cells proliferated and produced niche markers (collagen1 and phalloidin).

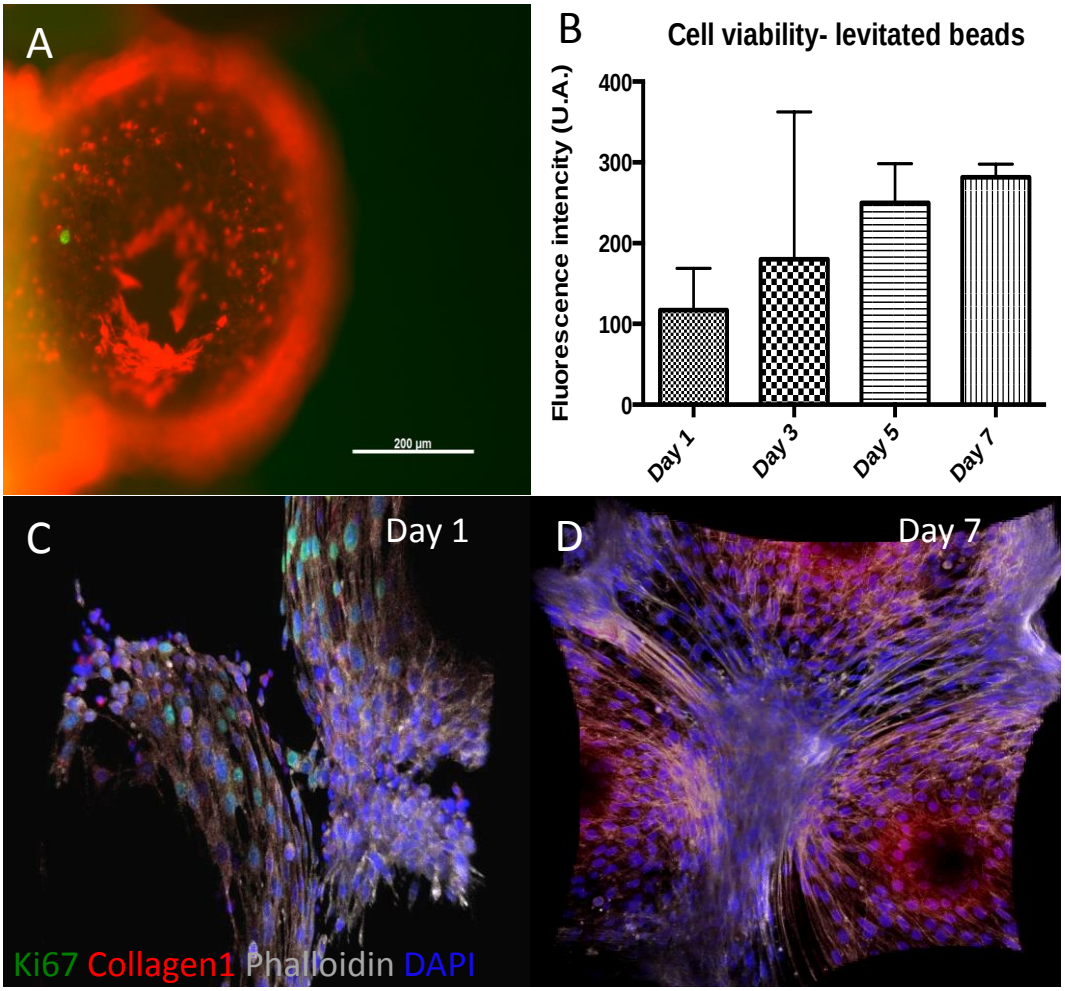

Figure 5.8: A) Viability with Live/Dead kit; B) Viability assay with Alamar Blue assay; C) Immunocytochemistry at day 1; and D) day 7 to ki67, collagen1, phalloidin and DAPI.

Based on the conducted experiments, we showed that GD salt has mild stress effect on cells depends on the salt concentration and time exposure. Thus, before application of this method in tissue engineering, the proper working concentration and time exposure has to be evaluated for each specific cell line. The experiments with NIH3T3, model cell line has stable resistant phenotype, showed that concentration of GD salt higher than 50mM might be lethal, but for more sensitive cells like stem cells, this threshold can be lower, so as for the time exposure. It was shown that viability of NIH3T3 cell-laden blocks exposed to 50mM GD salt for 15 min was comparable to the control samples that were not exposed to GD salt. Moreover, there was also analyzed cells functionality and activity in long-terms (7 days) with expression of ECM marker collagen1 and ki67 proliferation marker. Besides observed high level of above mentioned markers, it was also observed with brightfield images that cells within 2 weeks were adapting to artificial matrix environment and modified it to their functional niche which would support their proliferation and activity (Figure 5.3-5.4).

There was demonstrated the safety and flexibility of photolithographic encapsulation system and following levitational-based magnetic assembly of simple building units, moreover, its simplicity in manipulation, so as high level of control over the samples fabrication and assembly. The levitational assembly approach of photocured cell-laden hydrogels presented here offers a parallel precise patterning capability to create 3D complex microtissues [34, 35]. Additionaly to levitation of photocrosslinked cell-laden hydrogels, there was presented another building block type – cell-seeded beads, which as were easily and precisely assembled in complex 3D structures by magnetic levitation, and showed high viability, activity, proliferation and functionality levels (Figure 5.8).

The presented method of patterning and assembly of cell-encapsulating/seeded micro-components might find several broad applications in numerous fields including regenerative medicine, cell-based pharmaceutical

research and tissue engineering [24, 33, 36].

5.5 Conclusions

In summary, in this chapter there was demonstrated a strategy for cell-encapsulating/seeded building units fabrication such as microgels or beads and following patterned assembly in a contactless manner into 3D complex structure. The presented strategy allows programming of each building block by composition, stiffness, elastic modulus, porosity, or cell type and then levitationally assembled with other building blocks into complex constructs with unique spatially heterogeneous material properties. Moreover, it shows high scaling potential, good cell viability and functionality, but also simplicity in manipulation and guidance of hydrogels assembly, what makes levitational assembly approach very promising for bottom-up tissue engineering. Additionally, this strategy can be employed to generate soft living 3D hydrogel systems to be used in soft robotics, or heterogeneous microphysiological systems for pharmaceutical research and diagnostics.

Chapter 6

General conclusions

The overall objective of this thesis was detailed evaluation of the effect of organ fabrication process on cell parameters, like viability, activity, proliferation and ability to maintain homeostasis in artificial 3D environment, moreover selection of the best encapsulation conditions for successful tissue maturation.

The general idea was to analyze cell behavior during the organ printing steps on the molecular level. We hypothesized that viability testing immediately after encapsulation doesn't represent the whole picture of the cells state. Thus, we designed a detailed protocol to evaluate cell behavior during the all stages of tissue fabrication process that included a set of posibile changes on the molecular level in cell behavior. Next, for the successful tissue maturation, we evaluated the best encapsulation time based on the cells viability, proliferation rate, ability to maintain homeostasis, and adapt the artificial environment to their functional niche. At last, we developed an easy and safe way to assemble simple building units into more complex 3D structures, and proved it to be safe for cell behavior.

Initially, we evaluated the effect of EHDJ encapsulation system on cells stress state, viability, activity and proliferation. The results showed, that encapsulation process has mild stress effect on cell behavior, but within first week of encapsulation cells were able to completely recover, and started to modify the artificial alginate environment by production of extracellular matrix components. Within the following 2 weeks, we suppose the artificial microenvironment was adapted to the cell functional niche, because there was observed a drastic shift in cells activity and proliferation.

Thus, based on the conducted initial study, we hypothesized that the best encapsulation time for tissue maturation will be at least four weeks, by that time

cells would be recovered from fabrication process stress, and adapt the artificial environment for their proper functioning. To prove this hypothesis, we released cells from the artificial alginate matrix and reseeded them in control environments in tissue culture plates, to evaluate the cells behavior. The obtained results supported the hypothesis, and showed that cells encapsulated for four weeks had the best parameters and functionality for tissue transplantation. There was also suggested a variety of other applications of 3D microtissues fabricated with EHDJ method besides the tissue transplantation, based on the cell behavior parameters.

At last, the detailed effect of another encapsulation system (photo-crosslinking based) was evaluated for safe simple building units preparation, and applied in magnetic levitational assembly for fabrication of complex 3D structures with controlled composition and design. We presented a safe contactless way for tissue self-assembly and its application in different fields of science.

The further research will be focused on the direct soft tissue fabrication, like neural, cartiladge or liver and its *in vitro* functionality testing, followed by *in vivo* transplantation. Additionally, the modification of the artificial environments will be made to improve and speed up the tissue maturation process.

Bibliography

1. Vacanti, C.A. (2006) History of Tissue Engineering and A Glimpse into its Future, *Tissue Engineering 12*, 1137-1142.
2. Ikada, Y. (2006) Challenges in tissue engineering, *Journal of The Royal Society Interface 3*, 589-601.
3. Chang, C., Gupta, G. (2010) Tissue engineering for the hand: Research Advances and Clinical Applications. World scientific publishing group. Co. Pte. Ltd. Singapore
4. Langer, R., Vacanti, J.P. (1993) Tissue Engineering. *Science* 260, 920.
5. Atala, A. (2011) Tissue engineering of human bladder. *British Medical Bulletin* 97, 81-104.
6. Chen, M., Przyborowski, M., Berthiaume, F. (2009) Stem cells for skin tissue engineering and wound healing. *Critical reviews in biomedical engineering* 37, 399-421.
7. Yildirimer, L., Thanh, N.T.K., Seifalian, A.M. (2012) Skin regeneration scaffolds: a multimodal bottom-up approach. Trends in biotechnology 30, 638-648.
8. Chandrasekaran, A.R., Venugopal, J., Sundarrajan, S., Ramakrishna, S. (2011) Biomedical materials 6, 1-10
9. Madeira, C., Santhagunam, A., Salgueiro, J.B., Cabral, J.M.S. (2014) Advanced cell therapies for articular cartilage regeneration. Trends in Biotechnology 33, 35-42.
10. Amini, A.R., Laurencin, C.T., Nukavarapu S.P. (2012) Bone Tissue Engineering: Recent Advances and Challenges. *Critical reviews in biomedical engineering* 40, 363-408.
11. Pellegrini, G., De Luca, M. (2014) Eyes on the Prize: Limbal Stem Cells and Corneal Restoration. Cell Stem Cell 15, 121-122.

12. Tiruvannamalai-Annamalai, R., Armant, D.R., Matthew, H.W.T. (2014) A glycosaminoglycan based, modular tissue scaffold system for rapid assembly of perfusable, high cell density, engineered tissues. PLOS ONE 9, 1-15.
13. Rahfoth, B., Weisser, J., Sternkopf, F., Aigner, T., von der Mark, K. Brauer, R. (1998) Transplantation of allograft chondrocytes embedded in agarose gel into cartilage defects of rabbits. Osteoarthritis and cartilage/OARS, Osteoarthritis Research Society 6, 50-65.
14. Onoe, H., Takeuchi, S. (2014) Cell-laden microfibers for bottom-up tissue engineering. Drug Discovery today (in press).
15. Liu, Y., Mai, S., Li, N., Yiu, C.K.Y, Mao, J., Pashley, D.H., Tay, F.R. (2011) Differences between top-down and bottom-up approaches in mineralizing thick, partially demineralized collagen scaffolds. Acta Biomaterialia 7, 1742-1751.
16. Heden, P., Sellman, G., von Wachenfeldt, M., Olenius, M., Fagrell, D. (2009) Body shaping and volume restoration: the role of hyaluronic acid. Aesthetic plastic surgery 33, 274-282.
17. Holzman, S., Connolly, R.J., Schwaitzberg, S.D. (1994) Effect of hyaluronic acid solution on healing of bowel anastomoses. Journal of investigative surgery: the official journal of the Academy of Surgical Research 7, 431-437.
18. Silva, S.S., Motta, A., Rodrigues, M.T., Pinheiro, A.F.M., Gomes, M. E., Mano, J. a. F., Reis, R.L., Migliaresi, C. (2008) Novel genipin-cross-linked chitosan/silk-fibroin sponges for cartilage engineering strategies. Biomacromolecules 9, 2764-2774.
19. Motta, A., Fambri, L., Migliaresi, C. (2002) Regenerated silk fibroin films: thermal and dynamic mechanical analysis. Macromolecular chemistry and physics 203, 1658-1665.

20. Unger, R.E., Wolf, M., Peters, K., Motta, A., Migliaresi, C, James Kirkpatrick, C. (2004) Growth of human cells on a non-woven silk fibroin net: a potential or use in tissue engineering. Biomaterials 25, 1069-1075.
21. Nichol, J.W., Khademhosseini, A. (2009) Modular tissue engineering: engineering biological tissues from the bottom up. Soft matter 5, 1312-1319.
22. Liaudanskaya, V., Gasperini, L., Maniglio, D., Motta, A., Migliaresi, C. (2015) Assessing the impact of electrohydrodynamic jetting on encapsulated cell viability, proliferation, and ability to self-assemble in three-dimensional structures. Tissue Engineering Part C (in press).
23. Guillotin, B., Guillemot, F. (2011) Cell pattering technologies for organotypic tissue fabrication. Trends in biotechnology 29, 183-190.
24. Tasoglu, S., Yu, C.H., Gungordu, H.I., Guven, S., Vural, T., Demirci, U. (2014) Guided and magnetic self-assembly of tunable magnetoceptive gels. Nature Communications 5, 1-11.
25. Tasoglu, S., Diller, E., Guven, S., Sitti, M., Demirci, U. (2014) Untethered micro-robotic coding of three-dimensional material composition. Nature communications 5, 1-9.
26. Chen, P., Luo, Z., Guven, S., Tasoglu, S., Ganesan, A.V., Weng, A., Demirci, U. (2014) Microscale assembly directed by liquid-based template. Advanced materials 26, 5936-5941.
27. Murphy, S.V., Atala, A. (2014) 3D bioprinting of tissues and organs. Nature biotechnology 32, 773-785.
28. Mironov, V., Trusk, T., Kasyanow, V., Little, S., Swaja, R., Marward, R. (2009) Biofabrication: a 21st century manufacturing paradigm. Biofabrication 1, 1-16.
29. Mironov, V., Kasyanow, V., Drake, C., Marward, R. (2008) Organ printing: promises and challenges. Future Medicine 3, 93-103.

30. Melchels, F.J. Malda, N. Fedorovich, J. Alblas, and T. Woodfield (2011) Organ Printing. In: P. Ducheyne, ed. Comprehensive Biomaterials. Radarweg 29, Amsterdam, Netherlands: Elsevier Ltd., pp. 587–606.
31. Federovich, N.E., Albas, J., Wijn, J.R.D., Hennik, W.E., Verbout, A.J., Dhert W.J.A. (2007) Hydrogels as extracellular matrices for skeletal tissue engineering: state-of-the-art and novel application in organ printing. Tissue Engineering 13, 1905-1925.
32. Tasoglu, S., Demirci, U. (2013) Bioprinting for stem cell research. Trends in biotechnology 31, 10-19.
33. Gurkan, U., Tasoglu S., Kavaz, D., Demirel M.C., Demirci, U. (2012) Emerging technologies for assembly of microscale hydrogels. Advanced healthcare materials 1, 149-158.
34. Tasoglu, S., Yu, C.H., Liaudanskaya, V., Guven, S., Migliaresi, C., Demirci, U. (2015) Levitational assembly for biomaterial fabrication. Advanced healthcare materials (in press).
35. Tasoglu, S., Kavaz, D., Gurkan, U.A., Guven, S., Chen, P., Zheng, R., Demirci, U. (2013) Paramagnetic levitational assembly of hydrogels. Advanced materials 25, 1-15.
36. Namkoong, B., Guven, S., Ramesh, S., Liaudanskaya, V., Abzhanov, A., Demirci, U. (2015) Recapitulating cranial osteogenesis with neural crest cells in 3-D microenvironments. STEM CELLS (Submitted)
37. Mironov, V., Visconti, R.P., Kasyanov, V., Forgacs, G., Drake, C.J., Markwald, R.R. (2009) Organ printing: tissue spheroids as building blocks. Biomaterials 30, 2164-2174.
38. Mironov, V., Boland, T., Trusk, T., Forgacs, G., Markwald, R.R. (2003) Organ printing: computer-aided jet-based 3D tissue engineering. Trends in Biotechnology 21, 157-161.
39. Mironov, V., Prestwich, G., Forgacs, G. (2007) Bioprinting living structures. Journal of materials chemistry 17, 2054-2060.

40. Jakab, K., Norotte, C., Marga, F., Murphy, K., Vunjak-Novakovic, G., Forgacs, G. (2010) Tissue engineering by self-assembly and bioprinting of living cells. Biofabrication 2, 1-14.
41. Khademhosseini, A., Langer, R. (2007) Microengineered hydrogels for tissue engineering. Biomaterials 28, 5087-5092.
42. Zorlutuna, P., Annabi, N., Camci-Unal, G., Nikkhah, M., Cha, J.M., Nichol, J.W., Manbachi, A., Chen, S., Khademhosseini, A. (2012) Microfabricated biomaterials for engineering 3D tissues. Advanced materials 24, 1782-1804.
43. Peppas, N.A., Hilt, J.Z., Khademhosseini, A., Langer, R. (2006) Hydrogels in biology and medicine: from molecular principles to bionanotechnology. Advanced materials 18, 1345-1360.
44. Williams, D. F. (2008) On the mechanisms of biocompatibility. Biomaterials **29,** 2941-2953.
45. Williams, D. F. (2009) On the nature of biomaterials. Biomaterials **30,** 5897-5909.
46. Farnsworth, N.L., Antunez, L.R., Bryant, S.J. (2012) Influence of chondrocyte maturation on acute response to impact injury in PEG hydrogels. Journal of Biomechanics 45, 2556-2563.
47. Zhang, Y., Yu, Y., Chen, H., Ozbolat, I.T. (2012) Characterization of printable cellular micro-fluidic channels for tissue engineering. Biofabrication 5, 1-11.
48. Stoppato, M., Stevens, H.Y., Carletti, E., Motta, A., Migliaresi, C., Guldberg, R.E. (2013) Effects of silk fibroin fiber incorporation on mechanical properties, endothelial cell colonization and vascularization of PDLLA scaffolds. Biomaterials 34, 4573-4581.
49. Gorka, O., Hernandez, R.M., Gascon, A.R., Calafiore, R., Chang, T.M.S., de Vos, P., Hortelano, G., Hunkeler, D., Lacik, I., Pedraz, J.L. (2004) History,

challenges and perspectives of cell microencapsulation. Trends in biotechnology 22, 87-92.

50. Gorka, O., Hernandez, R.M., Gascon, A.R., Calafiore, R., Chang, T.M.S., de Vos, P., Hortelano, G., Hunkeler, D., Lacik, I., Shapiro, A.M., Pedraz, J.L. (2003) Cell encapsulation: Promise and progress. Nature Medicine, 9, 104-107.
51. Chang, T.M.S. (1964) Semipermeable microcapsules. Science 146, 524-525.
52. Gasperini, L., Mano, J.F., Reis, R.L. (2014) Natural polymers for the microencapsulation of cells. Journal of the royal society interface 11, 1-19.
53. Bhujbal, S.V., de Vos, P., Niclou, S.P. (2014) Drug and cell encapsulation: Alternative delivery options for the treatment of malignant brain tumors. Advanced drug delivery reviews (in press).
54. Kumachev, A., Greener, J., Tumarkin, E., Eiser, E., Zandstra, P.W., Kumacheva, E. (2011) High-throughput generation of hydrogel microbeads with varying elasticity for cell encapsulation. Biomaterials 32, 1477-1483.
55. Griffin, D.R., Kasko, A.M. (2012) Photodegradable macromers and hydrogels for live cell encapsulation and release. Journal of the American chemical society 134, 13103-13107.
56. Chien, H.W., Tsai, W.B., Jiang, S. (2012) Direct cell encapsulation in biodegradable and functionalizable carboxybetaine hydrogels. Biomaterials 33, 5706-5712.
57. Uludag, H., de Vos, P., Tresco, P.A. (2000) Technology of mammalian cell encapsulation. Advanced Drug Delivery 42, 29-64.
58. Suguira, S., Oda, T., Izumida, Y., Aoyagi, Y., Satake, M., Ochiai, A., Ohkohchi, N., Nakajima, M. (2005) Size control of calcium alginate

beads containing living cells using micro-nozzle array. Biomaterials 26, 3327-3331.

59. Belscak-Cvitanovic, A., Stojanovic, R., Manojlovic, V., Komes, D., Cindric, I.J., Nedovic, V., Bugarski, B. (2011) Encapsulation of polyphenolic antioxidants from medicinal plant extracts in alginate-chitosan system enhanced with ascorbic acid by electrostatic extrusion. Food research international 44, 1094-1101.
60. Gasperini, L., Maniglio, D., Migliaresi, C. (2013) Microencapsulation of cells in alginate through an electrohydrodynamic process. Journal of bioactive compatible polymers 28, 413-423.
61. Steele, J.A.M., Barron, A.E., Carmona, E., Halle, J.P., Neufeld, R.J. (2012) Encapsulation of protein microfiber networks supporting pancreatic islets. Society for biomaterials. DOI: 10.1002/jbm.a.34281
62. Kang, A., Park, J., Ju, J., Jeong, G.S., Lee, S.H. (2014) Cell encapsulation via microtechnologies. Biomaterials 35, 2651-2663.
63. Lu, H.F., Targonsky, E.D., Wheeler, M.B., Cheng, Y.L. (2006) Thermally induced gelable polymer networks for living cell encapsulation. Biotechnology and Bioengineering 96, 146-155.
64. Ringeisen, B. R., Othon, C. M., Barron, J. a, Young, D., Spargo, B.J. (2006) Jet-based methods to print living cells. Journal of Biotechnology **1,** 930-944.
65. Mazzitelli, S., Tosi, A., Balesta, C., Nastruzzi, C., Luca, G., Mancuso, F., Calafiore, R., Calvitti, M. (2008) Production and characterization of alginate microcapsules produced by a vibrational encapsulation device. Journal of biomaterials applications 23, 123-145.
66. Gupta, A., Seifalian, A.M., Ahmad Z., Edirisinghe, M.J., Winslet, M.C. (2007) Novel electrohydrodynamic printing of nanocomposite biopolymer scaffolds. Journal of bioactive compatible polymers 22, 265-280.

67. Gauvin, R., Chen, Y.C, Lee, J.W., Soman, P., Zorlutuna, P., Nichol, J.W., Bae, H., Chen, S., Khademhosseini, A. (2012) Microfabrication of complex porous tissue engineering scaffolds using 3D projection stereolithography. Biomaterials 33, 3824-3834.
68. Gurkan, U.A., Fan, Y., Xu, F., Erkmen, B., Urkac, E.S., Parlakgul, G., Bernstein, J., Xing, W., Boyden, E.S, Demirci, U. (2012) Simple precision creation of digitally specified, spatially heterogeneous, engineered tissue architectures. Advanced materials 8, 1192-1198.
69. Bratt-Leal, A., Carpenedo, R. (2009) Engineering the embryoid body microenvironment to direct embryonic stem cell differentiation. American institute of chemical engineers. DOI: 10.1021/bp.139.
70. Tan, Y.C., Hettiarachchi, K., Siu, M., Pan, Y.R., Lee, A.P. (2005) Controlled microfluidic encapsulation of cells, proteins, and microbeads in lipid vesicles. Journal of American Chemical Society 2006, 5656-5667.
71. Grigoriev, D.O., Burkeeva, T., Mohwald, H., Shchkin, D.G. (2008) New method for fabrication of loaded micro- and nanocontainers: emulsion encapsulation by polyelectrolyte layer-by-layer deposition on the liquid core. Langmuir 24, 999-1004.
72. Whitesides, G.M. (2006) The origins and the future of microfluidics. Nature 442, 368-373.
73. Martinez, C.J., Kim, J.W., Ye, C., Ortiz, I., Rowat, A.C., Marquez, M., Weitz, D. (2012) A microfluidic approach to encapsulate living cells in uniform alginate hydrogel microparticles. Macromolecular bioscience, DOI: 10.1002/mabi.201100351.
74. Tumarkin, E., Kumacheva, E. (2009) Microfluidic generation of microgels from synthetic and natural polymers. Chemical society reviews 38, 2161-2168.
75. Trivedi, V., Ereifej, E.S., Doshi, A., Sehgal, P., VandeVord, P.J., Basu, A.S. (2009) Microfluidic encapsulation of cells in alginate capsules for high

throughput screening. 31st Annual International conference of the IEEE EMBS, 7037.

76. Zhang, H., Tumarkin, E., Peerani, R., Nie, Z., Sullan, R.M.A., Walker, G.C., Kumacheva, E. (2006) Microfluidic Production of biopolymer microcapsules with controlled morphology. Journal of American chemical society 128, 12205-12210.
77. Chabert, M., Viovy, J.L. (2008) Microfluidic high-throughput encapsulation and hydrodynamic self-sorting of single cells. PNAS 105, 3191-3196.
78. Sugiura, S., Oda, T., Aoyagi, Y., Satake, M., Ohkohchi, N., Nakajima, M. (2008) Tubular gel fabrication and cell encapsulation in laminar flow stream formed by microfabricated nozzle array. Lab on chip 8, 1255-1257.
79. Gasperini, L., Maniglio, D., Motta, A., Migliaresi, C. (2015) An electrohydrodynamic bioprinter for alginate hydrogels containing living cells. Tissue engineering part C: Methods 21, 123-132.
80. Fedorovich, A.E., Wijn,J.R., Verbout, A.J., Alblas, J., Dhert, W.J.A. (2008) Three-dimensional fiber deposition of cell-laden, viable, patterned constructs for bone tissue printing. Tissue Engineering: Part A 14, 127-133.
81. Guo, Z., Liu, W., Su, B.L. (2010) Superhydrophobic surfaces: from natural to biomimetic to functional. Journal of colloid and interface science 353, 335-355.
82. Lee, K.Y., Mooney, D.J. (2012) Alginate: properties and biomedical applications. Progress polymer science, 37, 106-126.
83. Nicodemus, G.D., Bryant, S.J. (2008) Cell encapsulation in biodegradable hydrogels for tissue engineering applications. Tissue Engineering: Part B, 14, 149-165.

84. Murphy, S.V., Skardal, A., Atala, A. (2013) Evaluation of hydrogels for bio-printing applications. Journal of Biomedical Materials Research Part A **101,** 272-284.
85. Babensee, J.E., Sefton, M.V. (2000) Viability of HEMA-MMA Microencapsulated Model Hepatoma Cells in Rats and the Host Response. Tissue Engineering **6,** 165-182.
86. Hwang, C.M., Sant, S., Masaeli, M., Kachouie, N.N., Zamanian, B., Lee, S.H., Khademhosseini, A. (2010) Fabrication of three-dimensional porous cell-laden hydrogel for tissue engineering. Biofabrication 2, 1-12.
87. Chan, B.P., Hui, T.Y., Yeung, C.W., Li, J., Mo, I., Chan, G.C.F. (2007) Self-assembled collagen-human mesenchymal stem cell microspheres for regenerative medicine. Biomaterials, 28, 4652-4666.
88. Hopkins, A.M., Laporte, L.D., Toretelli, F., Spedden, E., Staii, C., Atherton, T.J., Hubbell, J.A., Kaplan, D.L. (2013) Silk hydrogels as soft substrates for neural tissue engineering. Advanced functional materials, 23, 5140-5149.
89. Seidlits, S.K., Khaing, Z.Z., Petersen, R.R., Nickels, J.D., Vanscoy, J.E., Shear, J.B., Schmidt, C.E. (2010) The effects of hyaluronic acid hydrogels with tunable mechanical properties on neural progenitor cell differentiation. Biomaterials, 31, 3930-3940.
90. Ramon-Azcon, J., Ahadian, S., Obregon, R., Camci-Unal, G., Ostrovidov, S., Hosseini, V., Kaji, H., Ino, K., Shiku, H., Khademhosseini, A., Matsue, T. (2012) Gelatin methacrylate as a promising hydrogel for 3D microscale organization and proliferation of dielectrophoretically patterned cells. Lab on chip 12, 2959-2969.
91. Hunt, N.C., Grover, L.M. (2010) Cell encapsulation using biopolymer gels for regenerative medicine. Biotechnology letters, 32, 733-742.
92. Li, Z., Kawashita, M., (2011) Current progress in inorganic artificial biomaterials. Journal artificial organs, 14, 163-170.

93. Daley, W.P., Peters, S.B., Larsen, M. (2008) Extracellular matrix dynamics in development and regenerative medicine. Journal of cell science 121, 255-264.
94. Hynes, R.O. (2009) The extracellular matrix: not just pretty fibrils. Science (New York, N.Y.) 326, 1216-1219.
95. Lu, P., Takai, K., Weaver, V.M., Werb, Z. (2011) Extracellular matrix degradation and remodeling in development and disease. Cold spring harbor perspectives in biology 3.
96. Frantz, C., Stewart, K.M., Weaver, V.M. (2010) The extracellular matrix at a glance. Journal of cell science 123, 4195-4200.
97. Kumar, D., Gerges, I., Tamplenizza, M., Lenardi, C., Forsyth, N.R., Liu, Y. (2014) Three-dimensional hypoxic culture of human mesenchymal stem cells encapsulated in photocurable, biodegradable polymer hydrogel: A potential injectable cellular product for nucleus pulposus regeneration. Acta biomaterialia 10, 3463-3474.
98. Krishnamurthy, N.V., Gimi, B. (2011) Encapsulated cell grafts to treat cellular deficiencies and dysfunction. Critical review of biomedical engineering 39, 473-491.
99. Li, X., Xu, J., Filion, T.M., Ayers, D.C., Song, J. (2013) pHEMA-nHA encapsulation and delivery of vancomycin and rhBMP-2 enhances its role as a bone graft substitute. Clinical orthopaedics and related research 471, 2540-2547.
100. Nie, L., Zhang, G., Hou, R., Xu, H., Li, Y., Fu, J. (2015) Controllable promotion of chondrocytes adhesion and growth on PVA hydrogels by controlled release of TGF-b1 from porous PLGA microspheres. Colloids and surfaces B: biointerfaces 125, 51-57.
101. Nafea, E.H., Poole-Warren, L.A., Marthens, P.J. (2014) Structural and permeability characterization of biosynthetic PVA hydrogels designed

for cell-based therapy. Journal of biomaterials science, polymer edition 25, 1771-1790.

102. Bozza, A., Coates, E.E., Incitti, T., Ferlin, K.M., Messina, A., Menna, E., Bozzi, Y., Fisher, J.P., Casarosa, S. (2014) Neural differentiation of pluripotent cells in 3D alginate-based cultures. Biomaterials 35, 4636-4645.
103. Nichol, J.W., Koshy, S.T., Bae, H., Hwang, C.M., Yamanlar, S., Khademhosseini, A. (2010) Cell-laden microengineered gelatin methacrylate hydrogels. Biomaterials 31, 5536-5544.
104. Benton, J.A., DeFrost, C.A., Vivekanandan, V., Anseth K.S. (2009) Photocrosslinking of gelatin macromers to synthesize porous hydrogels that promote valvular interstitial cell function. Tissue engineering: Part A 15, 3221-3230.
105. Hutson, C.B., Nichol, J.W., Aubin, H., Bae, H., Yamanlar, S., Al-Haque, S., Koshy, S.T., Khademhosseini, A. (2011) Synthesis and characterization of tunable poly (ethylene glycol): gelatin methacrylate composite hydrogels. Tissue engineering: Part A 17, 1713-1723.
106. Menendez, P., Bueno, C., Wang, L, Bhatia, M. (2005) Human Embryonic stem cells: Potential tool for achieving immunotolerance? Stem Cell reviews 1, 151-158.
107. Thomson, J.A., Itskovitz-Eldor, J., Shapiro, S.S., Waknitz., M.A., Swiergiel, J.J., Marshall, V.S., Jones, J.M. (1998) Embryonic stem cell lines derived from human blastocysts. Science 282, 1145-1147.
108. Reubinoff, B.E., Itsykson, P, Turetsky, T, Pera, M.F., Reinhartz, E., Itzik, A., Ben-Hur, T. (2001) Neural progenitors from human embryonic stem cells. Nature biotechnology 19, 1134-1140.
109. Levenberg, S., Golub, J.S., Amit, M., Itskovitz-Eldor, J., Langer, R. (2002) Endothelial cells derived from human embryonic stem cells. PNAS 99, 4391-4396.

110. Mummery, C., Ward, D., Van Den Brink, C.E., Bird, S.D., Doevendans, P.A., Opthof, T., De La Riviere, A.B., Tertoolen, L., Ven Der Heyden, M., Pera, M. (2002) Cardiomyocytes differentiation of mouse and human embryonic stem cells. Journal of anatomy 200, 233-242.
111. Kaufman, D.S., Hanson, E.T., Lewis, R.L., Auerbach, R., Thomson, J.A. (2001) Hematopoietic colony-forming cells derived from human embryonic stem cells. PNAS 98, 716-721.
112. Green, H., Easley, K., Iuchi, S. (2003) Marker succession during the development of keratinocytes from cultured human embryonic stem cells. PNAS 100, 625-630.
113. Rambhatla, L., Chiu, C.P., Kundu, P., Peng, Y., Carpenter, M.K. (2003) Generation of hepatocyte-like cells from human embryonic stem cells. Cell transplant 12, 1-11.
114. Sottile, V., Seuwen, K., Kneissel, M. (2004) Enhanced marrow adipogenesis and bone resorption in estrogen-deprived rats treated with the PPARgamma agonist BRL49653 (rosiglitazone). Calcified tissue international 75, 329-337.
115. Takahashi, K., Yamanaka, S. (2006) Induction of pluripotent stem cells from mouse embryonic and adult fibroblast culture by defined factors. Cell 126, 663-676.
116. Takahashi, K., Tanabe, K., Ohnuki, M., Narita, M., Ichisaka, T., Tomoda, K., Yamanaka, S. (2007) Induction of pluripotent stem cells from adult human fibroblasts by defined factors. Cell 131, 861-872.
117. Yamanaka, S. (2012) Induced pluripotent stem cells: past, present, and future. Cell Stem Cell 10, 678-684.
118. Yu, J., Vodyanik, A.M., Smuga-Otto, K., Antosiewicz-Bourget, J., Frane, J.L., Tian, S., Nie, J., Jonsdottir, G.A, Ruotti, V., Stewart, R., Slukvin, I.I., Thomson,J.A. (2007) Induced pluripotent stem cell lines derived from human somatic cells. Science 318, 1917-1920.

119. Lister, R., Pelizzola, M., Kida, Y.S., Hawkins, R.D., Nery, J.R., Hon, G., Antosiewicz-Bourget, J., O'Malley, R., Castanon, R., Klugman, S., Downes, M., Yu, R., Stewart, R., Ren, B., Thomson,J.A., Evans, R.M., Ecker, J.R. (2011) Hotspots of abberant epigenomic reprogramming in human induced pluripotent stem cells. Nature 471, 68-75.
120. Zhao, T., Zhang, Z.N., Rong, Z., Xu, Y. (2011) Immunogenicity of induced pluripotent stem cells. Nature 474, 212-216.
121. Robinton, D.A., Daley, G.Q. (2012) The promise of induced pluripotent stem cells in research and therapy. Nature 481, 295-305.
122. Pang, Z.P., Yang, N., Vierbuchen, T., Ostermeier, A., Fuentes, D.R., Yang, T.Q., Citri, A., Sebastiano, V., Marro, S., Sudhof,T., Wernig, M. (2011) Induction of human neuronal cells by defined transcription factors. Nature 476, 220-224.
123. Focosi, D., Amabile, G., Di Ruscio, A., Quaranta, D.G., Tenen, D.G., Pistello, M. (2014) Induced pluripotent stem cells in hematology: current and future application. Blood Cancer Journal 4, 1-8.
124. Bianco, P., Cao, X., Frenette, P.S., Mao, J.J., Robey, P.G., Simmons, P.J., Wang, C.Y. (2013) The meaning, the sense and the significance: translating the science of mesenchymal stem cells into medicine. Nature medicine 1, 35-42.
125. Nombela-Arrieta, C., Ritz, J., Silberstein, L.E (2011) The elusive nature and function of mesenchymal stem cells. Molecular cell biology 12, 126-131.
126. Lindroos, B., Suuronen, R., Miettinen, S. (2011) The potential of adipose stem cells in regenerative medicine. Stem Cell review 7, 269-291.
127. Ong, W.K., Sugii, S. (2013) Adipose-derived stem cells: fatty potentials for therapy. The international journal of biochemistry and cell biology 45, 1083-1086.

128. Ding, L., Morrison, S.J. (2013) Haemotopoietic stem cells and early lymphoid progenitors occupy distinct bone marrow niches. Nature 495, 231-236.
129. Ding, L., Saunders, T.L., Enikolopov, G., Morrison, S.J. (2012) Endothelial and perivascular cells maintain haematopoietic stem cells. Nature 481, 457-463.
130. Lutolf, M.P., Gilbert, P.M., Blau, H.M. (2009) Designing materials to direct stem-cell fate. Nature 462, 433-441.
131. Jabr, F. (2012) Know your neurons: How to classify different types of neurons in the brains forest. Scientific American.
132. Ransohoff, R.M., Stevens, B. (2011) How many cell types does it take to wire a brain? Science 333, 1391-1392.
133. Xu, F., Wu, C.M., Rengarajan, V., Finley, T.D., Keles, H.O., Sung, Y., Li, B., Gurkan, U.A., Demirci, U. (2011) Three-dimensional magnetic assembly of microscale hydrogels. Advanced materials 23, 4254-4260.
134. Li, Y., Huang, G., Zhang, X., Li, B., Chen, Y., Lu, T., Lu, T.J., Xu, F. (2013) Magnetic hydrogels and their potential biomedical applications. Advanced materials 23, 660-672.
135. Marx, V. (2015) Biophysics: using sound to move cells. Nature methods 12, 41-44.
136. Xu, F., Finley, T.D.,Turkaydin, M., Sung, Y., Gurkan, U.A., Yavuz, A.S., Guldiken, R.O., Demirci, U. (2011) The assembly of cell-encapsulating microscale hydrogels using acoustic waves. Biomaterials 32, 7847-7855.
137. Wang, H., Shi, Q., Yue, T., Nakajima, M., Takeuchi, M., Huang, Q., Fukuda, T. (2014) Micro-assembly of a vascular-like micro-channel with railed micro-robot team-coordinated manipulation. International Journal of Advanced Robotic systems 11, 1-12.

138. Pereira, R. C., Gentili, C., Cancedda, R., Azevedo, H. S., Reis, R. L. (2011) Encapsulation of Human Articular Chondrocytes into 3D hydrogel: Phenotype and Genotype Characterization. 3D Cell culture: Methods and protocols, methods in molecular biology 695, 167- 181.
139. Purcell, E. K., Singh, A., Kipke, D. R. (2009) Alginate composition effects on a neural stem cell-seeded scaffold. Tissue Engieering Part C Methods 15, 541-550.
140. Visted, T., Bjerkvig, R., Enger, P. O. (2001) Cell encapsulation technology as a therapeutic strategy for CNS malignancies. Neural Oncology 3, 201-210.
141. Sundararaghavan, H. G., Burdick, J. A. (2011) Cell encapsulation. In: Ducheyne, P., edc. Comprehensive Biomaterials. Elsevier, pp. 115-130.
142. Mahou, R., Tran, N. M., Dufresne, M., Legallais, C., Wandrey, C. (2009) Encapsulation of Huh-7 cells within alginate-poly(ethylene glycol) hybrid microspheres. Journal of Materials Science: Materials in Medicine 23, 171-179.
143. Mongkoldhumrongkul, N., Best, S., Aarons, E., Jayasinghe, S. N. (2009) Bio-electrospraying whole human blood : analysing cellular viability at a molecular level. Journal of Regenerative Medicine and Tissue Engineering 3, 562-566.
144. Melchels, F., Malda, J., Fedorovich, N., Alblas, J., Woodfield, T. (2011) Organ Printing. In: Ducheyne, P., eds. Comprehensive biomaterials.– Elsevier , pp. 587–606.
145. Krysko, D. V, Vanden Berghe, T., D'Herde, K., Vandenabeele, P. (2008) Apoptosis and necrosis: detection, discrimination and phagocytosis. Methods (San Diego, Calif.) 44, 205-221.
146. Porter, a G., and Jänicke, R. U. (1999) Emerging roles of caspase-3 in apoptosis. Cell Death and Differentiation 6, 99-104.

147. Shi, Y. (2002) Mechanisms of Caspase Activation and Inhibition during Apoptosis. Molecular Cell 9, 459-470.
148. Kurokawa, M., Kornbluth, S. (2009) Caspases and kinases in a death grip. Cell 138, 838-854.
149. Kornblit, B., Munthe-Fog, L., Petersen, S.L., Madsen, H.O., Vindelov, L., Garred, P. (2007) The genetic variation of the human HMGB1 gene. Tissue antigens 70, 151-156.
150. Scaffidi, P., Misteli, T., Bianchi, M.E. (2002) Release of chromatin protein HMGB1 by necrotic cells triggers inflammation. Nature 418, 191-195.
151. Luan, Z.G., Zhang, Z.J., Yin, X.H., Ma, X.C., Zhang, H. (2013) Downregulation of HMGB1 protects against the development of acute lung injury after severe acute pancreatitis. Immunology 218, 1261-1270.
152. Wei, W., Chen, M., Zhu, Y., Wang, J., Zhu, P., Li, Y., Li, J. (2012) Down-regulation of vascular HMGB1 and RAGE expression by n-3 polyunsaturated fatty acids is accomplished by amelioration of chronic vasculopathy of small bowel allografts. Journal of nutritional biochemistry 23, 1333-1340.
153. Jiang, W.L., Xu, Y., Zhang, S.P., Zhu, H.B., Hou, J. (2012) Tricin 7-glucoside protects against experimental cerebral ischemia by reduction of NF-kB and HMGB1 expression. European Journal of Pharmaceutical sciences 45, 50-57.
154. Ozawa, K., Kuwabara, K., Tamatani, M., Takatsuji, K., Tsukamoto, Y., Kaneda, S., Tohyama, M. (1999) 150-kDa Oxygen-regulated Protein (ORP150) Suppresses Hypoxia-induced Apoptotic Cell Death. The Journal of Biological Chemistry 274, 6397-6404.
155. Tamatani, M., Matsuyama, T., Yamaguchi, A., Mitsuda, N., Tsukamoto, Y., Taniguchi, M., Tohyama, M. (2001) ORP150 protects against

hypoxia/ischemia-induced neuronal death. Nature Medicine 7, 317-323.

156. Sato, M., Sugano, N., Ohzono, K., Nomura, S., Kitamura, Y., Tsukamoto, Y., Ogava, S. (2001) Apoptosis and expression of stress protein (ORP150, HO1) during development of ischaemic osteonecrosis in the rat. The journal of bone and joint surgery 83, 751-759.

157. Bando, Y., Tsukamoto, Y., Katayama, T., Ozawa, K., Kitao, Y., Hori, O., Stern, D.M., Yamauchi, A., Ogawa, S (2004) ORP150/HSP12A protects renal tubular epithelium from ischemia-induced cell death. The FASEB journal DOI: 10.1096/fj.03-1161fje.

158. Graven, K. K., Mcdonald, R. J., Farber, H. W., Graven, K. K., Donald, R. J. M. C., Farber, H. W. (1998) Hypoxic regulation of endothelial glyceraldehyde-3-phosphate dehydrogenase. American Journal of Physiology: Cell Physiology 274, 347-355.

159. Yamaji, R., Fujita, K., Takahashi, S., Yoneda, H., Nagao, K., Masuda, W., Nakano, Y. (2003) Hypoxia up-regulates glyceraldehyde-3-phosphate dehydrogenase in mouse brain capillary endothelial cells: involvement of Na+/Ca2+ exchanger. Biochimica et Biophysica Acta 1593, 269-276.

160. Collel, A., Green, D.R., Ricci, J.E. (2009) Novel roles for GAPDH in cell death and carcinogenesis. Cell death and differentiation 16, 1573-1581.

161. Samali, A., Orrenius, S. (1998) Heat shock proteins: regulators of stress response and apoptosis. Cell Stress and Chaperones 4, 228-236.

162. Mayer, M. P., Bukau, B. (2005) Hsp70 chaperones: cellular functions and molecular mechanism. Cellular and Molecular Life Sciences 62, 670-684.

163. Yenari, M.A., Giffard, R.G., Sapolsky, R.M., Steinberg, G.K. (1999) The neuroprotective potential of heat shock protein 70 (HSP70). Molecular medicine today 5, 525-531.

164. Gumbiner, B. M. (2005) Regulation of cadherin-mediated adhesion in morphogenesis. Nature reviews. Molecular Cell Biology 6, 622-634.
165. Niessen, C. M., Leckband, D., Yap, A. S. (2011) Tissue Organization by Cadherin Adhesion Molecules : Dynamic Molecular and Cellular Mechanisms of Morphogenetic Regulation. Physiological Reviews 91, 691-731.
166. Karabekian, Z., Gillum, N.D., Wong, E.W.P., Sarvazyan, N. (2009) Effects of N-cadherin overexpression on the adhesion properties of embryonic stem cells. Cell adhesion and migration 3, 305-310.
167. Lammens, T., Swerts, K., Derycke, L., De Craemer, A., De Brouwer, S., De Preter, K., Van Roy, N., Vandesompele, J., Speleman, F., Philippe, J., Benoit, Y., Beiske, K, Bracke, M., Laureys, G. (2012) N-cadherin in neuroblastoma disease: expression and clinical significance. PLos one 7, 1-8.
168. Bou-Gharios, G., Ponticos, M., Rajkumar, V., Abraham, D. (2004) Extra-cellular matrix in vascular networks. Cell proliferation 37, 207-220.
169. Forlino, A., Marini, J.C. (2000) Osteogenesis Imperfecta: Prespects for molecular therapeutics. Molecular genetics and metabolism 71, 225-232.
170. Rossert, J., Terraz, C., Dupont, S. (2000) Regulation of type 1 collagen genes expression. Nephrology dialysis transplantation 15, 66-68.
171. Csordas, A., Wick, G., Bernhard, D. (2006) Hydrogen peroxide-mediated necrosis induction in HUVECs is associated with an atypical pattern of caspase-3 cleavage. Experimental Cell Research 312**,** 1753-1764.
172. Plante, M. K., Arscott, W. T., Folsom, J. B., Tighe, S. W., Dempsey, R. J., Wesley, U. V. (2013) Ethanol promotes cytotoxic effects of tumor necrosis factor-related apoptosis-inducing ligand through induction of reactive oxygen species in prostate cancer cells. Prostate Cancer Prostatic Disease 16**,** 16–22.

173. Saito, Y., Nishio, K., Ogawa, Y., Kimata, J., Kinumi, T., Yoshida, Y., Noguchi, N., Niki, E. (2006) Turning point in apoptosis/necrosis induced by hydrogen peroxide. Free radical research 40, 619-630.
174. Wu, D., Yotnda, P. (2011) Induction and testing of hypoxia in cell culture. Journal of visualized experiments 54, 1-4.
175. Koch, F. P., Yekta, S. S., Merkel, C., Ziebart, T., Smeets, R. (2010) The impact of bisphosphonates on the osteoblast proliferation and collagen gene expression in vitro. Head and face medicine 6**,** 1-6.
176. Sabirzhanov, B., Stoica, B. A., Hanscom, M., Piao, C.-S., Faden, A. I. (2012) Over-expression of HSP70 attenuates caspase-dependent and caspase-independent pathways and inhibits neuronal apoptosis. Journal of Neurochemistry 123**,** 542-554.
177. Spandidos, A., Wang, X., Wang, H., Seed, B. (2010) PrimerBank: a resource of human and mouse PCR primer pairs for gene expression detection and quantification. Nucleic Acids Research 38**,** 792-799.
178. White, E. (2012) Life, death, and the pursuit of apoptosis. Genes and development 6, 1-15.
179. Denecker, G., Vercammen, D., Steemans, M., Berghe, T.V., Brouckaert, G., Van Loo, G., Zhivotovsky, B., Fiers, W., Grooten, J., Declercq, W., Vandenabeele, P. (2001) Cell death and differentiation 8, 829-840.
180. Sato, K., Saito, H., Matsuki, N. (1996) HSP70 is essential to the neuroprotective effect of heat-shock. Brain research 740, 117-123.
181. Mosser, D.D., Caron, A.W., Bourget, L., Merlin, A.B., Sherman, M.Y., Morimoto, R.I., Massie, B. (2000) The chaperone function of hsp70 is required for protection against stress-induced apoptosis. Molecular and cellular biology 20, 7146-7159.
182. Guzhova, I., Kislyakova, K., Moskaliova, O., Fridlanskaya, I., Tytell, M., Cheetham, M., Margulis, B. (2001) In vitro studies show that Hsp70 can

be released by glia and that exogenous Hsp70 can enhance neuronal stress tolerance. Brain research 914, 66-73.

183. Duval, E., Leclercq, S., Elissalde, J.-M., Demoor, M., Galéra, P., Boumédiene, K. (2009) Hypoxia-inducible factor 1alpha inhibits the fibroblast-like markers type I and type III collagen during hypoxia-induced chondrocyte redifferentiation: hypoxia not only induces type II collagen and aggrecan, but it also inhibits type I and type III collagen in the hypoxia-inducible factor 1alpha-dependent redifferentiation of chondrocytes. Arthritis and Rheumatism 60**,** 3038-3048.

184. Jaattela, M., Wissing, D., Kokholm, K., Kallunki, T., Egeblad, M. (1998) Hsp70 exerts its anti-apoptotic function downstream of caspase-3-like proteases. The EMBO Journal 17, 6124-6134.

185. Weise, J., Engelhorn, T., Dörfler, A., Aker, S., Bähr, M., Hufnagel, A. (2005) Expression time course and spatial distribution of activated caspase-3 after experimental status epilepticus: contribution of delayed neuronal cell death to seizure-induced neuronal injury. Neurobiology of Disease 18**,** 582-590.

186. Karabekian, Z., Gillum, N. D., Wong, E. W. P., Sarvazyan, N. (2009) Effects of N-cadherin overexpression on the adhesion properties of embryonic stem cells. Cell Adhesion and Migration 3**,** 305-310.

187. Wang, N., Adams, G., Buttery, L., Falcone, F. H., Stolnik, S. (2009) Alginate encapsulation technology supports embryonic stem cells differentiation into insulin-producing cells. The Journal of Biotechnology 144**,** 304- 312.

188. Lam, T.K.T. (2010) Neuronal regulation of homeostasis by nutrient sensing. Nature Medicine 16, 392-395.

189. Kotas, M.E., Medzhitov, R. (2015) Homeostasis, Inflamation and disease susceptibility. Cell 160, 816-827.

190. Folmes, C.D.L., Dzeja, P.P., Neslon, T.J., Terzic, A. (2012) Metabolic plasticity in stem cell homeostasis and differentiation. Cell Stem Cell 11, 596-606.

191. Jones, D.L., Wagers, A.J. (2008) No place like home: anatomy and function of the stem cell niche. Nature reviews: Molecular cell biology 9, 11- 21.

192. Scadden, D.T. (2006) The stem-cell niche as an entity of action. Nature 441, 1075-1079.

193. Chen, S., Lewallen, M., Xie, T. (2013) Adhesion in the stem cell niche: biological roles and regulation. Development 2, 255-265.

194. Mendelson, A., Frenette, P.S. (2014) Hemotopoietic stem cell niche maintenance during homeostasis and regeneration. Nature Medicine 20, 833-846.

195. Mason, C., Dunnil, P. (2008) A brief definition of regenerative medicine. Regenerative medicine 3, 1-5.

196. Annabi, N., Tamayol, A., Uquillas, J.A., Akbari, M., Bertassoni, L.E., Cha, C., Camci-Unal, G., Dokmeci, M.R., Peppas, N.A., Khademhosseini, A. (2014) 25th anniversary article: rational design and applications of hydrogels in regenerative medicine. Advanced materials 26, 85-124.

197. Wagers, A.J. (2012) The stem cell niche in regenerative medicine. Cell: Stem cell 10, 362-369.

198. Tabar, V., Studer, L. (2014) Pluripotent stem cells in regenerative medicine: challenges and recent progress. Nature Genetics 15, 82-92.

199. Barthes, J., Ozcelik, H., Hindie, M., Ndreu-Halili, A., Hasan, A., Vrana, N.E. (2014) Cell microenvironment engineering and monitoring for tissue engineering and regenerative medicine: the recent advances. BioMed Research International ID 921905, 1-18.

200. Ross, R.A., Spengler, B.A. (2007) Human neuroblastoma stem cells. Seminars in cancer biology 17, 241-247.

201. Tibbit, M.W., Anseth, K.S. (2009) Hydrogels as Extracellular matrix mimics for 3D cell culture. Biotechnology and Bioengineering 103, 655-663.

202. Kultz, D. (2005) Molecular and evolutionary basis of the cellular stress response. Annual review of physiology 67, 225-257.

203. Huh, D., Hamilton, G.A., Ingber, D.E. (2011) From 3D cell culture to organs-on-chips. Trends in cell biology 21, 745-754.

204. Yamada, K.M., Cukierman, E. (2007) Modeling tissue morphogenesis and cancer in 3D. Cell 130, 601-610.

205. Wefers, B., Meyer, M., Ortiz, O., De Angelis, M.H., Hansen, J., Wurst, W., Kuhn, R. (2013) Direct production of mouse disease models by embryo microinjection of TALENs and oligodeoxynucleotides. PNAS 110, 3781-3787.

206. Reininger-Mack, A., Thielecke, H., Robitzki, A.A. (2002) 3D-biohybrid systems: applications in drug screening. Trends in biotechnology 20, 56-61.

207. Chwalek, K., Bray, L.J., Werner, C. (2014) Tissue-engineered 3D tumor angiogenesis models: potential technologies for anti-cancer drug discovery. Advanced drug delivery reviews 79-80, 30-39.

208. Hopkins, A.M., DeSimone, E., Chwalek, K., Kaplan, D.L (2014) 3D in vitro modeling of the central nervous system. Progress in neurobiology (in press), 1-25.

209. Cole, K.A., Krizman, D.B., Emmert-Buck, M.R. (1999) The genetics of cancer – a 3D model. Nature genetics 21, 38-41.

210. Xu, F., Celli, J., Rizvi, I., Moon, S., Hasan, T., Demirci, U. (2011) A three-dimensional in vitro ovarian cancer coculture model using a high-throughput cell pattering platform. Journal of biotechnology 6, 204-212.

211. Cell culture basics. Handbook Invitrogen/Gibco. Online resource: www.invitrogen.com/cellculturebasics

212. Reininger-Mack, A., Thielecke, H., Robitzki, A.A. (2002) 3D-biohybrid systems: applications in drug screening. Trends in biotechnology 20, 56-61.
213. Meli, L., Jordan, E.T., Clark, D.S., Linhardt, R.J., Dordick, J.S. (2012) Influence of a three-dimensional, microarray environment on human cell culture in drug screening systems. Biomaterials 33, 9087-9096.
214. Yip, D., Cho, C.H. (2013) A multicellular 3D heterospheroid model of liver tumor and stromal cells in collagen gel for anti-cancer drug testing. Biochemical and biophysical research communications 433, 327-332.
215. Vorsmann, H., Groeber, F., Walles, H., Busch, S., Beissert, S., Walczak, H., Kulms, D. (2013) Development of a human three-dimensional organotypic skin-melanoma spheroid model for in vitro drug testing. Cell death and disease 4, 1-11.
216. Griffith, L.G., Swartz, M.A. (2006) Capturing complex 3D tissue physiology in vitro. Nature Reviews - Molecular Cell Biology 7, 211-224.
217. Whitesides, G.M., Grzybowski, B. (2002) Self-assembly at all scales. Science 295, 2418-2421.
218. Stauth, S.A., Parviz, B.A. (2006) Self-assembled single-crystal silicon circuits on plastic. PNAS 103, 13922-13927.
219. Tanase, M., Silevitch, D.M., Hultgren, A., Bauer, L.A., Searson, P.C., Meyer, G.J., Reich, D.H. (2002) Magnetic trapping and self-assembly of multicomponent nanowires. Journal of applied physics 91, 8549-8551.
220. Hulteen, J.C., Van Duyne, P. (1995) Nanosphere lithography: a materials general fabrication process for periodic particle array surfaces. Journal of vacuum science and technology A 13, 1553-1558.
221. Chung, S.E., Park, W., Shin, S., Lee, S.A., Kwon, S. (2008) Guided and fluidic self-assembly of microstructures using railed microfluidic channels. Nature materials 7, 581-587.

222. Yan, J., Bloom, M., Bae, S.C., Luijten, E., Granick, S. (2012) Linking synchronization to self-assembly using magnetic Janus colloids. Nature 491, 578-581.

223. Jacobs, H.O., Tao, A.R., Schwartz, A., Gracias, D.H., Whitesides, G.M. (2002) Fabrication of a cylindrical display by patterned assembly. Science 296, 323-325.

224. Xia, Y., Yin, Y., Lu, Y., McLellan, J. (2003) Template-assisted self-assembly of spherical colloids into complex and controllable structures. Advanced healthcare materials 13, 907-918.

225. Mirica, K.A., Philips, S.T., Shevkoplyas, S.S., Whitesides, G.M. (2011) Using magnetic levitation for three dimensional self-assembly. Advanced materials 23, 4134-4137.

Scientific production

Manuscripts in International journals

Liaudanskaya, V., Gasperini, L., Maniglio, D., Motta, A., Migliaresi, C. (2015) Assessing the impact of electrohydrodynamic jetting on encapsulated cell viability, proliferation, and ability to self-assemble in three-dimensional structures. Tissue Engineering Part C (in press).

Tasoglu, S., Yu, C.H., Liaudanskaya, V., Guven, S., Migliaresi, C., Demirci, U. (2015) Levitational assembly for biomaterial fabrication. Advanced healthcare materials (in press).

Namkoong*, B., Guven*, S., Ramesh, S., Liaudanskaya, V., Abzhanov, A., Demirci, U. (2015) Recapitulating cranial osteogenesis with neural crest cells in 3-D microenvironments. STEM CELLS (Submitted).

Liaudanskaya, V., Motta, A., Migliaresi, C. Homeostasis maintenance is critical parameter for application of cell encapsulation in tissue fabrication. In preparation.

Participation in Congresses and Schools

10–13 June, 2014

TERMIS, European Chapter Meeting, Genova, Italy.

Poster presentation. V. Liaudanskaya, A. Motta, C. Migliaresi: “Organ printing: self-assembly ability of cells encapsulated by EHDJ method”.

Congress proceedings: Journal of Tissue Engineering and Regenerative Medicine, Volume 8, Issue Supplement s1, pages 377-378 (PP297).

7-9 October, 2013

POLARIS 1st Workshop, Porto, Portugal.

10-12 October, 2013

TERM STEM 2013, Porto, Portugal.

2 oral presentations. V.Liaudanskaya, L. Gasperini, A. Motta, C. Migliaresi: “Influence of electrohydrodynamic jet (EHDJ) prinitg system on the cell behavior”.

Congress proceedings: Journal of Tissue Engineering and Regenerative Medicine Volume 7, Issue Supplement s1, page 8.

9-13 October, 2012

TERM STEM 2012, Guimaraes, Portugal.

Oral presentation. V.Liaudanskaya, L. Gasperini, A. Motta, C. Migliaresi: “Organ printing and stem cells as future of regenerative medicine: influence of the cell encapsulation system on cell behavior”

Congress proceedings: Journal of Tissue Engineering and Regenerative Medicine, Volume 6, Issue Supplement s2, page 21.

8-12 July, 2013

Summer school on Tissue Engineering and Regenerative medicine: “Biomaterials and regenerative medicine” - Riva del Garda, Italy.

9-13 July, 2012

Summer School on Biomaterials and Regenerative Medicine: “Bioinspired and biomimetic materials and scaffolds: from nature communication and design strategies” - Riva del Garda, Italy.

Lecture:

V. Liaudanskaya, L. Gasperini, A. Motta, C. Migliaresi: “Cell encapsulation within alginate hydrogels: biological evaluation on the process-dependent cell modifications”.

Other activities

January – May 2014

Stage abroad

Brigham and Women's Hospital at Harvard Medical School and Massachusetts Institute of Technology – Boston, USA.

Advisor: prof. Utkan Demirci

May - October 2014

Stage abroad

Stanford University, School of Medicine, Radiology department. Canary center at Stanford for early cancer detection – Stanford, USA.

Advisor: prof. Utkan Demirci

Acknowledgments

I consider myself very lucky person to have a chance to spend last three years in such a wonderful places as BIOtech and BAMM labs. More importantly meet so many fantastic people and get lots and lots of priceless knowledge and experience.

BIOtech, I can truly call this lab as my family that I never had before.
First of all, I would love to thank Prof. Claudio Migliaresi, my advisor, who give me this wonderful chance to join BIOtech group, moreover, for opportunity to spend almost a year in US, at last for his critical guidance in my research work.
Of course, my advisor Prof. Antonella Motta for her kind support and priceless advices in all aspects of my research and personal life.
Walter. My critical opponent and such a good friend :) I will never forget our lab meetings debates and your jokes :)
Filippo. My dear friend… I am lucky to be able to call you my friend.
All the other students and senior scientists I had honor to work with, who like "ECM" made BIOtech lab such a perfect "niche" for work and activity.
At last, I would love to express a separate gratitude to Filippo, Nicola, Rosa and Cristiano who made my last half year in BIOtech so wonderful and joyful.

BAMM labs at Harvard Medical school and Stanford Medical school (USA).
I want to say thank you to Prof. Utkan Demirci for letting me work and learn so much as a member of BAMM labs, participate in the cutting edge research projects in the field of tissue engineering. This experience is valuable and priceless. Savas and Sinan, my two mentors, who are so different, but so important for me. Each of them tought me how to be a better scientist, and I truly appreciate that.

My two girls Gizem and Charlene, who become my dearest and closest friends in BAMM group.

Next, very important part, I would like to acknowledge my very first lab in Belarus, in particular Dr. Danilenko Nina Genusovna, who saw in me something nobody could see before, starvation for scientific knowledge. She believed in me, and helped me to become a scientist.
My very first mentor, and at the same time my dear friend, my brother Oleg. He was the toughest teacher I have ever had in my life, but it worked ☺ I have learned how be a scientist.

Lastly… I would love to say thanks to my dearest friends who I know for many many years… To those who was always by my side no matter what… Who believed in me and supported me the best way they could….
Mam and dad…
Olya and Anuta: my dearest friends, you made me better and have changed my life because of your warm love.
Katusha and her family: you are my life example of clean love and family union☺; Nastena and her family: you are like sun shine in my life) Always make me smile.
Ilona ☺ life example how to be happy no matter what.
Vova and Rigo, for being these great reliable friends in my life.
And the most important of all, to Richard) You gave me what I never had in my life.

And to all those who I know … because every person you meet change your life in a certain way ☺ Maybe I will never be where I am, without them)